UNIVERSIDAD COMPLUTENSE DE MADRID
FACULTAD DE CIENCIAS QUÍMICAS

TESIS DOCTORAL

Supercritical extraction of bioactive compounds from vegetable matrices and their encapsulation with supercritical fluid advanced techniques

Extracción supercrítica de compuestos bioactivos a partir de matrices vegetales y su encapsulación con técnicas avanzadas supercríticas

MEMORIA PARA OPTAR AL GRADO DE DOCTOR

PRESENTADA POR

Diego Felipe Tirado Armesto

Directora

Lourdes Calvo Garrido

Madrid

UNIVERSIDAD COMPLUTENSE DE MADRID

FACULTAD DE CIENCIAS QUÍMICAS

Departamento de Ingeniería Química y Materiales

TESIS DOCTORAL

Supercritical extraction of bioactive compounds from vegetable matrices and their encapsulation with supercritical fluid advanced techniques

Extracción supercrítica de compuestos bioactivos a partir de matrices vegetales y su encapsulación con técnicas avanzadas supercríticas

MEMORIA PARA OPTAR AL GRADO DE DOCTOR

PRESENTADA POR

Diego Felipe Tirado Armesto

Directora

Prof. Dra. Lourdes Calvo Garrido

Madrid, 2019

COMPLUTENSE UNIVERSITY OF MADRID

SCHOOL OF CHEMICAL SCIENCES

Department of Chemical and Materials Engineering

DOCTORAL THESIS

Supercritical extraction of bioactive compounds from vegetable matrices and their encapsulation with supercritical fluid advanced techniques

THESIS SUBMITTED FOR THE DEGREE OF DOCTOR OF PHILOSOPHY

PRESENTED BY

Diego Felipe Tirado Armesto

Supervisor

Prof. Dr. Lourdes Calvo Garrido

Madrid, 2019

UNIVERSIDAD
COMPLUTENSE
MADRID

LOURDES CALVO GARRIDO, PROFESORA TITULAR DEL DEPARTAMENTO DE INGENIERÍA QUÍMICA Y MATERIALES DE LA FACULTAD DE CIENCIAS QUÍMICAS DE LA UNIVERSIDAD COMPLUTENSE DE MADRID

CERTIFICA:

Que el presente trabajo de investigación titulado "**Supercritical extraction of bioactive compounds from vegetable matrices and their encapsulation with supercritical fluid advanced techniques**", ha sido realizado bajo su dirección en el Departamento de Ingeniería Química y Materiales de la Universidad Complutense de Madrid, y constituye la memoria que presenta **Diego Felipe Tirado Armesto** para optar al grado de Doctor en Ingeniería Química, que a su juicio, reúne los requisitos de originalidad y rigor científico necesarios para ser presentada como Tesis Doctoral.

Y para que así conste, firma el presente certificado en Madrid a 15 de julio de 2019.

Prof. Dra. Lourdes Calvo Garrido

Doctoral thesis as a compendium of publications aiming to obtain the International Doctorate mention

This dissertation aims to obtain the International Doctorate mention. With this purpose, a research stay of three and a half months was conducted in the Department of Industrial Engineering at the University of Salerno, under the supervision of Professor Ernesto Reverchon.

Moreover, this thesis is presented as a compendium of five previously published scientific articles. The following are complete references to the articles that constitute the body of this thesis:

I. D.F. Tirado, E. de la Fuente, L. Calvo, A selective extraction of hydroxytyrosol-rich olive oil from alperujo, Journal of Food Engineering 263 (2019) 409-416. doi: 10.1016/j.jfoodeng.2019.07.030.

II. D.F. Tirado, M.J. Tenorio, A. Cabañas, L. Calvo, Prediction of the best cosolvents to solubilise fatty acids in supercritical CO_2 using the Hansen solubility theory, Chemical Engineering Science 190 (2018) 14–20. doi: 10.1016/j.ces.2018.06.017.

III. D.F. Tirado, A. Rousset, L. Calvo, The selective supercritical extraction of high-value fatty acids from *Tetraselmis suecica* using the Hansen solubility theory, Chemical Engineering Transactions 75 (2018) 133-138. doi: 10.3303/CET1975023.

IV. D.F. Tirado, L. Calvo, The Hansen theory to choose the best cosolvent for supercritical CO_2 extraction of β-carotene from *Dunaliella salina*, The Journal of Supercritical Fluids 145 (2019) 211–218. doi: 10.1016/j.supflu.2018.12.013.

V. D.F. Tirado, I. Palazzo, M. Scognamiglio, L. Calvo, G. Della Porta, E. Reverchon, Astaxanthin encapsulation in ethyl cellulose carriers by continuous supercritical emulsions extraction: A study on particle size, encapsulation efficiency, release profile and antioxidant activity, The Journal of Supercritical Fluids 150 (2019) 128-136. doi: 10.1016/j.supflu.2019.04.017.

"…Del lado hispánico, en cambio, tal vez nos venga el ser emigrantes congénitos con un espíritu de aventura que no elude los riesgos. Todo lo contrario: los buscamos. De unos cinco millones de colombianos que viven en el exterior, la inmensa mayoría se fue a buscar fortuna sin más recursos que la temeridad, y hoy están en todas partes... La cualidad con que se les distingue en el folclor del mundo entero es que ningún colombiano se deja morir de hambre. Sin embargo, la virtud que más se les nota es que nunca fueron tan colombianos como al sentirse lejos de Colombia.

Así es. Han asimilado las costumbres y las lenguas de otros como las propias, pero nunca han podido sacudirse del corazón las cenizas de la nostalgia, y no pierden ocasión de expresarle con toda clase de actos patrióticos para exaltar lo que añoran de la tierra distante, inclusive sus defectos…

…La paradoja es que estos conquistadores nostálgicos, como sus antepasados, nacieron en un país de puertas cerradas…

…Nuestra educación conformista y represiva parece concebida para que los niños se adapten por la fuerza a un país que no fue pensado para ellos, en lugar de poner el país al alcance de ellos para que lo transformen y engrandezcan. Semejante despropósito restringe la creatividad y la intuición congénitas, y contrataría la imaginación, la clarividencia precoz y la sabiduría del corazón, hasta que los niños olviden lo que sin duda saben de nacimiento: que la realidad no termina donde dicen los textos, que su concepción del mundo es más acorde con la naturaleza que la de los adultos, y que la vida sería más larga y feliz si cada quien pudiera trabajar en lo que le gusta, y sólo en eso.

Esta encrucijada de destinos ha forjado una patria densa e indescifrable donde lo inverosímil es la única medida de la realidad. Nuestra insignia es la desmesura. En todo…

… Pues somos dos países a la vez: uno en el papel y otro en la realidad. Aunque somos precursores de las ciencias en América, seguimos viendo a los científicos en su estado medieval de brujos herméticos, cuando ya quedan muy pocas cosas en la vida diaria que no sean un milagro de la ciencia…

…Creemos que las condiciones están dadas como nunca para el cambio social, y que la educación será su órgano maestro. Una educación, desde la cuna hasta la tumba, inconforme y reflexiva, que nos inspire un nuevo modo de pensar y nos incite a descubrir quiénes somos en una sociedad que se quiera más a sí misma… Que integre las ciencias y las artes a la canasta familiar, de acuerdo con los designios de un gran poeta de nuestro tiempo que pidió no seguir amándolas por separado como a dos hermanas enemigas. Que canalice hacia la vida la inmensa energía creadora que durante siglos hemos despilfarrado en la depredación y la violencia, y nos abra al fin la segunda oportunidad sobre la tierra que no tuvo la estirpe desgraciada del coronel Aureliano Buendía…"

Gabriel García Márquez

Taken from *LA PROCLAMA: POR UN PAIS AL ALCANCE DE LOS NIÑOS*

Colombia al filo de la oportunidad (1997).

Acknowledgements

I would first like to extend my deepest gratitude to Professor Lourdes Calvo, who welcomed me into her research group (and Spain) to develop my doctoral thesis. I couldn't be more grateful for your unending patience in teaching me the art of the supercritical fluids, a hidden jewel for me. Thank you for training me to become the researcher I am trying to be today.

I gratefully acknowledge the "Bolívar Gana con Ciencia" program from the Department of Bolívar (Colombia) for my Ph.D. grant.

I would also like to thank Professor Albertina Cabañas for allowing me to work in her Phase Equilibrium Lab at the Department of Physical Chemistry I. I really appreciate the time spent teaching me about phase equilibrium.

I want to thank also the "Centro Nacional de Microscopía Electrónica (CNME)" and the "Centros de Apoyo a la investigación (CAI)" of the university for their help and kindness when I required their services. Thanks also to the administrative staff and Professors from the School of Chemical Sciences.

I do appreciate Professor Diofanor Acevedo's support and advice from the distance and the guys who are members of his Research Group. Thanks to Professors Piedad Montero and Adriana Herrera as well.

I also want to thank the members of the Madrid Underwater Rugby Club, Osos, for their company and pleasant moments underwater.

I'm sure I'm not quoting hereby plenty of people who have supported me either from the distance or by having spent time in Europe with me, but I extend my most sincere gratitude to all of them, inasmuch as I believe I couldn't mention everyone. Among all these people, I would like to express my gratitude to all those "parceros": "Mis manitas" (Katy and Lourdes), Cris, Alexis, Flavia, Angy, Bárbara, Fanny, Rodri, Freddy, Sandrita, Mati, Nancy, Dra. Laura Hernández, Dr. Antonio Tabernero, Gallo, Ramiro, my cousin Bollini, Abbey and Lulu… Thanks Y'all. I also want to bring up to Ceci (my mother in Madrid), her husband Álvaro and all her family… I'll always cherish your presence in my life and mind.

I couldn't leave without showing my gratitude to the people who made the long and difficult days in the university much easier and manageable. Carlos, Patricia, Dani, Nacho: you were the best company I could ever wish for, and much more than I deserved. I take with me the memory of the family I have chosen in Madrid. Thank you for all that quality time at the "cespecillo".

Mariana, even if you're not here, I'll always carry you with me in my mind.

Finally, and most important, Nego. You were my driving force.

This Doctoral Thesis has been carried out thanks to the financial support of the PhD grant from the "Bolivar Gana con Ciencia" program granted by the Department of Bolivar (Colombia) under the strategic line of Science, Technology and Agricultural, Biodiversity and Habitat, Food and Nutrition Innovation.

Esta Tesis Doctoral se ha realizado gracias al soporte financiero de la beca doctoral del programa “Bolívar Gana con Ciencia” concedida por el Departamento de Bolívar (Colombia) bajo la línea estratégica de Ciencia Tecnología e Innovación Agropecuaria, Biodiversidad y Hábitat, Alimentos y Nutrición.

Table of contents

List of Figures

List of Tables

List of abbreviations

A_{470}	Absorbance at 470 nm
$A_{652.4}$	Absorbance at 652.4 nm
$A_{665.2}$	Absorbance at 665.2 nm
ANOVA	Analysis of variance
AOAC	Association of Official Agricultural Chemists
BF_3	Boron trifluoride
BPR	Back-pressure regulator
$C_{(x+c)}$	Carotenoid (xanthophylls and carotenes) concentration
C_a	Chlorophyll a concentration
CAGR	Compound annual growth rate
C_b	Chlorophyll b concentration
CO_2	Carbon dioxide
DAD	Diode array detector
d.b.	Dry basis
DLS	Dynamic light scattering
DPPH	1,1-diphenyl-2-picrylhydrazyl
E	Latent heat of vaporization of the fluid
E_d	Dispersion latent heat of vaporization
E_h	Hydrogen bonging latent heat of vaporization
E_p	Polar latent heat of vaporization
FAME	Fatty acid methyl esters
FDA	Food and Drug Administration

FE-SEM	Field Emission-Scanning Electron Microscope
FID	Flame Ionization Detector
FOSHU	Foods for Specific Health Uses
FUFOSE	Functional Food Science in Europe
GAE	Gallic acid equivalents
GC	Gas chromatography
GCM	Group contribution method
HPLC	High-performance liquid chromatography
HSP	Hansen solubility parameter
HST	Hansen solubility theory
IUPAC	International Union of Pure and Applied Chemistry
KH_2PO_4	Potassium di-hydrogen phosphate
L/G	Liquid/gas
LSD	Least Significant Difference
MD	Mean diameter
MR	Mass recovery
MUFA	Monosaturated fatty acid
N_2	Nitrogen
Na_2SO_4	Sodium sulphate anhydrous
NaCl	Sodium chloride
NaOH	Sodium hydroxide
NIST	National Institute of Standards and Technology
NTP	Normal temperature and pressure
O	Oil

P_C	Critical pressure
PDI	Polydispersity index
PID	Proportional Integral Derivative
PLGA	Poly(lactic-co-glycolic acid)
PUFA	Polyunsaturated fatty acid
R_a	Energy difference
RDI	Recommended Daily Intake
RED	Relative Energy Distance
REFPROP	Reference Fluid Properties
RESS	Rapid expansion of a supercritical solution
SAA	Supercritical assisted atomization
SAS	Supercritical antisolvent precipitation
sc-CO_2	Supercritical carbon dioxide
SCF	Supercritical fluid
SCM	Supercritical mixture
SEDS	Solution enhanced dispersion by supercritical fluids
SEE	Supercritical Emulsion Extraction
SEM	Scanning Electron Microscope
SFA	Saturated fatty acid
SFEE	Supercritical Fluid Extraction of Emulsion
SI	International System of Units
SIF	Simulated intestinal fluid
SSI	Supercritical solvent impregnation
T_C	Critical temperature

TEAC	Trolox equivalent antioxidant capacity
TEM	Transmission Electron Microscope
Trolox	(±)-6-hydroxy-2,5,7,8-tetramethylchromane-2-carboxylic acid
u	Solvent velocity
UFA	Unsaturated fatty acid
V	Molar volume of the fluid
V_{ref}	Reference molar volume
VLE	Vapour–liquid equilibria
W	Water
δ	Hildebrand solubility parameter
δ_d	Hansen dispersion solubility parameter
$\delta_{d\ ref}$	Reference Hansen dispersion solubility parameter
δ_h	Hansen hydrogen bonding solubility parameter
$\delta_{h\ ref}$	Reference Hansen hydrogen bonding solubility parameter
δ_p	Hansen polar solubility parameter
$\delta_{p\ ref}$	Reference Hansen polar solubility parameter
δ_T	Total Hansen solubility parameter

Abstract

1. Introduction

The search for natural sources of bioactive compounds with nutritional interest has received widespread attention. Microalgae represent one of the sources that are being most studied due to the high number of nutritional compounds within their structure. Moreover, research on this field has explored the valorisation of residues from mainstream processes. Some of these interesting compounds highlighted with nutritional benefits include antioxidants, phenolic compounds and mono (MUFAs), and polyunsaturated fatty acids (PUFAs). These target compounds have been commonly extracted by using organic solvents; however, this technique is non-selective and has been losing attractiveness since it generates products with traces of residual solvent.

This increasing awareness towards the environment and health issues that derive from the use of organic solvents has led to the implementation of stronger regulations; and for that reason, the use of the supercritical carbon dioxide (sc-CO_2) extraction has become a commercial and environmentally friendly alternative. The sc-CO_2 extraction is an important industrial process, enabled by overcoming the poor solvent nature of sc-CO_2 through the addition of entrainers (modifiers or cosolvents). However, choosing an appropriate cosolvent is an arduous task, because long and expensive experimental trials are needed. To fulfil this demand, the Hansen solubility theory (HST) has arisen as a suitable tool to reduce the number of experiments for the selection of a proper cosolvent for sc-CO_2.

On the other hand, products containing bioactive compounds such as those obtained in this research thesis could help to cover the nutritional necessities of society in terms of health and well-being. Nevertheless, these products do not provide the expected health benefits because of their low chemical or biochemical stability and their high reactivity. Among the various delivery systems available, biopolymer-based micro- and nanocarriers could be designed to transport these compounds to a specific site of action with minimal degradation; and the Supercritical Fluid Extraction of Emulsions (SFEE) has emerged, harnessing the unique thermodynamic and fluid-dynamic properties of sc-CO_2, to produce micro- and nanocarriers capable to protect and transport the interesting compounds. Additionally, SFEE can be performed in a continuous layout, avoiding the problems linked to the batch process.

2. Objectives

The main objective of this research thesis was to selectively obtain, from microalgae and an agro-industrial residue, oil extracts rich in bioactive compounds of considerable nutritional interest by supercritical fluid extraction with CO_2 as the main solvent. To do so, the best pre-treatment of the raw material and the best operating conditions of the process were selected in order to maximize the extraction yield. Moreover, the selectivity of the supercritical fluid regarding the target compound was enhanced by using cosolvents chosen via a theoretical solubility model. Finally, the potential of the SFEE technology, operating in a continuous layout, was explored in order to nanoencapsulate the obtained bioactive compounds.

3. A unifying discussion of the results of this thesis

First of all, the process parameters and solid conditions that affected the sc-CO_2 extraction were studied and optimised. To do so, hydroxytyrosol-rich oil extracts from alperujo, the solid-liquid waste generated by the current two-phase method of olive oil extraction, was extracted by using sc-CO_2. The oil extraction yield reached at optimised conditions (30 MPa, 323.2 K and 7.5 kg CO_2 h^{-1} kg $biomass^{-1}$) by sc-CO_2 extraction (13 %) was close to that obtained by solvent extraction with n-hexane (14 %) and the fatty acid profile of the supercritical extracts was similar to that of a commercial extra virgin olive oil. Moreover, the supercritical fluid extraction proved to be more selective than the solvent extraction, since no hydroxytyrosol was found in the n-hexane extracts. By optimising solid conditions, it was found that smaller particle sizes improved extraction rate. Sea-sand was mixed with alperujo to enhance the bed porosity. Extractions from samples with particle size diameter < 0.80 mm had a 40 % higher oil extraction yield compared with the supercritical fluid extraction process involving samples with the whole range of particles size. Also, the sample must be dried, because the excess of water creates a barrier to mass transfer. The fastest and highest extraction was achieved when the sample was dried till a water mass fraction of 1 %, which was the equilibrium moisture with the environment humidity in Madrid (average relative humidity of 57 %).

On the other hand, two pressures (20 MPa and 30 MPa) and two temperatures (323.2 K and 373.2 K) were assessed to study the influence of operating conditions. The increase in pressure improved the oil and the hydroxytyrosol extraction yield, as this is directly related to the increase in solvent density and solvent capacity. Temperature

played a singular role. Its increase reduced oil extraction yields due to the fact that it causes a reduction in CO_2 density; however, a higher hydroxytyrosol content was found in extracts obtained with the highest temperature (373.2 K), at which the total phenol content, and therefore the antioxidant capacity, were uppermost. Moreover, the oil extraction yield improved with solvent flow rate, but a minimum residence time was required. The optimum was 0.18 kg h^{-1} (7.5 kg CO_2 h^{-1} alperujo^{-1}).

This study of solid conditions and operating variables was then extended to subsequent supercritical fluid extractions from microalgae (*Tetraselmis suecica* and *Dunaliella salina*). Even though they were different plant matrices, the model of mass transfer from the cells was considered similar to that of alperujo. Due to the small particle size (45 μm) and the high total extract content in *D. salina* (21 % in mass fraction based on the Soxhlet extraction), sea-sand was also used in this case to prevent the material bed compaction and the formation of preferential channels that reduced the extraction yield. Despite the fact that *T. suecica* had the same particle size (45 μm), no sea-sand was used in that case since the low total extract content in the microalgae (3 % in mass fraction based on extraction with n-hexane). Finally, by using 18 kg CO_2 kg dried *D. salina*$^{-1}$ at 30 MPa and 328.2 K, roughly 30.5 % of the total extractable oil in the microalgae was obtained. In the case of *T. suecica*, at 305.2 K and 20 MP, 54 kg CO_2 kg dried *T. suecica*$^{-1}$ were needed to obtain 50 % of the total extract.

Afterwards, the prediction of the best cosolvents for sc-CO_2 by using the HST to achieve the selective extraction of compounds with nutritional interest from microalgae was performed. The calculations were made with several organic solvents used in the

food and pharmaceutical industry. A cosolvent volume fraction of 5 % (0.05 m^3 m^{-3}) was used to ensure a supercritical homogeneous mixture. β-carotene and oleic, linoleic and α-linolenic acids, as examples of valuable carotenoids and fatty acids respectively, were used as target compounds for the extractions. The order of the cosolvent ability was deduced based on minima R_a values in a wide range of operating conditions suitable for supercritical extraction. According to the theory, the lower the value of R_a, the higher the miscibility of the compound of interest in the supercritical mixture. The cosolvent order depended on the target compound, but in general, ethanol was the best to solubilise all the bioactive compounds in sc-CO_2. The differences in the R_a values and therefore the cosolvent order regarding each compound were mainly due to the different structures of the compounds and the operating conditions tested.

Predictions were first validated with bubble pressures of β-carotene, oleic, linoleic and α-linolenic acids in sc-CO_2 and its mixtures with the different cosolvents. The experimental data were obtained in a high-pressure variable volume view cell, following the static synthetic method. Experimental results agreed with predictions; however, cosolvents with a ring structure performed worse than predicted since the ring avoided strong interactions with the solute. As a result, the best cosolvent for the solubilisation of the target compounds at the conditions specified was ethanol. Subsequently, the estimations were tested against extraction yields of oleic, linoleic and α-linolenic acids from *T. suecica* and β-carotene from *D. salina*. The addition of a mass fractions of 5 % ethanol to sc-CO_2 improved the selective extraction of oleic, linoleic and α-linolenic acids from *T. suecica*, which agreed with the predictions based on the R_a values. The obtained extract with pure sc-CO_2 contained approximately 14.9 %, 3.7 % and 15.7 % of oleic,

linoleic and α-linolenic acid, respectively; while the obtained extract with the mixture sc-CO_2 + ethanol contained 53 %, 54 % and 61 % more. On the other hand, with ethanol as cosolvent, at 318.2 K and 20 MPa, the carotenoids extraction yield from *D. salina* was more than four times (25 g carotenoids kg microalgae^{-1}) than with pure sc-CO_2 (6 g carotenoids kg microalgae^{-1}). The justification for why ethanol was the best cosolvent for CO_2 in both, the solubilization of fatty acids and carotenoids, lies in the increase of the dispersion and dipole-dipole interactions.

The Hansen theory was also used to predict the best operation conditions. The effect of pressure was well predicted via the direct relationship between pressure and the solvent density; however, the impact of temperature was not properly foreseen because neither the variation of solute vapour pressure nor mass transfer kinetics were considered. This could be a limiting factor in implementing Hansen theory, since both factors play an important role in supercritical extractions.

Additionally, the Hansen approach was explored to establish the optimum cosolvent concentration. A non-linear miscibility enhancement with increasing cosolvent fraction was predicted, being higher at small concentrations and low pressures. This behaviour agreed with experimental data and was related to the reduction of the molar volume of the solvent mixture with the increase of cosolvent fraction and pressure and; to the self-association of the cosolvent molecules occurring at large concentrations. However, the impact of the cosolvent concentration depended on the specific interactions to the target solute.

Lastly, it was studied how to protect the extracts obtained, mainly from oxidation and the action of light. For that purpose, encapsulation in a protecting polymer was studied using the SFEE technique. As an example, astaxanthin, another extractable carotenoid from the microalgae, was encapsulated in ethyl cellulose. In this method, astaxanthin and ethyl cellulose were dissolved in ethyl acetate. This formed the organic phase of an emulsion in water that was stabilized by a surfactant (Tween 80). Then sc-CO_2 was used to remove the ethyl acetate causing the fast precipitation of ethyl cellulose and astaxanthin forming solid aggregates suspended in water. The extraction took place in a packing column operating with the CO_2 stream in countercurrent flow with the emulsion.

After setting the oil in water (O/W) ratio in the emulsion to 20/80 (ethyl acetate/water), the micronisation of ethyl cellulose and the impact of its concentration (from 1.0 % to 2.5 %) in the organic phase were first studied. Tween 80 concentration in the aqueous phase was also varied. By increasing the amount of this surfactant from 0.1 % to 0.6 %, smaller particles were generated, and aggregation was observed from 0.3 % on. By operating at 8 MPa, 311.2 K with a CO_2/emulsion ratio of 0.1 and a CO_2 flow rate of 1.4 kg CO_2 h^{-1}, the optimised formulation (1.0 % ethyl cellulose and 0.1 % Tween 80) resulted in spherical smooth particles with narrow mean diameter (PDI of 0.15), nanoscale particle size (240 nm) and a polymer mass recovery of about 90 %. Higher mean particle size was measured when the bioactive compound was encapsulated (363 nm), achieving an encapsulation efficiency of 84 % (2.1 10^{-2} kg astaxanthin kg $powder^{-1}$). During the procedure, the antioxidant capacity of astaxanthin was preserved being equivalent to 3,900 M Trolox equivalent per kg pure $astaxanthin^{-1}$ due to the mild

conditions of the operation. Finally, an *in vitro* release evaluation performed in a simulated intestinal fluid at pH 7.2 and 310.2 K (physiological temperature), showed a fast release rate for the first 6 h but slowed down after about 7 h. As much as 70 % of astaxanthin was released after 10 h.

4. Conclusions

The initial solid condition of the raw material to be submitted to supercritical fluid extraction is very important to maximize the extraction yield and to improve the quality of the extract. On the one side, particles with large diameter hinder the penetration of the supercritical solvent and the solubilisation of the solute. However, caution should be taken since too small particles could represent a risk of formation of preferential channels and blockages during extraction. On the other hand, an insufficient amount of water inside the plant material could cause the cell structure to shrink and consequently hinders diffusion and reduces yield; whereas an excess of water would represent an extra barrier to transport generate the co-extraction of polar substances. For the specific raw materials used in this work, small particles (< 0.80 mm) with moisture content in equilibrium with the environment in Madrid improved fluid contact and therefore extraction rate. Nevertheless, drying demands a considerable amount of energy and milling is a very expensive pre-treatment. These operations together with the supercritical extraction itself can lead to high production costs; but the oil quality with a high bioactive compounds content could be used to formulate nutraceuticals, cosmetics or even pharmaceuticals with a high added value.

As expected, the extraction yields significantly increased with pressure, as it is directly related to the increase in solvent density and solvent capacity. Temperature, on the other hand, plays a very important role in the extraction processes, since its increase may reduce oil extraction yields due to a reduction in the sc-CO_2 density, but it could also improve the extraction of bioactive compounds, if their vapour pressure is high and because it has a positive impact on diffusion and kinetics; not to mention that temperature could also help to improve the cell opening in vegetable matrices. Therefore, the optimal temperature to selectively extract oil extract rich in the bioactive compound should be well established in each case as it is not possible to anticipate the temperature impact as it affects many different aspects of the thermodynamics and mass transfer. Finally, the flow rate rise enhances superficial solvent velocity, which benefits turbulence and reduces the film layer of stagnant fluid around the solid, thus increasing the external mass transfer coefficients; but an excessively large flow rate lessens the residence time in the extractor, which reduces the time for oil solubilization and transport into the bulk of the solvent.

When the yield or the selectivity of the extraction is low, or the operating pressure or CO_2 consumption are to be reduced, a cosolvent may be added to the supercritical solvent. However, considering the economic and practical difficulties involved in choosing a cosolvent at supercritical conditions, theoretical evaluations must be implemented, and the HST provides a useful estimation. The Hansen approach can be used to predict the best cosolvent for sc-CO_2 in the solubilization of bioactive compounds from natural matrices within a specific interval of operating conditions. Besides, the approach is able to predict the non-linear miscibility enhancement with increasing cosolvent fraction, which agreed with experimental data and was related to the reduction

of the molar volume of the solvent mixture with the increase of pressure and the cosolvent fraction and to the self-association of the cosolvent molecules occurring at large concentrations.

The Hansen theory also demonstrated that the best cosolvent was not the same that under conventional conditions. Interestingly, another fact demonstrated by this theory is that a similar benefit cannot be attributed a priori to cosolvents of the same functional type. Despite the above, some considerations must be taken into account when implementing the theory: *i*) the stability of the ring in cyclic solvents is not well predicted; *ii*) it takes into account neither the increase of the solute vapour pressure with temperature nor the enhancement of the kinetic and *iii*) when supercritical fluid extractions from vegetable matrices are performed, the presence of oil in the system could play an important role as matrix cosolvent.

Finally, the SFEE technology is an effective tool for the micronisation ethyl cellulose and to encapsulate astaxanthin within it. The use of a packed column offers the possibility of a high production capacity of nanoparticles with a small volume plant in only a few minutes, along with greater product homogeneity and recovery. Moreover, it is possible by tuning the initial emulsion formulation to obtain ethyl cellulose particles of varied sizes within a narrow distribution and low polydispersity. The technique demonstrates its effectiveness in encapsulating the bioactive compound without compromising its antioxidant activity and provided an adequate structure for its subsequent controlled release; however, some drawbacks should be taken into account when considering this technology: a) materials are obtained in aqueous suspensions that

should be dried off if solid particles are required; b) the toxicological hazards related to the addition of nanoparticles in food has yet to be reviewed; c) consumption of CO_2 to exhaust the organic solvent could be quite high; d) after CO_2 and organic solvent separation, the CO_2 should be recycled and e) SFEE is strongly protected by patents which could jeopardize its commercialization. To evaluate the feasibility of commercial production by using this technology it would be essential to conduct a rigorous economic evaluation.

Resumen

1. Introducción

La búsqueda de fuentes naturales de compuestos bioactivos de interés nutricional ha recibido una amplia atención. Las microalgas representan una de las fuentes más estudiadas debido al elevado número de compuestos nutricionales dentro de su estructura. La investigación en este campo también ha explorado la valorización de residuos desde procesos convencionales. Entre los compuestos de interés destacados con beneficios nutricionales están los antioxidantes, fenólicos y ácidos grasos mono (AGMI) y poliinsaturados (AGPI). Estos compuestos se han extraído comúnmente utilizando disolventes orgánicos; sin embargo, esta técnica no es selectiva y ha ido perdiendo atractivo, ya que genera productos con trazas residuales de disolvente.

Esta creciente conciencia hacia el medio ambiente y la salud que se deriva del uso de disolventes orgánicos ha llevado a la implementación de regulaciones más estrictas; y por esa razón, el uso de la extracción con dióxido de carbono supercrítico (sc-CO_2) se ha convertido en una alternativa comercial y amigable con el medio ambiente. La extracción con sc-CO_2 es un importante proceso industrial, que se consigue superando el bajo poder disolvente del sc-CO_2 mediante la adición de *entrainers* (modificadores o cosolventes). Sin embargo, la elección de un cosolvente adecuado es una tarea ardua, ya que se necesitan largos y costosos ensayos experimentales. Para satisfacer esta demanda, se propone la teoría de solubilidad de Hansen (TSH) como una herramienta adecuada para reducir el número de experimentos para la selección de un cosolvente adecuado para el sc-CO_2.

Por otro lado, los productos que contienen compuestos bioactivos como los obtenidos en esta tesis de investigación podrían ayudar a cubrir las necesidades nutricionales de la sociedad en términos de salud y bienestar. Sin embargo, estos productos no proporcionan los beneficios para la salud esperados debido a su baja estabilidad química o bioquímica y a su alta reactividad. Entre los diversos sistemas de suministro disponibles, se podrían diseñar micro y nanotransportadores basados en biopolímeros para transportar estos compuestos a un sitio específico de acción con una degradación mínima. Para ello, ha surgido la Extracción Supercrítica de Emulsiones (ESE), aprovechando las propiedades termodinámicas y fluidodinámicas únicas del sc-CO_2 para producir micro y nanotransportadores capaces de proteger y transportar los compuestos de interés. Además, la ESE se puede realizar en una disposición continua, evitando los problemas relacionados con el procesado por lotes.

2. Objetivos

El objetivo principal de esta tesis de investigación fue obtener selectivamente, a partir de microalgas y un residuo agroindustrial, extractos de aceite ricos en compuestos bioactivos de considerable interés nutricional mediante la extracción con fluidos supercríticos (EFS), usando CO_2 como principal disolvente. Para ello, se seleccionó el mejor pretratamiento de la materia prima y las mejores condiciones de operación del proceso para maximizar el rendimiento de extracción. Además, la selectividad del gas supercrítico con respecto al compuesto objetivo se mejoró mediante el uso de cosolventes elegidos mediante un modelo teórico de solubilidad. Finalmente, se exploró el potencial

de la tecnología ESE, operando en disposición continua, para nanoencapsular los compuestos bioactivos obtenidos.

3. Discusión integradora de los resultados de esta tesis

En primer lugar, se estudiaron y optimizaron los parámetros del proceso y las condiciones del sólido que afectaron la extracción con sc-CO_2. Para ello, se extrajeron con sc-CO_2 los extractos de aceite ricos en hidroxitirosol del alperujo, el residuo sólido-líquido generado por el actual sistema de extracción de aceite de oliva de dos fases. El rendimiento de extracción de aceite alcanzado en condiciones optimizadas (30 MPa, 323,2 K y 7,5 kg CO_2 h^{-1} kg biomasa^{-1}) mediante la extracción con sc-CO_2 (13 %) fue similar al obtenido mediante la extracción Soxhlet con n-hexano (14 %) y el perfil de ácidos grasos de los extractos supercríticos fue similar al de un aceite de oliva virgen extra comercial. Además, la extracción supercrítica demostró ser más selectiva que la extracción convencional con disolvente orgánico, ya que no se encontró hidroxitirosol en los extractos obtenidos con n-hexano. Al optimizar las condiciones del sólido, se encontró que tamaños de partículas más pequeños mejoraban la tasa de extracción. El alperujo se mezcló con arena de mar para mejorar la porosidad del lecho. Las extracciones a partir de muestras con un diámetro de tamaño de partícula < 0,80 mm tuvieron un rendimiento de extracción de aceite un 40% mayor en comparación con el proceso EFS en el que se usaron muestras con todo el rango de tamaño de partículas. Además, la muestra debía estar seca, ya que el exceso de agua creó una barrera para la transferencia de masa. La extracción más rápida y máxima se consiguió cuando el alperujo se secó hasta una

fracción másica de agua del 1 %, que era la humedad en equilibrio con la humedad ambiental de Madrid.

Por otro lado, se evaluaron dos presiones (20 MPa y 30 MPa) y dos temperaturas (323,2 K y 373,2 K) para estudiar la influencia de las condiciones de proceso. El aumento de la presión mejoró el rendimiento de extracción del aceite y del hidroxitirosol, ya que está directamente relacionado con el aumento de la densidad y la capacidad disolvente. La temperatura jugó un papel complejo. Su aumento redujo los rendimientos de extracción de aceite debido a que provocó una reducción de la densidad del CO_2; sin embargo, se encontró un mayor contenido de hidroxitirosol en los extractos obtenidos a la temperatura más alta (373.2 K), en los que el contenido total de fenoles, y por lo tanto la capacidad antioxidante, fueron los más altos. Además, el rendimiento de extracción de aceite mejoró con el caudal de disolvente, pero se requería un tiempo mínimo de residencia. El óptimo fue de 0,18 kg h^{-1} (7,5 kg CO_2 h^{-1} alperujo^{-1}).

Este estudio de condiciones del sólido y variables de operación se extendió luego a las extracciones supercríticas posteriores a partir de microalgas (*Tetraselmis suecica* y *Dunaliella salina*). A pesar de ser matrices vegetales diferentes, el modelo de transferencia de masa desde las células se consideró similar al del alperujo. Debido al pequeño tamaño de las partículas (45 μm) y al alto contenido de extracto total en *D. salina* (21 % en fracción másica, basada en extracción Soxhlet), la arena de mar también se utilizó en este caso para evitar la compactación del lecho y la formación de canales preferentes que redujeran el rendimiento de extracción. A pesar de que *T. suecica* tenía el mismo tamaño de partícula (45 μm), no se utilizó arena de mar en ese caso, ya que el bajo

contenido de extracto total en la microalga (3 % en fracción másica, basada en extracción con n-hexano). Finalmente, utilizando 18 kg de CO_2 kg de *D. salina* seca^{-1} a 30 MPa y 328,2 K, se obtuvo aproximadamente el 30,5 % del aceite total extraíble en la microalga. En el caso de *T. suecica*, a 305,2 K y 20 MPa se necesitaron 54 kg CO_2 kg de *T. suecica* seca^{-1} para obtener el 50 % del extracto total contenido en la microalga.

A continuación, se realizó la predicción de los mejores cosolventes para sc-CO_2 utilizando la TSH para conseguir la extracción selectiva de compuestos con interés nutricional a partir de microalgas. Los cálculos se realizaron con varios disolventes orgánicos utilizados en la industria alimentaria y farmacéutica. Se utilizó una fracción volumétrica de cosolvente del 5 % (0,05 m^3 m^{-3}) para asegurar una mezcla supercrítica homogénea. Se usaron β-caroteno y los ácidos oleico, linoleico y α-linolénico, como ejemplos de valiosos carotenoides y ácidos grasos respectivamente, como compuestos objetivo para las extracciones. El orden de la capacidad cosolvente se dedujo en base a valores mínimos de R_a en un amplio rango de condiciones de operación adecuadas para la extracción supercrítica. Según la teoría, cuanto menor es el valor de R_a, mayor es la miscibilidad del compuesto de interés en la mezcla supercrítica. El orden cosolvente dependió del compuesto objetivo, pero en general, el etanol fue el mejor para solubilizar todos los compuestos bioactivos en sc-CO_2. Las diferencias en los valores de R_a y, por lo tanto, en el orden cosolvente de cada compuesto se debieron principalmente a las diferentes estructuras de los compuestos y a las condiciones de operación evaluadas.

Las predicciones se validaron primero con presiones de burbuja de β-caroteno y ácidos oleico, linoleico y α-linolénico en sc-CO_2 y sus mezclas con los diferentes

cosolventes. Los datos experimentales se obtuvieron en una celda de visión de volumen variable de alta presión, siguiendo el método sintético estático. En general, los resultados experimentales estuvieron de acuerdo con las predicciones; sin embargo, los cosolventes con una estructura de anillo se desempeñaron peor de lo previsto ya que el anillo evitó fuertes interacciones con el soluto. Como resultado, el mejor cosolvente para la solubilización de los compuestos objetivo en las condiciones especificadas fue el etanol. Posteriormente, las estimaciones se contrastaron con los rendimientos de extracción de los ácidos oleico, linoleico y α-linolénico desde *Tetraselmis suecica* y β-caroteno a partir *Dunaliella salina*. La adición de una fracción másica de etanol del 5 % al sc-CO_2 mejoró la extracción selectiva de los ácidos oleico, linoleico y α-linolénico desde *T. suecica*, lo que coincidió con las predicciones basadas en los valores de R_a. El extracto obtenido con sc-CO_2 contenía aproximadamente 14,9 %, 3,7 % y 15,7 % de ácido oleico, linoleico y α-linolénico, respectivamente; mientras que el extracto obtenido con la mezcla sc-CO_2 + etanol contenía 53 %, 54 % y 61 % más. Por otro lado, con el etanol como cosolvente, a 318,2 K y 20 MPa, el rendimiento de extracción de carotenoides desde *D. salina* fue cuatro veces mayor (25 g de carotenoides kg microalgas^{-1}) que con sc-CO_2 solo (6 g de carotenoides kg microalga^{-1}). La justificación de por qué el etanol fue el mejor cosolvente para el CO_2 tanto en la solubilización de los ácidos grasos como en la de los carotenoides radica en el aumento de las interacciones de dispersión y dipolo-dipolo.

La teoría de Hansen también se utilizó para predecir las mejores condiciones de operación. El efecto de la presión se predijo bien a través de la relación directa entre la presión y la densidad del disolvente; sin embargo, el impacto de la temperatura no se previó adecuadamente porque no se tuvieron en cuenta ni la variación de la presión de

vapor del soluto ni la cinética de transferencia de masa. Esto podría ser un factor limitante en la implementación de la teoría de Hansen, ya que ambos factores juegan un papel importante en las extracciones supercríticas.

Además, se exploró el enfoque de Hansen para establecer la concentración óptima de cosolventes. Se predijo una mejora no lineal de la miscibilidad con el aumento de la fracción cosolvente, siendo mayor en pequeñas concentraciones y bajas presiones. Este comportamiento coincidió con los datos experimentales y se relacionó con la reducción del volumen molar de la mezcla a medida que aumentaba la fracción de cosolvente y la presión; y con la autoasociación de las moléculas de cosolventes, la cual se produce más fácilmente a mayores concentraciones. Sin embargo, el impacto de la concentración de cosolventes dependía de las interacciones específicas del soluto objetivo.

Por último, se estudió cómo proteger los extractos obtenidos, principalmente de la oxidación y de la acción de la luz. Para ello, se estudió la encapsulación en un polímero protector mediante la técnica ESE. Como ejemplo, la astaxantina, otro carotenoide extraíble de microalga, se encapsuló en etilcelulosa. En este método, la astaxantina y la etilcelulosa se disolvieron en acetato de etilo. Esto formó la fase orgánica de una emulsión en agua que fue estabilizada por un surfactante (Tween 80). Luego se utilizó sc-CO_2 para eliminar el acetato de etilo, lo que provocó la rápida precipitación de etilcelulosa y astaxantina, formando agregados sólidos suspendidos en agua. La extracción se llevó a cabo en una columna de relleno que operaba con el flujo de CO_2 en contracorriente con la emulsión.

Después de establecer la relación aceite en agua (O/W) en la emulsión a 20/80 (acetato de etilo/agua), se estudió en primer lugar la micronización de la etilcelulosa y el impacto de su concentración (de 1,0 % a 2,5 %) en la fase orgánica. La concentración de Tween 80 en la fase acuosa también fue variada. Al aumentar la cantidad de este tensioactivo de 0,1 % a 0,6 %, se generaron partículas más pequeñas y se observó una agregación de 0,3 % en adelante. Operando a 8 MPa, 311,2 K con una relación CO_2/emulsión de 0,1 y un caudal de CO_2 de 1,4 kg CO_2 h^{-1}, la formulación optimizada (1,0 % de etilcelulosa y 0,1 % de Tween 80) dio como resultado partículas lisas y esféricas con un diámetro medio estrecho (PDI de 0,15), un tamaño de partícula a nanoescala (240 nm) y una recuperación de la masa del polímero de aproximadamente el 90 %. Se midió un mayor tamaño medio de partículas cuando se encapsuló el compuesto bioactivo (363 nm), alcanzando una eficacia de encapsulación del 84 % (2,1 10^{-2} kg de astaxantina kg de sólido^{-1}). Durante el procedimiento, la capacidad antioxidante de la astaxantina fue preservada, siendo equivalente a 3.900 M Trolox equivalentes por kg de astaxantina pura^{-1} debido a las suaves condiciones de operación. Finalmente, una evaluación de liberación *in vitro* realizada en un líquido intestinal simulado a pH 7,2 y 310,2 K (temperatura fisiológica), mostró una rápida tasa de liberación de la astaxantina durante las primeras 6 h, la cual se ralentizó después de unas 7 h. Finalmente, hasta un 70 % de astaxantina fue liberado después de 10 h.

4. Conclusiones

El estado inicial de la materia prima a ser sometida a EFS es muy importante para maximizar el rendimiento de extracción y mejorar la calidad del extracto. Por un lado, las

partículas de gran diámetro dificultan la penetración del disolvente supercrítico y la solubilización del soluto. Sin embargo, se debe tener cuidado, ya que partículas demasiado pequeñas podrían representar un riesgo de formación de canales preferenciales y obstrucciones durante la extracción. Por otro lado, una cantidad insuficiente de agua en el interior del material vegetal podría hacer que la estructura celular se encoja y, en consecuencia, dificulte la difusión y reduzca el rendimiento; mientras que un exceso de agua representaría una barrera adicional para el transporte, lo que generaría la co-extracción de sustancias polares. Para las materias primas específicas utilizadas en este trabajo, pequeñas partículas (< 0,80 mm) con contenido de humedad en equilibrio con el medio ambiente en Madrid mejoraron el contacto con el fluido y por lo tanto la tasa de extracción. Sin embargo, el secado requiere una cantidad considerable de energía y la molienda es un pretratamiento muy costoso. Estas operaciones, junto con la extracción supercrítica propiamente dicha, pueden dar lugar a elevados costes de producción; pero la calidad del aceite con un alto contenido en compuestos bioactivos podría utilizarse para formular nutracéuticos, cosméticos o incluso productos farmacéuticos con un alto valor añadido.

Como era de esperar, el rendimiento de la extracción aumentó significativamente con la presión, ya que está directamente relacionado con el aumento de la densidad y la capacidad de disolvente. La temperatura, por otro lado, jugó un papel muy importante en los procesos de extracción, ya que su aumento puede reducir los rendimientos de extracción de aceite debido a la reducción de la densidad de sc-CO_2, pero también podría mejorar la extracción de compuestos bioactivos, si su presión de vapor es alta y porque tiene un impacto positivo en la difusión y la cinética; por no mencionar que la temperatura

también podría ayudar a mejorar la apertura de las células en las matrices vegetales. Por lo tanto, la temperatura óptima para extraer selectivamente el extracto de aceite rico en el compuesto bioactivo debe estar bien establecida en cada caso, ya que no es posible anticipar el impacto de la temperatura, debido a que afecta muchos aspectos diferentes de la termodinámica y la transferencia de masa. Finalmente, el aumento del caudal aumenta la velocidad superficial del solvente, lo que beneficia la turbulencia y reduce la capa de película de fluido alrededor del sólido, aumentando así los coeficientes de transferencia de masa externa; pero un caudal excesivamente grande disminuye el tiempo de residencia en el extractor, lo que reduce el tiempo de solubilización del aceite y su transporte a la fase global del disolvente.

Cuando el rendimiento o la selectividad de la extracción es baja, o cuando la presión de funcionamiento o el consumo de CO_2 deben reducirse, se puede añadir un cosolvente al disolvente supercrítico. Sin embargo, considerando las dificultades económicas y prácticas involucradas en la elección de un cosolvente en condiciones supercríticas, se deben implementar evaluaciones teóricas, y la TSH proporciona una estimación útil. El enfoque de Hansen puede ser usado para predecir el mejor cosolvente para sc-CO_2 en la solubilización de compuestos bioactivos de matrices naturales dentro de un intervalo específico de condiciones de operación. Además, el enfoque es capaz de predecir la mejora no lineal de la miscibilidad con el aumento de la fracción cosolvente, lo que concuerda con los datos experimentales y está relacionado con la reducción del volumen molar de la mezcla con el aumento de la presión y de la fracción de cosolvente; y con la auto-asociación de las moléculas cosolventes que se producen en grandes concentraciones.

La teoría de Hansen también demostró que el mejor cosolvente no era el mismo que en condiciones convencionales. Curiosamente, otro hecho demostrado por esta teoría es que un beneficio similar no puede atribuirse a priori a los cosolventes del mismo tipo funcional. A pesar de lo anterior, se deben tener en cuenta algunas consideraciones a la hora de implementar la teoría: *i)* la estabilidad del anillo en disolventes cíclicos no se predice bien; *ii*) no tiene en cuenta ni el aumento de la presión de vapor del soluto ni la mejora de la cinética con la temperatura y *iii*) cuando se realiza EFS a partir de matrices vegetales, la presencia de aceite en el sistema podría jugar un papel importante como cosolvente de la matriz sólida.

Por último, la tecnología ESE es una herramienta eficaz para la micronización de la etilcelulosa y para encapsular la astaxantina en su interior. El uso de una columna de relleno ofrece la posibilidad de una alta capacidad de producción de nanopartículas con una planta de pequeño volumen en pocos minutos, junto con una mayor homogeneidad y recuperación del producto. Además, es posible afinar la formulación inicial de la emulsión para obtener partículas de etilcelulosa de tamaños variados dentro de una distribución estrecha y baja polidispersidad. La técnica probó su eficacia en la encapsulación del compuesto bioactivo sin comprometer su actividad antioxidante y proporcionó una estructura adecuada para su posterior liberación controlada; sin embargo, se deben tener en cuenta algunos inconvenientes al considerar esta tecnología: a) los materiales se obtienen en suspensiones acuosas que deben secarse si se requieren partículas sólidas; b) los riesgos toxicológicos relacionados con la adición de nanopartículas en los alimentos aún no han sido revisados; c) el consumo de CO_2 para

agotar el disolvente orgánico podría ser bastante elevado; d) luego de la separación del CO_2 y el disolventes orgánicos, el CO_2 debería reciclarse y e) la ESE está fuertemente protegida por patentes que podrían poner en peligro su comercialización. Para evaluar la viabilidad de la producción comercial mediante el uso de esta tecnología, sería esencial realizar una evaluación económica rigurosa.

1. Introduction

Increasing work, living speed, stress, and various psychological pressures have changed drastically the current lifestyles of human beings. All these aspects have led to a bigger incidence of increasingly common illnesses nowadays, such as diabetes, obesity, various cancers and vascular diseases. For this reason, natural products and health-promoting foods have received widespread attention in the world population [1].

To improve the quality of life and avoid these illnesses, people are trying to change eating habits by increasing consumption of vegetables, fruits, dietary supplements, nutraceuticals, phytotherapeutic substances and other foods with potential health benefits for the consumer, either to maintain a healthy lifestyle or obtain therapeutic results. For this reason, the demand for bioactive compounds from natural sources is increasing [2].

Microalgae represent one of these sources that are being studied due to the high amounts of bioactive compounds within their structure. Some of these valuable compounds include carotenoids, mono (MUFAs) and polyunsaturated fatty acids (PUFAs), phenolic compounds and others [3]. In addition, research on this field has also explored the valorisation of residues from mainstream processes, such as the isolation of organic compounds with high added values from agro-industrial solid wastes [4].

1.1 Bioactive compounds

Apart from providing nutrients, the food contains a series of non-nutritive substances involved in the secondary metabolism of the plant kingdom. These ingredients could be

pigments, aromatics constituents and growth regulators, which work as natural protectors against parasites and other external agents. They do not have a classically defined nutritional function but can have a significant impact on the course of a disease. These substances may be known as phytochemicals or bioactive compounds [5]. Some of them cannot be considered essential substances in the diet of human beings, since they are not required for our metabolism, but they are indispensable in the long term for our health. They work by providing a protective effect on the cardiocirculatory system, reducing blood pressure, regulating blood sugar and cholesterol, reducing the risk of cancer and improving the immune defensive response of our body [6].

These bioactive compounds act on human metabolism and cause beneficial effects on health, generally associated with their action on the expression of genes, such as antioxidants, anti-inflammatories, anticarcinogenic or chemopreventives, immunomodulators, neuroprotectors, fat metabolism regulators, among others [7]. They can also influence gastrointestinal health, such as probiotics and prebiotics, or other functions of the body, such as the nervous system, through the modulation of appetite and satiety, or the ability to learn, the memory and mood. Basically, they could help to prevent disease and maintain health. Consequently, the effect of these dietary factors on health promotion and disease prevention is a topic of great attention in current research [8].

As mentioned before, bioactive compounds are in the limelight of research laboratories in the pharmaceutical and food industries. In the scientific literature, this field of research is called functional foods [9], a concept which was first coined in Japan in 1984

when the Japanese government allocated research funds for studying functional food or Foods for Specific Health Uses (FOSHU) and defined as "food products fortified with special constituents that possess advantageous physiological effects" [9]. Afterwards, when functional food science migrated to Europe, researchers defined functional food using the statement that "food products can only be considered functional if together with the basic nutritional impact it has beneficial effects on one or more functions of the human organism thus either improving the general and physical conditions or/and decreasing the risk of the evolution of diseases" [10].

Currently, there is no official definition of functional foods common to all the countries, but the European Union project called Functional Food Science in Europe (FUFOSE) [11] gives an appropriate working definition: "A food can be regarded as functional if it is satisfactorily demonstrated to affect beneficially one or more target functions in the body, beyond adequate nutritional effects, in a way that is relevant to either an improved state of health and well-being and/or reduction of risk of disease. Functional foods must remain foods and they must demonstrate their effects in amounts that can normally be expected to be consumed in the diet: they are not pills or capsules, but part of a normal food pattern".

According to the Joint Research Centre of the Institute for Prospective Technological Studies from the European Commission [12], due to limited data and differences in definitions, information and figures on the absolute size of the bioactive compounds market within the European Union and globally are not consistent across different studies and reports

and vary widely. However, the global bioactive ingredient market is expected to reach more than € 45 billion by 2024 while the estimates for the European Union market was worth, roughly speaking, € 6 billion in 2018 and estimated to be growing at a compound annual growth rate (CAGR) of 7 %, to reach € 9 billion by 2024. The United States, for its part, ranks first in consumption with around € 7 billion in 2018 and almost € 11 billion by 2024 [13]. Thus, the information from all sources indicates consistently that this market is growing and that it is expected to continue to do so for the foreseeable future. Industry sources and reports confirm that new products are constantly marketed, and new target groups are targeted [12].

A wide range of bioactive compounds have been studied in this research thesis. Most of them came from microalgae and, in another particular case, from alperujo, the solid-liquid waste generated by the current two-phase method of olive oil extraction. In the case of compounds of interest from microalgae, β-carotene, astaxanthin and oleic (C18:1 *cis*-9; ω-9), linoleic (C18:2 *cis*-9,12; ω-6) and α-linolenic (C18:3 *cis*-9,12,15; ω-3) acids were studied. On the other hand, hydroxytyrosol-rich oil from alperujo was obtained.

In this thesis, the selective extraction of hydroxytyrosol from alperujo (**Publication I**), high-value fatty acids from *Tetraselmis suecica* (**Publication III**) and β-carotene from the microalgae *Dunaliella salina* (**Publication IV**) was explored. The selective extraction of the compounds was achieved by using a theoretical approach (**Publication II, III** and **IV**) and finally; the encapsulation of astaxanthin (**Publication V**), which main natural source is the microalgae *Haematococcus pluvialis*, was also accomplished. In conclusion, model

compounds from the group of phenols (hydroxytyrosol), carotenoids (β-carotene and astaxanthin) and fatty acids (oleic, linoleic and α-linolenic acids) were studied.

1.2 Microalgae as a source of bioactive compounds

Microalgae are microscopic organisms (2 μm - 200 μm), photosynthetic and eukaryotes, able to grow in an autotrophic or heterotrophic way. In general, they are highly efficient in carbon dioxide (CO_2) fixation and the use of solar energy to produce biomass. They are found in all water sources, such as lakes, seas and rivers, but they are not restricted only to water. They are also available in the soil and most terrestrial environments, even in the most extreme ones, which allows them to be found widely distributed in the biosphere, adapted to a large number of conditions [14].

Microalgae are rich in a wide range of bioactive compounds that are able to meet the needs of the population for nutrients and energy. Various processes have demonstrated the potential of these microorganisms in the food, feed, cosmetics and pigment and additive production industries [15]. One of the most interesting reasons is that microalgae do not compete with food crops because they do not require arable land and can use wastes as nutrients for development [14].

Some of the health-enhancing ingredients contained in these microorganisms are carotenoids, fatty acids, dietary fibres, phenolic compounds, flavonoids and sterols [16]. The antioxidant, antimicrobial and antiviral properties of these bioactive compounds have been

widely observed in the literature [15] and today, there is increasing interest in the use of these antioxidants in foods, as they have been shown to have important beneficial effects on health [17].

1.2.1 Carotenoids

Carotenoids have been receiving increasing attention due to their potential health benefit and microalgae are recognized as a natural source [18]. They are a class of organic pigments from the group of isoprenoids, with the main chain of 40 carbon atoms. These compounds represent highly important pigments thanks to their numerous biological functions. They are fat-soluble and therefore, present high solubility in non-polar solvents [19]. The anti-oxidants astaxanthin, β-carotene, lutein, lycopene, and canthaxanthin are the major carotenoids of commercial value found in microalgae [18].

β-carotene is one of the main types of carotenes (a specific type of carotenoids which are completely composed by hydrocarbons and without oxygen within their structure) and it is mainly known for being a natural precursor of vitamin A. It is a high-molecular-weight compound that is formed by a hydrocarbon chain ($C_{40}H_{56}$). It is easily degradable by light, heat and air, and its colour can vary from yellow to dark red, depending on its pureness, source and location [20]. One of the main sources of this compound is the microalga *D. salina*, a unicellular green microalga that can produce and accumulate β-carotene in response to stress conditions. Up to 14 % of its dry body mass could be β-carotene, more than any other organism that produces the compound [21]. This microorganism produces β-carotene

in response to UV stress and localizes it to lipid droplets within its chloroplasts. In that location, it is able to absorb and neutralize the damaging oxygen radicals produced from excessive UV and sun exposure [22]. Figure 1.1 shows the structure of β-carotene.

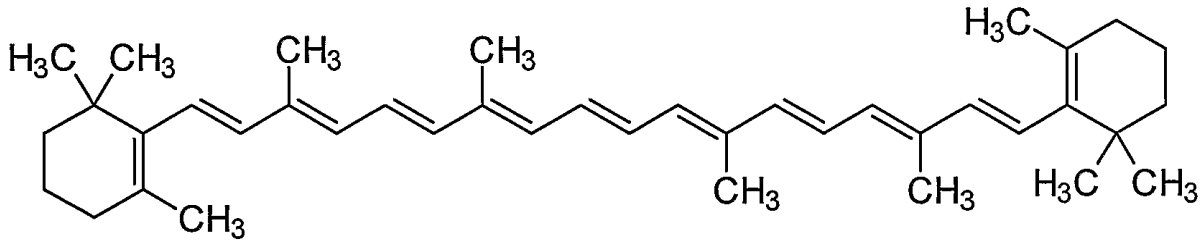

Figure 1.1. Structure of β-carotene.

The estimated global market size for β-carotene was valued at over € 375 million in 2015 and is likely to exceed € 440 million in 2023, growing at a CAGR of more than 3 % from 2016 to 2023. Europe β-carotene market size was the largest due to the presence of key countries such as France and Germany [23].

Astaxanthin (3,3′-dihydroxy-β,β′-carotene-4-dione), on the other hand, belongs to the xanthophyll family of carotenoids and the presence of a terminal hydroxyl and ketones in the ionone rings causes the esterification ability, antioxidant activity, and greater polar configuration of these compounds compared to other carotenoids. It is an oxycarotenoid with a molecular weight of 0.597 kg mol^{-1}; and its molecule is highly unsaturated and sensitive to high temperatures, light, and oxidative conditions [24]. Many studies have reported the high antioxidant capacity of astaxanthin, compared to other carotenoids, due to the presence of keto groups at the 4 and 4′ position and hydroxyl groups at the 3 and 3′ position in the β-

ionone ring [25]. More details about the structure of astaxanthin can be visualized in Figure 1.2.

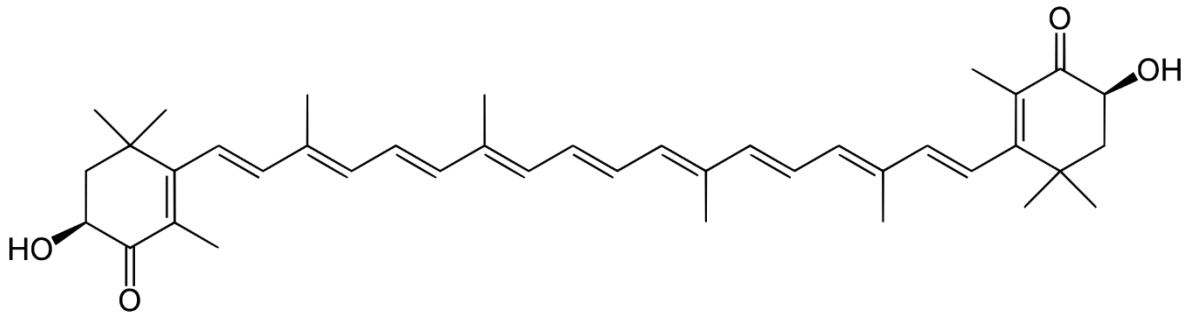

Figure 1.2. Structure of astaxanthin.

The astaxanthin market size was over € 485 million in 2017 and is estimated to exhibit over 4.8 % CAGR from 2018 to 2024 [26]. Recently, its application has gained popularity as a nutraceutical and a medicinal ingredient for the prevention and treatment of various diseases such as cancer [27], age-related macular degeneration [28], inflammation [29], *Helicobacter pylori* infection [29] and cardiovascular oxidative stress [30], as well as for general enhancement of immune responses [31].

The source of astaxanthin can be natural or synthetic. The synthetic comes from petrochemicals, whereas the natural is derived from marine microalgae, red yeast and many other plant and animal sources. However, it is mainly found in the microalgae *H. pluvialis*. Natural astaxanthin has been proven to be over 50 times stronger than synthetic astaxanthin in singlet oxygen quenching and approximately 20 times stronger in free radical elimination

[32]. Moreover, natural astaxanthin has been widely used over the last 15 years as a human nutraceutical supplement, after extensive safety data and several health benefits were established. Synthetic astaxanthin, which is synthesised from petrochemicals, has been used as a feed ingredient, primarily to pigment the flesh of salmonids. However, synthetic astaxanthin has never been demonstrated to be safe for use as a human nutraceutical supplement and has not been tested for health benefits in humans [32]. For this reason and considering that the objective of this thesis was to produce food-grade products, the astaxanthin used in this thesis (**Publication V**) came from vegetable and non-synthetic sources.

1.2.2 Fatty acids

Fatty acids are divided into two main groups according to their structural characteristics: saturated fatty acids (SFA) and unsaturated fatty acids (UFA). The latter, depending on their degree of unsaturation, can be classified as MUFAs and PUFAs. Depending on the position of the double bond, counting from the extreme carbon to the carboxylic functional group, MUFAs and PUFAs can be classified into three main series: omega-9 (ω-9) fatty acids (first double bond in carbon 9), omega-6 (ω-6) fatty acids (first double bond in carbon 6) and omega-3 (ω-3) fatty acids (first double bond in carbon 3) [33]. ω-9 fatty acids are not essential, because humans can introduce an unsaturation to an SFA in that position. In this way, oleic acid (C18:1 *cis*-9), for example, to which beneficial nutritional properties are attributed (as the main fatty acid in olive oil), does not need to be present in human diet. Even though, its consumption is recommended because, as well as

other ω-9 fatty acids, oleic acid helps to reduce the risk of heart diseases by raising levels of high-density lipoprotein and lowering low-density lipoprotein [34]. It is not the same with ω-3 and ω-6 fatty acids since our organism cannot introduce unsaturations in these positions. In this way, fatty acids such as linoleic (C18:2 *cis*-9,12) and α-linolenic acid (C18:3 *cis*-9,12,15) are essential; so our diet is required to contain them in well-determined proportions as their lack or imbalance in intake produces serious metabolic alterations [35].

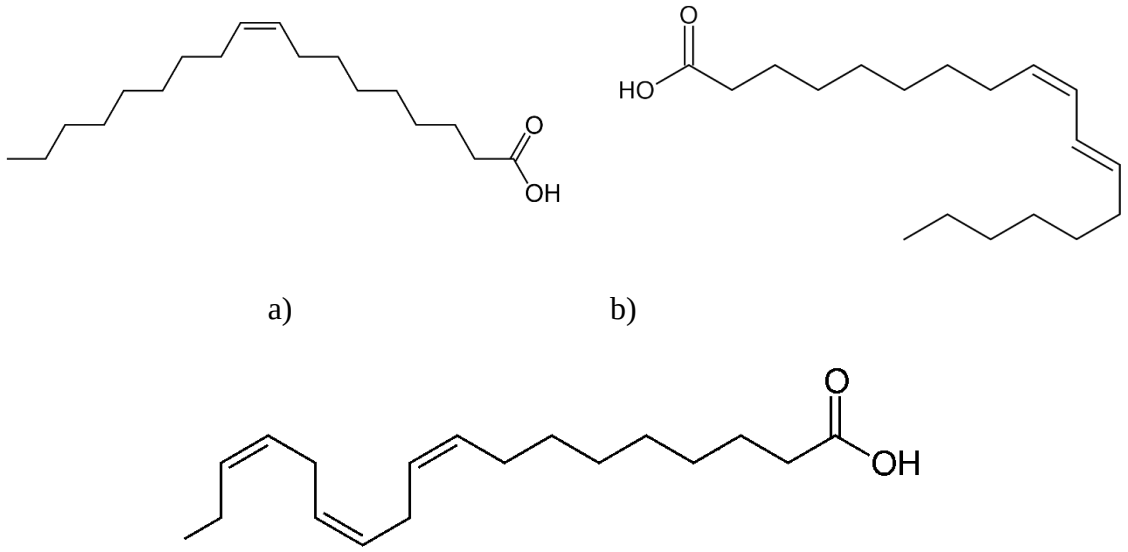

a) b)

c)

Figure 1.3. Structure of the fatty acids studied in this thesis: oleic (a), linoleic (b) and α-linolenic (c) acids.

Considering the above, there is a special interest in the extraction of these fatty acids from natural matrices; and the supercritical fluids (SCF), with the supercritical carbon dioxide (sc-CO_2) in particular, seem to be a suitable technology to achieve the above purpose

[36]. Regarding that, **Publication II**, aimed to predict the best cosolvents for the sc-CO_2 solubilisation of oleic and linoleic acids by using a theoretical approach; and **Publication III** validated this theory to choose the best supercritical mixture (SCM) to reach the selective supercritical fluid extraction of oleic (Figure 1.3a), linoleic (Figure 1.3b) and α-linolenic (Figure 1.3c) acids from *T. suecica*.

1.3 Bioactive compounds from agro-industrial residues

The intensification and globalization of agricultural production has led to a decrease in natural resources and an increase in the amount of waste generated. It is, therefore, necessary to manage these wastes, whose primary objective must be their use through environmentally friendly processes. Consequently, the worldwide concern about waste use has gained strength among the scientific community and at the industrial level, where by-product transformation processes may be useful for other activities and source of compounds of interest.

Olive tree cultivations, for example, have a long history in Mediterranean countries, and even today constitute important cultural, economic and environmental aspect of the area. Together with the production of extra virgin olive oil, large amounts of agricultural by-products are produced every year, causing significant environmental problems. Then, the olive oil production industry is an actual problem of waste generation on a global scale, and Spain, as the world's leading producer of olive oil, must deal with solutions that help to overcome these problems. Moreover, the problem of uncontrolled disposal of by-products to

the environment can be reduced by the exploitation and purification of their phenolic content [4].

1.3.1 Hydroxytyrosol-rich oil from by-products of the oil industry

The olive industry has been an important and traditional business in Mediterranean countries since antiquity. The rising interest in the consumption of olive oil as an integral ingredient of the Mediterranean diet has increased the importance of the olive oil sector in the last decades [37]. In 2017/18 period, world production of olive oil was roughly 2.854.000 tonnes; and Spain, the biggest producer worldwide, produced 1.150.000 tonnes (more than 40 % of world production) and production is likely to continue increasing because of the substantial increment recorded in olive tree cultivation [38].

Until the nineties, the olive oil production process was based on the so-called three-phase system, which produced three streams: pure olive oil, a watery liquid called *alpechín* and a solid cake called orujo or olive cake. To eliminate the *alpechín*, which represented a serious environmental problem, a new process technology with only two effluent streams (olive oil and alperujo) emerged, saving both water and energy compared with the three-phase system. Moreover, the wet solid stream or alperujo contains all the substances that in the three-phase system were contained in the *alpechín* and in the olive cake and it still has a significant oil content [39]. In Figure 1.4 a comparison of the three and two-phase centrifugation systems for olive oil extraction can be seen.

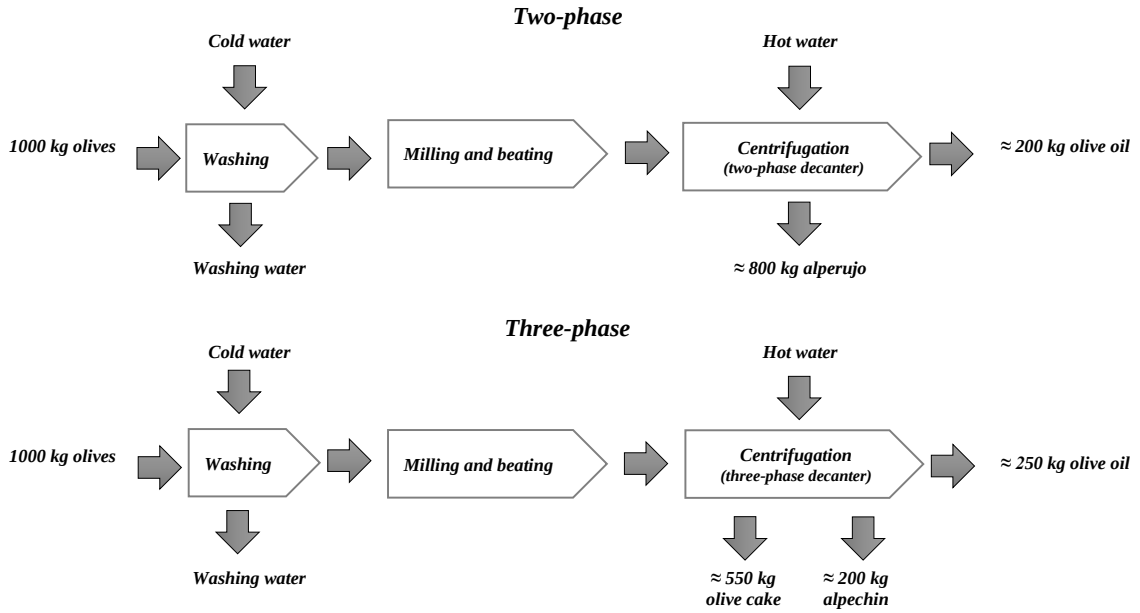

Figure 1.4. The three and two-phase centrifugation systems for olive oil extraction.

During the olive oil mechanical process, the major proportion of the phenolic compounds is found in the aqueous phase, while only a minor percentage (< 1 % in mass fraction) is in the olive oil. This explains why the most phenols (about 98 % in mass fraction) remain in the alperujo, with a higher concentration than in the residues obtained by the three-phase mode and 10 to 100-fold higher than that of olive oil. However, the production of olive oil in Spain with the new two-phase system centrifugation system is estimated to represent about 80 % of the total and the system is used by roughly 90 % of olive-mills [40]. The previous means that the yearly production of this by-product from the whole Spanish olive oil industry may approach 4.600.000 tonnes [41]; then the alperujo represents a serious environmental problem, and could be used as a source of bioactive compounds taking into

account that alperujo seems to be an affordable and abundant source of natural antioxidants and interesting compounds, hydroxytyrosol among the most important ones [42].

Regarding that, hydroxytyrosol is an amphipathic phenol with a phenyl ethyl-alcohol structure, as can be seen in Figure 1.5. It is also called 3,4-dihydroxyphenylethanol, 3,4-dihydroxyphenolethanol or 4-(2-Hydroxyethyl)-1,2-benzenediol by the International Union of Pure and Applied Chemistry (IUPAC) system [43]. It is one of the major phenolic compounds present in the olive fruit and has been pinpointed as being of most interest, because of its remarkable pharmacological and antioxidant activity [42]. The origin of hydroxytyrosol is the hydrolysis of oleuropein which happens during the ripening of the olives and during the storage and elaboration of table olives [44]. Many studies have demonstrated the antioxidant, antimicrobial, anti-inflammatory and antiatherogenic effects of hydroxytyrosol contained in different types of olive oils, enriched or not with this compound. Thanks to all those findings, hydroxytyrosol has been postulated as a nutraceutical for preventing and treating different diseases [43].

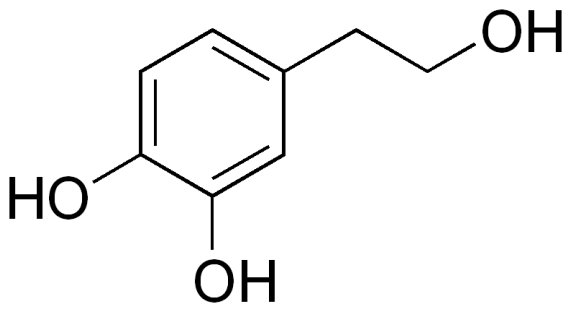

Figure 1.5. Structure of hydroxytyrosol.

Several methods and systems have been developed to obtain hydroxytyrosol-rich extracts from olives and their by-products, as well as from olive leaves. In most cases, solvent extraction techniques [45], ultrafiltration [46], reverse osmosis [47] and evaporation [37] are used. Nonetheless, these all involve several steps, organic solvents and even low yields. Because of that SCF, and in particular sc-CO_2, could be offered as a suitable organic solvent-free tool to achieve a selective extraction of this type of oil rich in active compounds. Regarding that, **Publication I** dealt with the selective sc-CO_2 extraction of hydroxytyrosol-rich olive oil from alperujo.

1.4 Supercritical carbon dioxide extraction as an effective green technology

The bioactive compounds involved in this research work have been commonly extracted using organic solvents or mechanical techniques. The organic solvent extraction gives better extraction yield, but the technique requires solvent recovery through distillation which may degrade thermally labile compounds. Moreover, the organic solvent extraction is non-selective and achieves the simultaneous removal of non-volatile pigments and waxes, resulting in viscous, dark-coloured extracts contaminated with solvent residues. This makes them difficult to handle without further refinement and may even dictate the future commercial viability of the oil extract. Furthermore, the presence of traces of residual solvent in the final product makes the process less attractive [48]. This increasing awareness towards the environmental and health issues that derive from the use of these substances has led to the implementation of stronger regulations. In this regard, the use of SCF has become an environmentally friendly alternative.

SCF are those gases and liquids at temperatures and pressures above their critical points (T_C – critical temperature; P_C – critical pressure), as can be seen in Figure 1.6. They have properties between those of a gas and a liquid i.e., higher diffusivity than gases and lower viscosity than liquids, which facilitates mass transfer [49]. Furthermore, they have density values that enable appreciable solvation power. Also, they are highly compressible, particularly near the critical point, and their density, and thus the solvation power, can be carefully controlled by small changes in temperature and/or pressure [50].

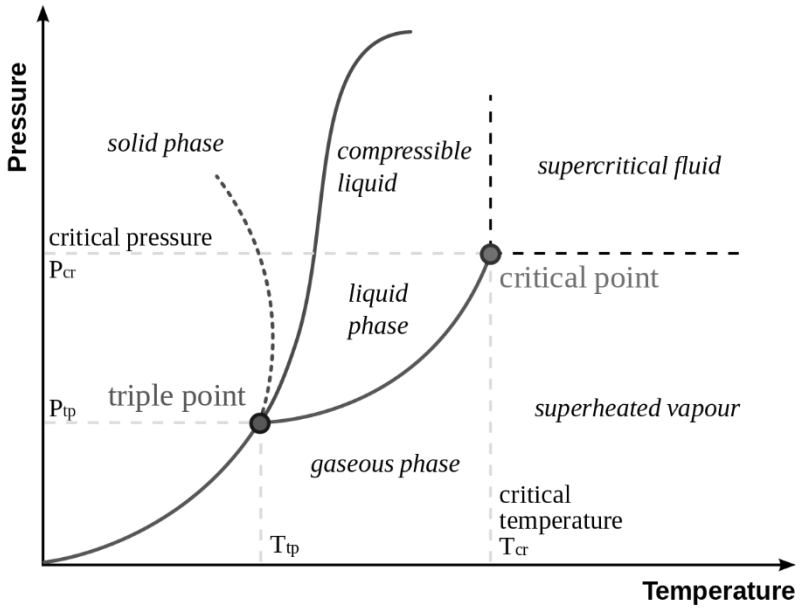

Figure 1.6. Definition of supercritical fluid state for a pure component.

All gases and liquids are able to form SCF above specific sets of critical conditions, although extremely high temperatures and/or pressures may be required. However, among

all the possibilities, sc-CO_2 is by far the most used SCF for supercritical fluid extractions because of its low T_C and P_C (304.13 K and 7.38 MPa, respectively). Moreover, sc-CO_2 has become an alternative solvent for oil extraction from microalgae and plants matrices, because it can achieve good oil yield with respect to the conventional organic solvent extraction, with better product quality and offering the possibility of obtaining a product without the presence of traces of residual solvent in the final product, which makes the process attractive from the health and environmental point of view [51].

In addition, sc-CO_2 is essentially non-toxic, non-flammable, non-corrosive, inexpensive at the industrial level, readily available in large quantities with high purity, totally dissipated from extracts at atmospheric pressure avoiding the necessity of further expensive and harmful refining treatments, can be recycled, and as said before has easily accessible supercritical conditions [49]. In fact, a significant number of reviews regarding supercritical fluid extractions of extracts rich in interesting compounds from vegetable matrices are available in the literature. Some examples are the reviews published by Melo *et al.,* [52], Sahena *et al.,* [53], Reverchon and De Marco [54], da Silva et al., [55], and Pereira and Meireles [56]. Some others have published reviews about obtaining bioactive compounds from microalgae [15,57–61] and other works have dealt with the extraction of these compounds from residues of the olive industry [62–64].

The sc-CO_2 extraction is an important industrial process, enabled by overcoming the poor solvent nature of CO_2 through the addition of entrainers. Basically sc-CO_2 is the perfect solvent to extract neutral lipids from natural matrices [65]; however, its disadvantage is its

lack of polarity for the extraction of polar analytes, and for that reason, a cosolvent (modifier or entrainer) should be sometimes added to a supercritical gas in order to: increase the solubility of a specific compound, increase separation factor and reduce operating pressure and CO_2 consumption [66]. In order to achieve so, the cosolvent changes some characteristics of the main supercritical solvent such as polarity, specific interactions with the solute or interaction with the active sites of the solid matrix [67]. However, the selection of the best cosolvent requires long and expensive experimental effort.

1.5 Increasing selectivity of supercritical carbon dioxide extraction by using the Hansen solubility approach

Miscibility assessments of bioactive compounds should be performed at supercritical conditions in order to optimize the extraction conditions. However, these evaluations at such extreme temperatures and pressures represent economical and practical difficulties. For that reason, theoretical estimations are implemented. As an example, the Hansen solubility theory (HST) has already been demonstrated to be a useful tool for this sort of evaluations [68,69].

The solubility parameter (δ) was initially introduced by Hildebrand [70] and it offered a numerical estimation of the level of interaction between two materials. This numerical estimation was known as the Hildebrand solubility parameter (δ). Thus, materials with similar δ are more likely to be miscible with each other. However, the solubility parameter proposed by Hildebrand was limited to solutions with low interactions with the solute and did not consider association between molecules; for that reason, Hildebrand´s work dealt

with a theory where the assumptions were not directly applicable to the real world: hydrogen bonding and polar solvents were not included since the theory was based on the behaviour of hydrocarbon solvents. As such Hildebrand was dealing with abstract entities rather than real-world solvents. The assumptions behind the theory were therefore very restrictive [71].

For that reason, Hansen [72] proposed in 1967 the division of δ into three components: dispersion (δ_d), polar (δ_p) and hydrogen bonding forces (δ_h) later on, known as Hansen solubility parameters (HSP) [73]. From then on, HSP found many applications, from academic laboratories to industrial facilities to judge miscibility of mainly polymers, but also of biopolymers, pharmaceuticals, pigments, colourants and some biological materials in different solvents. Some of these applications could be found in Hansen's handbook [73]. The utility of the Hansen approach for the selection of cosolvents to increase the selectivity of sc-CO_2 extraction of specific compounds was investigated in this thesis (**Publications II**, **III** and **IV**).

Hildebrand initially introduced δ as the square root of cohesive energy density, which could be calculated from the total cohesion energy or latent heat of vaporization of a fluid (E) and the molar volume (V) of the involved fluid, such as it is described in Equation (1.1).

$$\delta = \sqrt{\left(\frac{E}{V}\right)} \tag{1.1}$$

In the three-parameter Hansen approach, E can be obtained as the sum of three contributions (Equation 1.2): the non-polar atomic (dispersion) interactions, E_d, permanent dipole-permanent dipole interactions, E_p, and the hydrogen bonding interactions, E_h. E can be experimentally measured by determining the energy required to evaporate the liquid (Equation 1.3).

$$E = E_d + E_p + E_h \quad (1.2)$$

$$E = \Delta H - RT \quad (1.3)$$

ΔH is the latent heat of vaporization, R is the universal gas constant, and T is the absolute temperature. Dividing Equation (1.2) by the molar volume, V, the respective Hansen cohesion energy parameters (Equation 1.4) are obtained.

$$\frac{E}{V} = \left(\frac{E_d}{V}\right) + \left(\frac{E_p}{V}\right) + \left(\frac{E_h}{V}\right) \quad (1.4)$$

Taking into account that δ is defined by Equation (1.1), the total Hansen solubility parameter (δ_T) will be the square root of a sum of each Hansen component squared, including the dispersion (δ_d), polar (δ_p) and hydrogen bonding (δ_h) contributions (Equation 1.5). The International System of Units (SI) used in this work for HSP were $MPa^{1/2}$, which are 2.0455 times larger than the older Hildebrand units of $(cal\ cc^{-1})^{1/2}$.

$$\delta_T = \sqrt{\delta_d^2 + \delta_p^2 + \delta_h^2} \quad (1.5)$$

Moreover, miscibility judgments can be performed by using the Hansen sphere as shown in Figure 1.7. For this purpose, a group of solvents with known HSP is used to test their capabilities to solubilize a target compound. The internal part of the sphere is constituted by every solvent that dilutes the compounds of interest, also called the target compound. These solvents can be appreciated in Figure 1.7 as white circles. The ones that are not able to dilute the target compound can be found outside the sphere (black circles in Figure 1.7). The centre of the sphere corresponds to the three-dimensional HSP coordinates of the target compound (δ_{d1}, δ_{p1} and δ_{h1}). The radius is defined by the largest distance between the coordinates of the target compound and those of the solvent (δ_{d2}, δ_{p2} and δ_{h2}) that dilutes the solute at the limit of the sphere. As can be seen in Figure 1.7, this radius is known as R_0 and is only related to the target compound. In Figure 1.7 can also be seen that the distance between coordinates of the target compound or centre of mass of the Hansen sphere and those of the solvent is represented by R_a and can be calculated by Equation (1.6). In this thesis (**Publications II**, **III** and **IV**), the energy difference (R_a) between the solubility parameters of the target compound and the SCF (sc-CO_2 and SCM) was the parameter calculated to evaluate their miscibility. The smaller the value of R_a, the larger the miscibility between the compound and the solvent (SCF in this case).

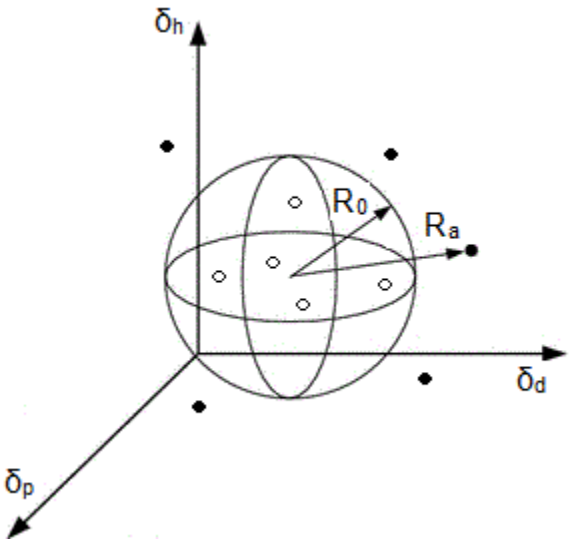

Figure 1.7. Representation of the Hansen sphere and its components.

$$R_a = \sqrt{4(\delta_{d1} - \delta_{d2})^2 + (\delta_{p1} - \delta_{p2})^2 + (\delta_{h1} - \delta_{h2})^2} \quad (1.6)$$

1.6 Encapsulation of bioactive compounds

Products containing bioactive compounds such as the ones dealt in this thesis could help to cover the nutritional necessities of society in terms of health and well-being. However, these products do not provide the expected health benefits because of their low chemical or biochemical stability and their high reactivity, failing their biological functionality and bioavailability [74]. Therefore, the development of functional foods, cosmetics or drugs through the addition of bioactive compounds holds many technological challenges.

Several scientists and researchers have been drawing attention to the exploitation of nanostructures as carriers for controlling the release of these compounds in specific times and sites of the human body. As a response to these demands, it has been suggested to encapsulate these compounds into micro- and nanometric sizes, which in turn isolates and protects them from the external environment [75]. This procedure is called microencapsulation and is the technology of packaging a solid, liquid or gaseous material in small capsules that release their contents at controlled rates over prolonged periods of time [76]. Due to their versatility, such technologies are of significant interest to the food and pharmaceutical sector.

Among the various delivery systems available, biopolymer-based micro and nanocarriers can be designed to transport the bioactive compound to a specific site of action with minimal degradation [77]. About this, recently there has been an increasing interest in the development of efficient food-grade nanocarrier systems for encapsulation, protection and target delivery of nutraceuticals, pharmaceuticals or bioactive compounds to enhance their bioavailability or stability. As an answer to the attempts to obtain food-grade micro and nanocarriers, the starch ethyl cellulose has been recently proposed. Ethyl cellulose is an inert hydrophobic polymer and its properties such as lack of toxicity, stability during storage [78] and permitted status as a food additive in the European Union as E 462 [79] make it suitable for designing sustained matrices.

On the other hand, several techniques have been developed and investigated by scientists throughout the years for the production of capsules for food and pharma

applications; from coacervation to solvent evaporation and spray-drying [75]. However, these traditional techniques usually do not allow to produce particles with a narrow and controlled size distribution as needed; and for that reason, SCF-based techniques represented an interesting chance to meet all the required process characteristics gaining the attention of researchers [50].

1.6.1 Supercritical Fluid Extraction of Emulsions (SFEE)

The unique thermodynamic and fluid-dynamic properties of SCF can be used for the formation of micro and nanocarriers. The lower viscosity and the higher diffusivity of SCF with respect to liquid solvents improve the mass transfer, that is often a limiting factor for particles formation and particle design processes. Due to these favourable properties, SCF and mainly sc-CO_2, are currently proposed [80]. Rapid expansion of a supercritical solution (RESS) [81] and its variations [82], supercritical antisolvent precipitation (SAS) [83], supercritical assisted atomization (SAA) [84], solution enhanced dispersion by supercritical fluids (SEDS) [85], and supercritical solvent impregnation (SSI) [86] have been used so far for encapsulation purposes. However, the principal shortcoming of all these methods lies in the lack of particle size control, being difficult to produce particles below the micrometric range and the lack of control of the morphology (shape and structure) [87].

To overcome these drawbacks, and to fabricate micro/nanocarriers with a low content of solvents, the Supercritical Fluid Extraction of Emulsion (SFEE) technology [88], also known as Supercritical Emulsion Extraction (SEE) [89], has been recently proposed. The

basis of this method relies on the use of sc-CO_2 to rapidly extract the organic phase from an oil-in-water (O/W) emulsion, in which a polymer has been previously dissolved. A bioactive compound could be dissolved in the organic phase, allowing its encapsulation. By removing the solvent, both materials precipitate in water, generating micro/nanocapsules with core-shell structure [90,91] or aggregates, depending on the material. The produced particles have a controlled size and morphology, due to the fast kinetics of the organic phase extraction through the use of sc-CO_2 [88].

Additionally, this technology can be performed in a continuous layout, using a high-pressure packed tower for the emulsion/sc-CO_2 contact in counter-current mode, avoiding the problems linked to the batch process, such as reproducibility and reduction of the process yield [92].

Finally, bearing in mind that the dispersed phase of the emulsion acts as a template for the particles to be produced by SFEE, special attention must be paid to the emulsion formulation, as it is on this basis that the future drop size is designed, and hence its structure and stability [90]. Considering the above, the initial emulsion formulation is the starting point of the SFEE process and for this reason, attention was given to the selection of components and composition in the emulsion formulations involved in this work (see **Publication V**). Moreover, emulsion rheology strongly relies on the droplet size of the dispersed phase; and for that reason, the influence of the viscosity of the organic phase on the final particle size was also studied (see **Publication V**).

2. Objectives

The main objective of this research thesis was to selectively obtain, from microalgae and an agro-industrial residue, high quality oil extracts rich in bioactive compounds of considerable nutritional interest by sc-CO_2 extraction; and subsequently to explore the potential of the SFEE technology, operating in a continuous layout, to nanoencapsulate the obtained active compounds, looking for pharmaceutical and food applications.

First of all, the process parameters and solid conditions that affected the sc-CO_2 extraction of hydroxytyrosol-rich oil extracts from alperujo were optimised. This was done to extend this optimization and study of these variables to supercritical fluid extractions from microalgae. On the other hand, to achieve the selective extraction of the compounds, the prediction of the best cosolvents for sc-CO_2 by using the Hansen approach was carried out. The calculations were made with several organic cosolvents, using a 5 % volume fraction to ensure a supercritical homogeneous mixture. β-carotene and oleic, linoleic and α-linolenic acids as examples of valuable carotenoids and fatty acids, respectively, were used as target compounds from microalgae. The order of the cosolvent ability was deduced based on minima R_a values in a wide range of operating conditions suitable for supercritical extraction. These predictions were first validated with equilibrium data measured by the static method in a variable volume view cell. Afterwards, the estimations were tested against extraction yields of β-carotene from *D. salina* and oleic, linoleic and α-linolenic acids from *T. suecica*.

Finally, an Erasmus research stay at the University of Salerno (Italy) was carried out to investigate the effectiveness of the SFEE technology in a continuous layout for the encapsulation of astaxanthin in ethyl cellulose. Astaxanthin, a compound in the current

research focus for its wide range of nutritional properties, was selected as a model carotenoid from microalgae. Ethyl cellulose, for its part, was chosen as covering polymer due to due to its approval as a food additive. Moreover, ethyl acetate and Tween 80 were used as the organic solvent of the emulsions and surfactant respectively, since both are approved by the Food and Drug Administration (FDA) [93]. Additionally, the antioxidant capacity of the elaborated particles and the astaxanthin release behaviour in simulated intestinal fluid (SIF) were investigated.

3. Materials and methods

The most important experimental and computational procedures used in the methodological section of this doctoral thesis are detailed below. These were described in a general way, and practical details may be found in the publications contained in the Appendices.

*3.1 Materials and reagents (**All Publications**)*

Table 3.1 shows the specifications of the raw materials subjected to supercritical fluid extractions. Both *D. salina* and *T. suecica* were used freeze-dried, as received from the supplier. The addition of sea-sand prevented the material bed compaction avoiding the formation of preferential channels that reduced the extraction yield. No sea-sand was used in the case of supercritical fluid extraction from *T. suecica* due to the low extract content in this microalgae (see Table 3.1). The particle sizes showed in Table 3.1 were obtained on Tyler series sieves. The total extract content was assessed by Soxhlet with n-hexane as organic solvent and the oil extraction yield with sc-CO_2 was reported at the most favourable conditions. The percentage of extract is reported on a dry basis of the vegetable material.

Finally, Table 3.2 shows the suppliers and purities of all the materials and reagents used in this thesis. These were used as received. The distilled water used was self-supplied.

Table 3.1. Specifications of the raw materials subjected to supercritical extraction

Raw material	**Particle size (µm)**	**Water content (%)**	**Total extract (%)***	**sc-CO_2 oil extraction yield (%)**	**Supplier**
Alperujo	100 - 1000	70	14	13.0	Natac Biotech
Dunaliella salina	45	6	21	6.4	Algalimento
Tetraselmis suecica	45	6	3	1.5	Algalimento

* Expressed on dry basis (d.b.)

Table 3.2. Materials and reagents used together with their suppliers.

Materials and reagents	**Supplier**	**Specifications**
(±)-6-hydroxy-2,5,7,8-tetramethylchromane-2-carboxylic acid (Trolox)	Sigma-Aldrich	≥ 0.97 kg kg^{-1}
1,1-diphenyl-2-picrylhydrazyl (DPPH)	Alfa Aesar™	≥ 0.98 kg kg^{-1}
Acetic acid solution	Sigma-Aldrich	for HPLC
Acetone	Sigma-Aldrich	≥ 0.999 kg kg^{-1}
Astaxanthin	Sigma-Aldrich	≥ 0.98 kg kg^{-1}

Materials and reagents	Supplier	Specifications
Benzene	Panreac	≥ 0.99 kg kg^{-1}
Boron trifluoride (BF_3)	ACROS Organics™	1.5 M in methanol
Butylated hydroxytoluene	Sigma-Aldrich	≥ 0.99 kg kg^{-1}
Butylated hydroxytoluene	Sigma-Aldrich	≥ 0.99 kg kg^{-1}
Carbon dioxide (CO_2)	Air Products	≥ 0.9998 kg kg^{-1}
Cyclohexane	Sigma-Aldrich	≥ 0.995 kg kg^{-1}
Diethyl ether	Sigma-Aldrich	≥ 0.997 kg kg^{-1}
Ethanol	Fisher Chemical	≥ 0.998 kg kg^{-1}
Ethyl acetate	Sigma-Aldrich	≥ 0.999 kg kg^{-1}
Ethyl cellulose	Sigma-Aldrich	Viscosity 100 cps in solution 40/40 toluene/ethanol, 455 kDa
Fatty acid methyl esters (FAMEs)	Sigma-Aldrich	FAME Mix C8 - C22
Folin-Ciocalteu reagent	Sigma-Aldrich	2 M with respect to acid
Gallic acid	ACROS Organics™	Monohydrate

Materials and reagents	Supplier	Specifications
Helium (He)	Air Liquide	≥ 0.9999 kg kg-1
Heptadecanoic acid	Sigma-Aldrich	≥ 0.98 kg kg^{-1}
Hydrogen (H)	Air Liquide	≥ 0.9999 kg kg^{-1}
Linoleic acid	Sigma-Aldrich	≥ 0.99 kg kg^{-1}
Methanol	Sigma-Aldrich	≥ 0.999 kg kg^{-1}
n-Hexane	Sigma-Aldrich	≥ 0.99 kg kg^{-1}
Nitrogen (N_2)	Air Liquide	≥ 0.9999 kg kg^{-1}
Oleic acid	Sigma-Aldrich	≥ 0.99 kg kg^{-1}
Potassium di-hydrogen phosphate (KH_2PO_4)	Panreac	≥ 0.99 kg kg^{-1}
Sea-sand	Sigma-Aldrich	0.315 mm - 1 mm, ≥ 0.90 kg kg^{-1}
Sodium chloride (NaCl)	Sigma-Aldrich	≥ 0.995 kg kg^{-1}
Sodium hydroxide (NaOH)	Sigma-Aldrich	≥ 0.98 kg kg^{-1}, pellets anhydrous
Sodium sulphate anhydrous (Na_2SO_4)	Sigma-Aldrich	United States Pharmacopeia (USP) Reference Standard

Materials and reagents	**Supplier**	**Specifications**
Sulfuric acid (H_2SO_4)	Sigma-Aldrich	0.95 kg kg^{-1}
Toluene	Merck	≥ 0.995 kg kg^{-1}
Tween 80	Sigma-Aldrich	Polyoxyethylene (20) sorbitan monooleate
α-Linolenic acid	ACROS Organics™	≥ 0.99 kg kg^{-1}
β-carotene	Sigma-Aldrich	≥ 0.97 kg kg^{-1}

*3.2 Supercritical fluid extractions (**Publications I**, **III** and **IV**)*

Supercritical fluid extractions were done in a homemade semi-continuous flow apparatus that consisted of a CO_2 feeding line and a 316 stainless-steel vessel. Table 3.3 shows the geometrical characteristics of the cylindrical extraction vessel used and Figure 3.1 shows a schematic representation of the experimental installation for supercritical extractions. Operating conditions are described in each publication.

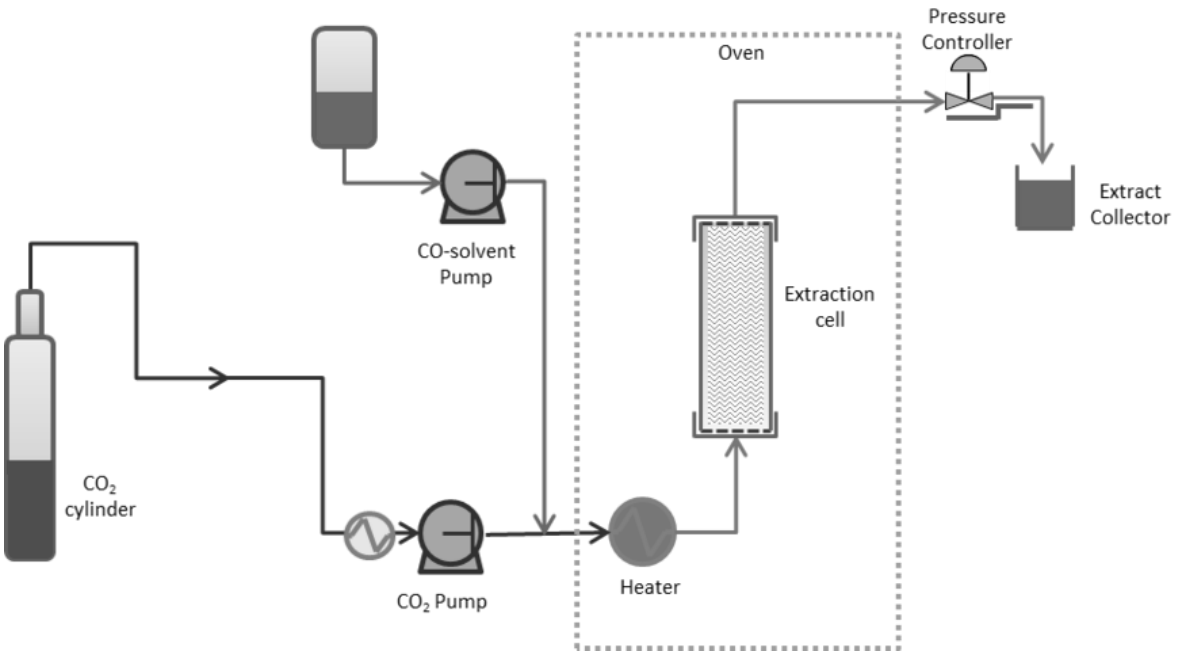

Figure 3.1. Schematic representation of the experimental installation used for supercritical fluid extractions.

Table 3.3. Geometrical characteristics of the cylindrical extraction vessel used.

Characteristic	Value
Internal diameter (m)	0.025
Length (m)	0.170
L/D ratio	6.8
Cross-flow area (m^2)	0.00049
Volume (m^3)	0.00008

A high purity CO_2 was used to reduce the oxygen concentration, which could degrade the activity of the desired bioactive compounds during the extraction [94]. Moreover, the air from all pipes and valves and from the extractor was purged before experiments. A heating jacket was placed around the extractor to control the temperature inside (within ± 0.5 K). Two membrane pumps (Milroyal D; Dosapro Milton Roy, Spain) connected in parallel were used to pump the CO_2 and the cosolvent (when used) up to the extraction pressure. The pump for the CO_2 had an attached chamber in which a cooling fluid flowed to avoid the CO_2 cavitation during pumping. The CO_2 flow rate was measured in the mass-flow meter (M-10 SLPM-D, Alicat Scientific, USA) placed at the end of the line, while pressure was controlled by a back-pressure regulator (within ± 0.5 MPa, BPR, 26-1761-24-161, TESCOM Europe, Germany).

The amount and the way in which the raw material was introduced into the extractor is described in **Publications I**, **III** and **IV**; however, in general, the solid material was

deposited with a spatula in the extraction vessel forming a fixed bed. Alperujo and *D. salina* were mixed with sea-sand. The use of sea-sand enhanced the bed porosity and prevented the material bed compaction avoiding the formation of preferential channels that reduced the extraction yield. In the case of *D. salina*, for example, at 20 MPa and 318.2 K, by using sea-sand as packing material there was an increase of approximately 76 % carotenoid extraction compared to the bed without sea-sand. Furthermore, no adsorption of the extracts on the sea sand particles was observed. No sea-sand was used in the case *T. suecica* due to its low initial extract content. Table 3.4 shows the amount of raw materials and the geometry of the fixed bed formed in the cylindrical extraction vessel used in this work.

Table 3.4. Characteristics of the fixed bed formed by the raw materials subjected to supercritical fluid extraction

Raw material	**Mass loaded (kg)**	**Sand loaded (kg)**	**Bed bulk density (kg m^{-3})**	**Bed length (L, m)**	**Bed diameter (D, m)**	**L/D**
Alperujo	0.024	0.020	899	0.100	0.025	4.0
Dunaliella salina	0.010	0.016	1158	0.046	0.025	1.8
Tetraselmis suecica	0.014	-	609	0.100	0.025	4.0

A wire mesh was placed on top of the bed to prevent particles' entrainment. The extractor was then closed, and the fluid (or the fluid mixture when used) was pumped in to achieve the working conditions. After that, the BPR was opened to provide a continuous flow

of the fluid through the bed. After the BPR, the fluid was depressurized, the solvent power of the SCF dropped, and the extract was precipitated in a previously weighed glass flask. Samples were collected at the required time (see details in each publication). When a cosolvent was used, this one was removed from the extract with a nitrogen stream after the extraction process was completed. The extraction curves were constructed by plotting the extraction yield based on the total biomass loaded in the extractor *versus* the solvent ratio that passed through the bed (kg CO_2 kg solid material^{-1}) at constant intervals of time.

The results shown are the average of at least two measurements. The experimental standard deviations were deduced from selected tests that were repeated six times. These values and the appearance of the oil extracts are described in each publication.

*3.3 Hansen approach for the selective extraction of bioactive compounds (**Publications II**, **III** and **IV**)*

As it has been indicated in previous sections, this thesis implemented computational procedures in order to choose the best cosolvents to increase the selectivity of sc-CO_2. Here, the way in which these methodologies were implemented is described in general terms. The target compound and cosolvents used are described in each publication. All HSP calculations were done with Microsoft Excel.

3.3.1 Hansen solubility parameters of target compounds

There was not enough data in the literature regarding the physical properties and solubility parameters of the solute-solvent pairs studied in this research thesis. Consequently, the HSP at normal temperature and pressure (NTP, assumed as 298.2 K and 0.1 MPa) of the fatty acids (oleic, linoleic and α-linoleic acid) and β-carotene from the dispersion, polar and H-bonding forces were calculated by using the group contribution method (GCM) proposed by Hansen [73]. Figure 1.1, Figure 1.2, Figure 1.3a, Figure 1.3b and Figure 1.3c show the structures used to perform this procedure.

On the other hand, the influence of temperature on the HSP values of the target compounds was calculated by using the Jayasri and Yaseen method [95] described by Equation (3.1). Working below the critical points of the target compounds, pressure does not exert a considerable influence on their HSP [96]; therefore, this influence was not considered. In Equation (3.1) T_r is the reduced temperature at temperatures 1 (298.2 K) and 2 (desired temperature). The critical temperatures required in Equation (3.1) were obtained by using the GCM proposed by Joback [97]. This technique is a modification of the Lydersen method [98] and is the best method to use overall to predict the critical temperature. For this, the Aspen Plus V 10.0 software was used [99].

$$\frac{\delta_2}{\delta_1} = \left(\frac{1 - T_{r2}}{1 - T_{r1}}\right)^{0.34} \tag{3.1}$$

3.3.2 Hansen solubility parameters of solvents

Estimations of miscibility order of the target compounds in CO_2 and its mixtures with a volume fraction of 5 % cosolvent were done. Predictions were performed with several organic solvents used in the manufacture of food [100] and pharmaceutical products [101]. As a general rule, the thermodynamic properties required in the HST of these solvents must have been well predicted by the Reference Fluid Properties (REFPROP) model from the National Institute of Standards and Technology (NIST). Water was not preselected as a cosolvent since a mixture of sc-CO_2 with a volume fraction of 5 % water was not a homogeneous supercritical phase at the operating conditions tested. Besides, based on our experience, water forms emulsions with oily extracts, hampering the extraction.

First, the influence of temperature and pressure on δ_T and the individual HSP of CO_2 and the organic solvents were calculated by using Equations (3.2), (3.3) and (3.4) as a function of V (which include temperature and pressure influence). In these equations, subscript "ref" refers to HSP and V of the fluid at NTP. These reference solubility parameters values for CO_2 and the cosolvents at NTP were obtained from the Hansen Handbook [73]; while V as a function of the temperature and pressure studied (specified in each publication) were calculated by using REFPROP model from NIST, with help of the Aspen Plus V 10.0 software [99].

$$\frac{\delta_{d\ ref}}{\delta_d} = \left(\frac{V_{ref}}{V}\right)^{-1.25} \tag{3.2}$$

$$\frac{\delta_{p\ ref}}{\delta_P} = \left(\frac{V_{ref}}{V}\right)^{-0.5} \tag{3.3}$$

$$\frac{\delta_{h\ ref}}{\delta_h} = \exp\left[-1.32\ x\ 10^{-3}(T_{ref} - T) - \ln\left(\frac{V_{ref}}{V}\right)^{-0.5}\right] \tag{3.4}$$

Table 3.5 shows the critical properties, reference values and the valid temperature and pressure range limits of the REFPROP property method used for the molar volume calculation. Critical points were obtained from the NIST database with the help of the Aspen Plus V 10.0 software [99] and reference values from the Hansen Handbook [73]. As can be seen in Table 3.5, the REFPROP property method was valid within the range of conditions evaluated in this work for all the used solvents. Finally, for the mixtures consisting of sc-CO_2 and the cosolvent, the solubility parameters were determined with a linear blend rule, given by Equation (3.5). The total HSP value of the mixture was equal to the sum of the product of the respective volume fractions (v_i) of the components present in the mixture, and their corresponding HSP value (δ_i). In Equation (3.5), the word "any," used as a subscript, refers to any solubility parameter (δ_d, δ_p, δ_h or δ_T).

$$\delta_{any} = \sum\{v_i . \delta_i\} \tag{3.5}$$

Table 3.5. Critical temperature (T_C) and pressure (P_C); reference molar volume (V_{ref}); reference values of dispersion ($\delta_{d\ ref}$), polar ($\delta_{p\ ref}$) and hydrogen-bonding ($\delta_{h\ ref}$) contributions, and limits of the REFPROP model for the used solvents.

Solvent	**T_C**	**P_C**	**Limits of the model**	**$\delta_{d\ ref}$**	**$\delta_{p\ ref}$**	**$\delta_{h\ ref}$**	**V_{ref}**
	K	**MPa**		**$MPa^{1/2}$**	**$MPa^{1/2}$**	**$MPa^{1/2}$**	**$10^6\ m^3\ mol^{-1}$**
CO_2	304.13	7.38	(217 -2000) K, 800 MPa	15.6	5.2	5.8	39.1
Acetone	508.07	4.70	(179 – 550) K, 700 MPa	15.5	10.4	7.0	74.0
Benzene	562.02	4.89	(279 – 635) K, 78 MPa	18.4	0.0	2.0	89.4
Cyclohexane	553.4	4.07	(279 – 700) K, 80 MPa	16.8	0.0	0.2	108.8
Diethyl ether	466.78	3.65	(270 – 500) K, 40 MPa	14.5	2.9	5.1	104.8
Ethanol	514.57	6.23	(250 – 650) K, 280 MPa	15.8	8.8	19.4	58.5
n-Hexane	507.55	3.03	(178 – 600) K, 100 MPa	14.9	0.0	0.0	131.6
Methanol	512.68	7.95	(176 – 620) K, 800 MPa	15.1	12.3	22.3	40.7
Toluene	591.89	4.13	(178 – 700) K, 500 MPa	18.0	1.4	2.0	106.8

3.3.3 Miscibility predictions for the selection of the best cosolvent

The miscibility order of the target compounds in sc-CO_2 and its SCM was predicted by using the R_a parameter described in Equation (3.6). The smaller the R_a value of the supercritical solvent, the more the miscibility of the target compound. Consequently, and according to the Hansen theory, supercritical systems with lowest R_a would represent the most suitable one.

In addition to the above, the miscibility enhancement was predicted. For this, this concept was defined as the percentage reduction of the R_a values of the mixture CO_2 - cosolvent in relation to pure CO_2 (see Equation 3.6) as a function of the cosolvent volume fraction at different pressures.

$$\text{Miscibility enhancement (\%)} = \left[1 - \left(\frac{R_{a\ CO_2+\text{cosolvent}}}{R_{a\ \text{pure}\ CO_2}}\right)\right] \text{x100 \%} \tag{3.6}$$

3.3.4 Validation of predictions

As mentioned before, predictions made through the Hansen approach were first validated with equilibrium data by the static method in a high-pressure variable volume view cell at the set temperature and molar fraction (see **Publication II, III** and **IV** for more details) in sc-CO_2 and its mixtures with the cosolvents studied were obtained. A cosolvent mass fraction of 5 % ± 0.1 % was used.

Figure 3.2 shows a schematic diagram of the homemade apparatus used to perform phase equilibria measurements. Its main component was a high-pressure, variable-volume cell constructed of stainless steel, working volume of 1.5 10^{-5} m^3 and fitted with a sapphire window. The image of the mixture in the cell was obtained by means of a boroscope (Fiegert-Endotech, Germany) placed against the sapphire window, fitted with a camera (Motic 2000, Moticam, China) and connected to a computer. The cell was electrically heated (up to 373.2 K) by means of a silicone heating tape (SRT051-040, Omegalux, United States) connected to a Proportional Integral Derivative (PID) temperature controller (model CN77322, Micromega, Italy). The temperature controller was connected to a type J thermocouple in direct contact with the fluid mixture with a resolution of ± 0.5 K. CO_2 was transferred into the view cell gravimetrically by means of an auxiliary cell. The mole fraction precision was estimated to be ± 0.1 %. The contents of the cell were mixed using a magnetic stirrer. The mixture inside could be compressed to the desired operating pressure (up to 30 MPa) by displacing a movable piston fitted within the cell using water pressurized by means of a high-pressure generator. This high-pressure generator was connected to a water reservoir through valve V1 and to the cell through valve V2 (see Figure 3.2). The water pressure was determined using a Swagelok pressure gauge. The pressure inside the cell was determined using a relative transducer (model PTX7511-1, Druck Industries, United States) provided with a digital display. The pressure deviation estimated to be ± 0.1 MPa.

The phase transition was determined visually as described by Perez *et al.*, [102]. For that, at a fixed temperature, the mixture in the cell was compressed to a single phase. The pressure was then slowly decreased until the condensed phase appeared. The contents

of the cell were periodically agitated using the magnetic stirrer. The solute could be alternatively solubilized and precipitated to obtain a precise bubble pressure value. The solubility was determined from the amounts of CO_2, cosolvent (when used) and solute loaded into the cell.

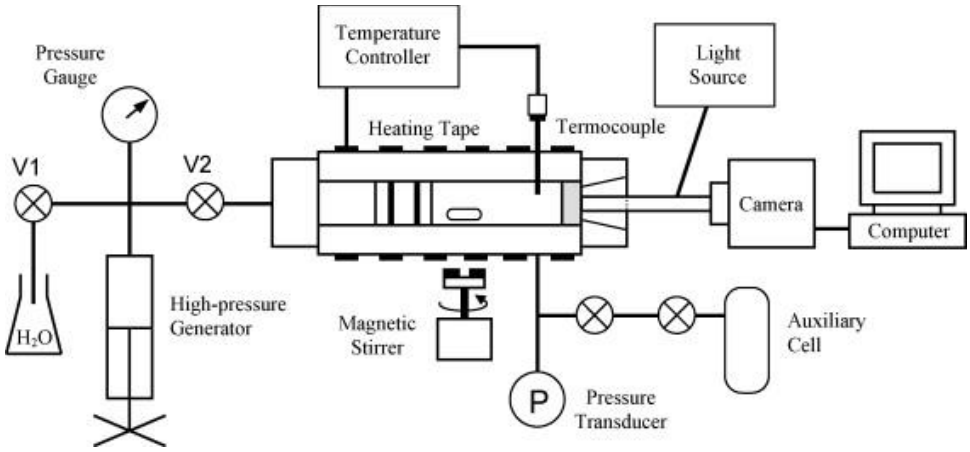

Figure 3.2. Schematic diagram of the static view cell apparatus used to perform phase equilibria measurements.

The estimations were also tested against extraction yields of oleic, linoleic and α-linolenic acids from *T. suecica (***Publication III)** and β-carotene from *D. salina* (**Publication IV**). Supercritical fluid extractions of the target compounds were carried out in our laboratory at different conditions of pressure and temperature using CO_2 and its mixtures with a mass fraction of 5 % cosolvent. The procedures for the fill up of the raw material, start-up and stop of the equipment could be consulted in Section 3.2 of this thesis.

For both validation methods, mass fraction and not volume fraction was used due to practical limitations. e.g., during supercritical fluid extractions, the flow rate in the

experimental set up was measured in mass. However, taken into account the low amount of cosolvent, the variation with respect to the volume fraction was insignificant in the range of conditions tested.

Finally, the assays were repeated at least twice, and the standard deviations were deduced from selected tests that were repeated six times (n = 2 x 3). These values were reported in each publication.

3.4 Characterization of oil extracts

The following are the experimental procedures used to characterize the oil extracts obtained in **Publication I**, **III** and **IV;** and the material and particles produced in **Publication V.**

*3.4.1 Total phenol content (**Publication I**)*

The oil extracts were analysed according to the Folin–Ciocalteu method [103], with minor modifications. In brief, after 2.5 10^{-7} m^3 of oil extract diluted in a mixture methanol – water (L L^{-1}) was well mixed in a vortex (Heidolph REAX top, Heidolph Instruments, Germany) with 2.5 10^{-6} m^3 of distilled water and 5 10^{-7} m^3 of the Folin–Ciocalteu stock reagent; 1 10^{-6} m^3 of the Na_2CO_3 reagent (75 kg m^{-3}) was added to the mixture and then incubated at room temperature for 30 min. Then, the absorbance was measured spectrophotometrically (MRC, model UV-1800, Tel-Aviv, Israel) at 765 nm. The total phenol content was expressed in milligrams of gallic acid equivalents per gram

of oil extract (mg GAE g oil extract^{-1}). The calibration curve was established from 0 kg gallic acid m^{-3} to 0.1 kg gallic acid m^{-3}.

*3.4.2 Hydroxytyrosol content by HPLC analysis (**Publication I**)*

An acid hydrolysis of the extract was performed before the analytical quantification to convert the hydroxytyrosol derivatives into free hydroxytyrosol and tyrosol. For that, 1 g oil was mixed with 2 mL of a 1 M H_2SO_4 solution. The mixture was maintained in a water bath at 353.2 K for 2 h, and then, diluted to 10 mL with methanol. Then, it was vortexed for 2 min and centrifuged for 10 min at 3500 rpm. Afterwards, the supernatant was filtered through a 0.45 μm membrane into an HPLC vial. To measure the hydroxytyrosol content, samples were analysed through high-performance liquid chromatography (HPLC) coupled to a diode array detector (DAD), equipped with a Luna C18 (2), 150 mm × 4.6 mm x 5 μm column, purchased from Phenomenex (Torrance, United States). Methanol was used as mobile phase A and 0.2 % in volume fraction of acetic acid as mobile phase B. The elution program was A (%)/B (%): 10/90, 0 min; 37/63, 10 min; 10/90, 11-15 min; eluent flow 1 10^{-6} m^3 min^{-1}. The injection quantity was 2 10^{-8} m^3. The wavelength was fixed at 280 nm.

*3.4.3 Fatty acids analysis (**Publication I** and **III**)*

Extracts were derivatized following the procedure described by the Official Method 969.33 of the Association of Official Agricultural Chemists (AOAC) [104]. For this, approximately 1 10^{-4} kg of oil extract was placed into a screw cap glass tube. As

much as 1 10^{-5} kg of heptadecanoic acid as internal standard and 4 10^{-6} m^3 of NaOH in methanol (0.5 N) were added into the tube and then nitrogen was blown for 15 s. The tube was covered tightly, vortexed, heated in a water bath (mod. W350, Memmert GmbH and Co, Germany) for 5 min at 358.2 K and then cooled. Furthermore, the tube was added by 5 10^{-6} m^3 of BF_3 in methanol (11.4 % in mass fraction), vortexed and then nitrogen was blown. The tube was covered tightly, heated for 15 min at 358.2 K and then cooled. In this stage, fatty acids were converted to FAMEs. Extracting solvent, 3 10^{-6} m^3 of hexane, was added and then the mix was vortexed. Furthermore, 3 10^{-6} m^3 of saturated NaCl solution was added and then the solution was vortexed. Finally, the upper layer was transferred through a small amount of Na_2SO_4 (placed on the top of a filter liner) into a test tube with a Pasteur pipette.

Subsequently, the samples were analysed by gas chromatography (GC) with a Shimadzu 2010 Plus gas chromatograph (Shimadzu Corporation, Japan) equipped with a Flame Ionization Detector (FID) and a Zebron ZB-1HT capillary column (20 m × 0.18 mm i.d. × 0.18 μm film thickness). The separation was carried out with helium (1.8 10^{-6} m^3 min^{-1}) as a carrier gas. The column temperature was programmed starting at a constant value of 393.2 K during 3 min, heated to 458.2 K at 3 K min^{-1}, held at 458.2 K during 3 min, heated again to 523.2 K at 15 K min^{-1} and finally held at 523.2 K for 5 min. The equilibration time was 5 min. A split injector (50:1) at 523.2 K was used. The FID was also heated at 553.2 K. The injection volume was 1 10^{-9} m^3. Most of the FAMEs were identified by comparison of their retention times with those of chromatographic standards. The compounds were quantified related to the area of the internal standard.

*3.4.4 Free radical scavenging capacity (**Publication I** and **V**)*

The method principle relies on the fact that the scavenging of free radicals by samples or standards causes a reduction in DPPH absorbance. Briefly, 2 10^{-7} m^3 of a methanolic solution of the sample was added to 3.8 10^{-6} m^3 of a freshly prepared methanolic solution containing 60 μM DPPH. This solution exhibited a deep purple colour with maximum absorption at 517 nm. The reaction mixture was then kept at room temperature in a dark chamber for 30 min. The change in colour from deep violet to light yellow was measured at 517 nm in the spectrophotometer. A standard curve was prepared using the reference synthetic antioxidant Trolox diluted in methanol, and the antioxidant capacity of the samples was measured as Trolox equivalent antioxidant capacity (TEAC, Trolox equivalent per kg of the sample).

*3.4.5 Carotenoid content in oil extracts (**Publication IV**)*

The extract was dissolved in methanol and stabilized with a volume fraction of 0.025 % BHT, and immediately analysed to avoid degradation of the carotenoids. The total concentration of carotenoids was determined by measuring the absorbance of the samples using a UV-Vis spectrophotometer and the Equations (3.7), (3.8) and (3.9) proposed by Wellburn [105]. Based on the analysis of the microalgae provider, β-carotene represented a mass fraction of 86 % of the total carotenoids content.

$$C_{\text{total carotenoids (x+c)}}\left(\frac{\mu g}{mL}\right) = \frac{1000A_{470} - 1.63C_a - 104.96C_b}{221} \quad (3.7)$$

$$C_a\left(\frac{\mu g}{mL}\right) = 16.72A_{665.2} - 9.16A_{652.4} \quad (3.8)$$

$$C_b\left(\frac{\mu g}{mL}\right) = 34.09A_{652.4} - 15.28A_{665.2} \quad (3.9)$$

Where $C_{(x+c)}$, C_a and C_b are total carotenoid (xanthophylls and carotenes), chlorophyll a and chlorophyll b concentration respectively and A_{470}, $A_{652.4}$ and $A_{665.2}$ are the absorbances at 470 nm, 652.4 nm and 665.2 nm respectively.

*3.5 Encapsulation by advanced supercritical techniques (**Publication V**)*

This section included the methodology implemented to produce ethyl cellulose particles and the further encapsulation of astaxanthin in **Publication V**.

3.5.1 Preparation of the starting emulsions

Oil in water (O/W) emulsions with an O-W ratio of 20:80 were prepared. The organic phase was prepared by dissolving ethyl cellulose in ethyl acetate. Concentrations of 1.0 %, 1.5 %, 2.0 % or 2.5 % of ethyl cellulose were tested. To dissolve the polymer, a fixed amount of ethyl cellulose was added to the ethyl acetate and then, it was well mixed in a vortex (Velp Scientifica ZX3, Italy) for 1 min. On the other side, Tween 80 was dissolved in an ethyl acetate-saturated water solution to create the aqueous phase. Concentrations of 0.1 %, 0.2 %, 0.3 % or 0.6 % of Tween 80 were tried. Afterwards, the organic phase was added to the aqueous phase, drop by drop, and agitated by using a high-speed stirrer (mod. L4RT, Silverson Machines Ltd., United Kingdom) operating at

3200 rpm during 4 min. Then, the emulsion was subjected to the SFEE process. When astaxanthin was encapsulated, this one was added in the mixture ethyl acetate–polymer and then dissolved by sonication using a VCX130-Vibra Cell (Sonics and Materials, United States) at 30 % of amplitude for 1.5 min. All the percentages in this work are expressed as a mass fraction.

The influence of the polymer content in the organic phase and the surfactant content in the aqueous phase was analysed in terms of mass recovery (MR) of the polymer, mean diameter (MD), polydispersity index (PDI) and morphology. The best formulation was selected to perform the encapsulation of astaxanthin.

Moreover, to analyse the influence of the viscosity of the organic phase on the final particle size, the increment of the viscosity of the organic phase with the concentration of the polymer was studied. For this purpose, the apparent viscosity as a function of shear rate was analysed using a Brookfield dial viscometer (Model LVT, serial 24078, United States) using the #1 spindle and maintaining the sample at 298.2 K ± 0.1 K. A frequency sweep was performed in a range between 0.3 rpm and 60 rpm. However, the limit of detection was found at 60 rpm, which is why only the apparent viscosity value was reported at this frequency.

3.5.2 Continuous Supercritical Fluid Extraction of Emulsions

The organic solvent was removed from the emulsion by SFEE. For this, 1 10^{-4} m^3 of the emulsion was pumped into a packed column to obtain a continuous counter-current

contact with sc-CO_2. Briefly, the apparatus consisted of a column (height 0.16 m, i.d. 1 10^{-2} m) packed with stainless steel packings (Pro-Pak, 4 10^{-3} m nominal size, 1889 m^{-1} specific surface and 0.94 voidage). The column was thermally insulated, and its temperature profile was controlled by temperature controllers. CO_2 was pumped from the bottom of the column by a high-pressure diaphragm pump (mod. Milroyal B, Milton Roy, France). The emulsion was taken from a reservoir and pumped into the column using a high-pressure piston pump (mod. 305, Gilson, United States) at the top of the column. Before starting the emulsion delivery, the column was wetted with a fixed amount of the external water phase. A separator located downstream the top of the column was used to recover the extracted solvent. The procedure was performed at 8 MPa and 311.2 K considering the vapour–liquid equilibrium diagram of the ethyl acetate–sc-CO_2 system [99]. A liquid/gas (L/G) ratio of 0.1 and a CO_2 flow rate of 1.4 kg CO_2 h^{-1} were fixed according to the optimisation performed in previous work for the ethyl acetate–sc-CO_2 system [92]. Finally, nanoparticles suspension was continuously collected at the bottom of the column using a needle valve, washed several times with distilled water and then recovered by membrane filtration. A wet powder was obtained in all cases and this was left overnight to ensure drying. After this, samples were submitted to analysis. A schematic representation of the equipment is shown in Figure 3.3.

The MR of polymer was defined according to Equation (3.10):

$$\mathrm{MR} = \left(\frac{\text{Mass of polymer charged in emulsion}}{\text{Polymer mass recovered after the drying process}}\right) \text{x } 100\ \% \qquad (3.10)$$

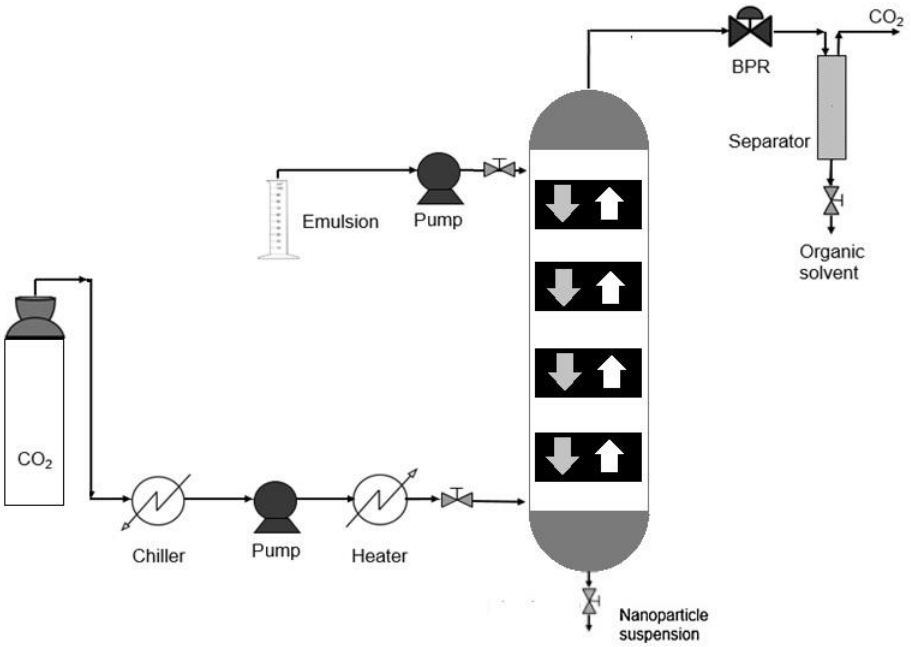

Figure 3.3. Representation of the continuous Supercritical Fluid Extraction of Emulsions layout used in this thesis.

3.5.3 Morphology and particle size

The morphology of the produced particles was studied using a Field Emission-Scanning Electron Microscope (FE-SEM mod. LEO 1525; Carl Zeiss SMT AG, Germany). For this, the powder was dispersed on a carbon tab previously stuck to an aluminium stub. Samples were coated with gold (layer thickness 250 A) using a sputter coater (mod.108 A, Agar Scientific, United Kingdom). Moreover, the morphology of the encapsulated astaxanthin was assessed by Transmission Electron Microscope (TEM, JEOL JEM 1010, JEOL, United States). To do this, an aqueous suspension of nanoparticles was centrifuged (Digicen 21, Orto Alresa, ES) at 15,000 rpm for 10 min. After that, the supernatant was removed. Then, a drop of concentrated aqueous suspension was negatively stained for 1 min with a 1 % sodium phosphotungstic acid solution and

placed on a carbon-coated copper grid. Afterwards, TEM pictures were taken. Finally, the MD was measured by dynamic light scattering (DLS) by using a Malvern Zetasizer instrument (Zetasizer Nano S, United Kingdom). For this, 1 10^{-6} m^3 of the produced suspension was used without any further dilution step.

3.5.4 Astaxanthin encapsulation efficiency

The maximum absorbance of astaxanthin dissolved in acetone was observed at 470 nm using a UV–Vis spectrophotometer (Lambda 25 UV/VIS Spectrometer; PerkinElmer, United States). A standard calibration curve of this compound in acetone was previously obtained and the dried powder containing it was dissolved in acetone. Then, the supernatant was recollected and analysed in the spectrophotometer. The encapsulation efficiency was calculated by the ratio between astaxanthin content inside the particles produced by SFEE and the amount of compound initially loaded, expressed as Equation (3.11).

$$\text{Encapsulation efficiency} = \left(\frac{\text{Mass of astaxanthin detected by UV} - \text{Vis}}{\text{Mass of astaxanthin loaded in the emulsion}}\right) \text{x } 100\ \% \quad (3.11)$$

3.5.5 Astaxanthin release study

A release profile under sink conditions (i.e. the maximum concentration of dissolved astaxanthin never exceeded 20 % of its solubility) was performed in 1 10^{-4} m^3 SIF: a phosphate buffered saline at pH 7.2, according to the method developed by

Verhoeven *et al.,* [106] with slight modifications. For this, 10 10^{-5} kg powder were immersed in the SIF and incubated at 310.2 K ± 0.1 K (physiological temperature) in a thermostatic water bath (mod. WNB 14, Memmert GmbH and Co, Germany) equipped with a horizontal shaking device (SV1422, Memmert, Germany). The *in vitro* astaxanthin release study was conducted for a period of 10 h. At every 1 h interval, samples of 5 10^{-6} m^3 were withdrawn from the dissolution medium and replaced with fresh medium to maintain sink conditions. Then, samples were spectrophotometrically analysed. Finally, the astaxanthin dissolved was plotted as a cumulative percent release versus time.

Additionally, the antioxidant activity of the produced particles and the pure astaxanthin was measured according to Section 3.4.4.

3.5.6 Statistical analysis

The experiments were repeated at least twice, and the analyses were performed in triplicate for each replicate (n = 2 × 3). Mean and standard deviation were calculated for all data. Response variables (MD and PDI) were submitted to analysis of variance (ANOVA). When statistical differences at a significance level of 5 % ($p < 0.05$) were found, a Fisher's Least Significant Difference (LSD) test was performed to determine the influence of the selected factors. Data processing was carried out using STATGRAPHICS Centurion XVI (Statpoint Technologies, Inc., United States).

4. A unifying discussion of the results

In this chapter, the most relevant results obtained during the performance of this doctoral research thesis are discussed in a unified manner. This discussion was based on five (5) previously published research papers in the Chemical Engineering field, which are attached in the Appendices section of this manuscript. Each of the aforementioned manuscripts contains in detail the computational and experimental procedures developed in the course of this research, as well as the totality of the results and their discussions.

To summarize the results of this thesis, this chapter was organized into five sections, which describe in a consolidated way the main findings:

i) Study of the main process parameters and solid conditions that affected the sc-CO_2 extraction from vegetable matrices (**Publication I**).

ii) Use of the Hansen approach to predict the best cosolvents for sc-CO_2 to selectively extract bioactive compounds (**Publication II, III and IV**).

iii) Validation of predictions through equilibrium data and supercritical extraction curves from microalgae (**Publication II, III and IV**).

iv) Encapsulation of astaxanthin by SFEE (**Publication V**).

4.1 Study of the main process parameters and solid conditions that affected the sc-CO_2 extraction from vegetable matrices

This section describes the effect of the main process variables and solid conditions affecting the supercritical fluid extractions from vegetable matrices. The operation was carried out using alperujo, the solid-liquid waste generated by the new two-phase method of olive oil extraction, as a model fixed bed. The objective was to extend the influence of the parameters studied to the others supercritical fluid extractions applied in this doctoral thesis because although they were different plant matrices, the model of mass transfer from the cells was considered similar.

Analysis of the oil extraction yield from alperujo as function of particle size (< 0.80 mm and without sieving), initial moisture of the sample (equilibrium moisture, 0.1 kg water kg alperujo^{-1}, 0.3 kg water kg alperujo^{-1} and 0.7 kg water kg alperujo^{-1}), pressure (20 MPa and 30 MPa), temperature (323.2 K and 373.2 K) and CO_2 mass flow (0.06 kg h^{-1}, 0.18 kg h^{-1} and 0.30 kg h^{-1}) is described below. Particle size and the initial moisture in the sample represented the initial solid conditions studied. Pressure, temperature and flow rate, on the other hand, represented the main operating parameters. The results were expressed as extraction curves constructed by plotting the oil extraction yield expressed in mg extract g alperujo^{-1} *versus* the solvent ratio (kg CO_2 kg alperujo^{-1}) passed through the fixed bed. When a constant mass in the vial was reached, the extraction was stopped. In the case of samples to be analysed, the extraction was stopped when an appropriate amount of extract was obtained, and the analyses were carried out immediately after extraction. This was done to avoid a possible degradation of the interesting compounds.

In the case of samples to be analysed by HPLC, these were stored at 253.2 K until analysis.

Additionally, a conventional extraction was carried out for comparison, using 0.01 kg of dried alperujo and 1.5 10^{-4} m^3 of n-hexane in a 2.5 10^{-4} m^3 Soxhlet apparatus during 8 h. Afterwards, the optimised supercritical extractions from alperujo proved to reach extraction yields (13 % d.b.) equivalent to those achieved by conventional Soxhlet extraction with n-hexane (14 % d.b.) (see Table 3.1). However, this slightly higher oil extraction yield with the organic solvent was probably due to its lower selectivity, taking into account that the extract obtained with n-hexane contains neutral and polar lipids and pigments [107]. Moreover, the supercritical extracts showed a fatty acid composition close to that of an extra virgin olive oil of an Arbequina variety. This comparison can be appreciated in Table 4.1, with a mean standard deviation of the fatty acid composition of 6 % in mass fraction. The aforementioned demonstrates the versatility in the use of sc-CO_2 to obtain high-quality oil extracts.

Table 4.1. Fatty acid profile of supercritical extracts and a commercial virgin olive oil.

Fatty acid	**Oil extract (%)**	**Extra virgin olive oil (%)**
Palmitic acid	13.5	14.4
Stearic acid	1.8	1.7
Oleic acid	69.4	71.4
Linoleic acid	11.3	9.1
Linolenic acid	0.6	0.3

The study of the initial solid conditions of the materials before a supercritical fluid extraction has proven to be important to maximize the extraction yield, to reduce operating costs and to improve the quality of the extract [107]. On the one side, an insufficient water content in vegetable matrices could cause the cell structure to shrink and consequently hinders diffusion, which reduces yield [49]. However, excess water may create an extra barrier for transportation and may generate the co-extraction of polar substances, thereby reducing selectivity [108]. Moreover, high moisture, together with the sugars and fine solids contained in the raw material, such as the studied in this thesis, could give it a doughy consistency, hindering the contact to the solvent. Specifically, for alperujo, its high moisture content demanded energy and the sugars present in it made it sticky and difficult to dry. Therefore, this parameter must be optimised before any extraction. On the other side, the particle size of the raw material must be reduced so that the extract contained within the plant material is more accessible to the fluid and thus to maximize the extraction and reduce costs. However, care should be taken not to reduce particle size excessively, as this could compromise process performance (e.g. promoting channelling) and cause safety problems due to small particles entrainment [49].

The alperujo used in this work as a raw material had approximately an initial water content of 70 % (0.70 kg water kg^{-1} alperujo) and 0.14 kg oil kg^{-1} alperujo (see Table 3.1). To obtain samples with different moisture content, these were dried at 376.2 K until they reached the desired humidity. Figure 4.1 shows the drying curve obtained. On the other hand, Figure 4.2 shows the particle size distribution in terms of the MD obtained after milling and sieving the dried alperujo. In Figure 4.2, particles with dissimilar sizes could

be appreciated since the alperujo is made up of different types of waste from the olive oil industry, such as pulp, pit, seed, peels and leaves [40].

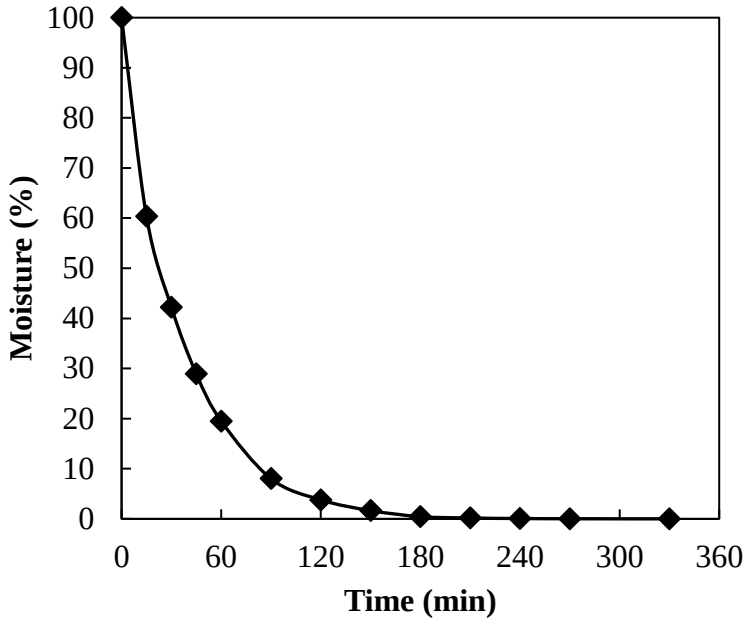

Figure 4.1. Drying curve of alperujo at 376.2 K.

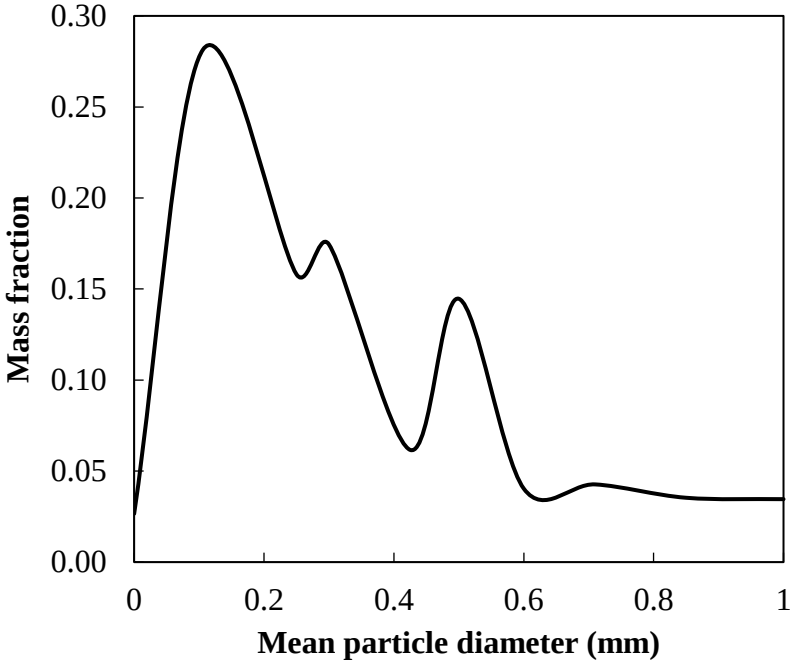

Figure 4.2. Particle size distribution of the milled dried alperujo.

4.1.1 Study of solid pre-treatment: Particle size and initial water content

In order to study the influence of the initial particle size of the raw material on the supercritical extraction process, supercritical fluid extractions from dried alperujo without sieving (the whole range of particle sizes in Figure 4.2) and with a particle size less than 0.80 mm were performed to check out the effect of particle size on the oil extract recoveries. It is well known that particles smaller than 0.40 mm could represent a risk of formation of preferential channels and blockages during the supercritical extraction [49]; however, this fraction represented slightly more than 60 % of the raw material, as can be corroborated in Figure 4.2. Because of this, shorter milling times were used, but the results were similar considering that alperujo was composed of particles with dissimilar sizes, as mentioned before. Consequently, alperujo with a particle size distribution less than 0.80 mm was used for the rest of the assays.

Two extraction curves representing the extraction from alperujo with two different initial particle sizes are shown in Figure 4.3. As expected, the oil yield increased with the lowest particle size, due to the fact that particles with a diameter greater than 0.80 mm hindered the penetration of the supercritical solvent and the solubilisation of the solute [49]. On the other hand, the influence of the initial water content in the raw material to be processed by supercritical fluid extraction was also studied. Regarding this, Figure 4.4 shows the extraction curves, working at 30 MPa, 323.2 K, 0.18 kg h^{-1} CO_2 flow rate and initial water content of the fixed bed of 1 %, 10 % and 70 %. The last value was the initial water content of the raw material. As can be appreciated in Figure 4.4, the fastest extraction was achieved when the sample had a water mass fraction of 1 %, which

corresponded to the equilibrium moisture of the atmosphere in Madrid. Apparently, the reduction in particle size was good enough to allow the oil extract to be available to the SCF.

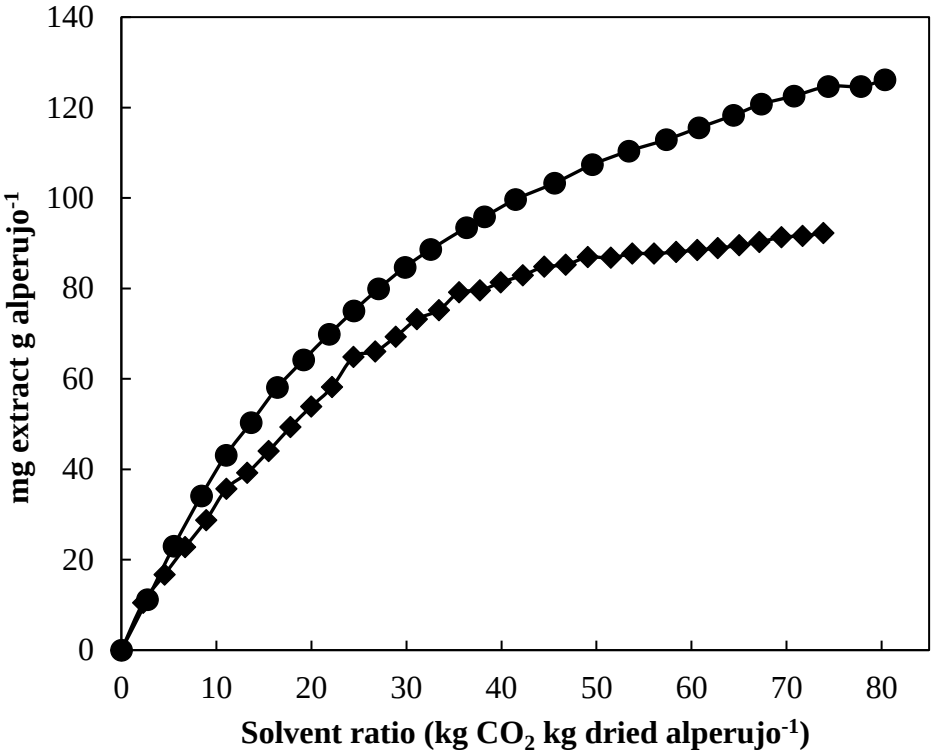

Figure 4.3. Effect of particle size on oil yield: < 0.80 mm (●) and without sieving (♦). Conditions: P = 30 MPa; T = 373.2 K; Q = 0.18 kg h^{-1} and alperujo water mass fraction, 1 %.

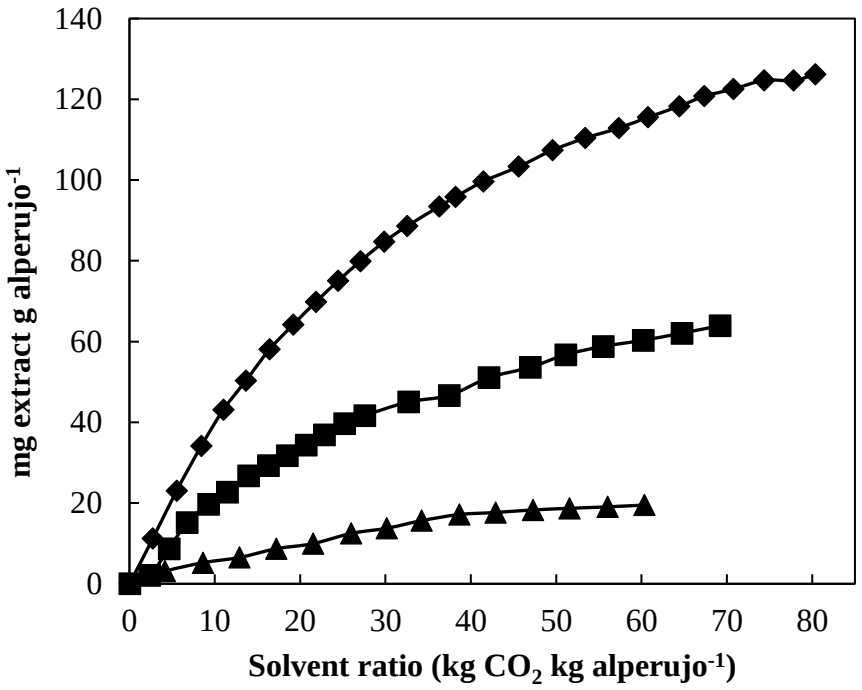

Figure 4.4. Extraction curves using different initial alperujo water mass fraction: 1 % (♦), 10 % (■), and 70 % (▲). Conditions: P= 30 MPa, T = 323.2 K; Q = 0.18 kg h^{-1} and MD = < 0.80 mm.

4.1.2 Influence of operating parameters: Effect of pressure, temperature and mass flow

Sudden changes in pressure and temperature cause drastic changes in the density of the SCF and hence in its solvating power. Solvent ratio, for its part, is the most important parameter for the supercritical fluid extraction, once approximate values of pressure and temperature are selected. In this section, the main effects of these variables during the course of the supercritical extraction were studied.

So far, it seemed that dried samples with reduced particle sizes improved to perform the supercritical extractions. In view of the above, these parameters were set to study the influence of the operating variables, which will be discussed below.

The effect of pressure on the oil extraction yield from alperujo was investigated with sc-CO_2 at pressures of 20 MPa and 30 MPa. The results are shown in Figure 4.5 and, as expected, extraction yield strongly increased with pressure, according to the basic principles of the supercritical fluid extractions [49]. Studies on oil extraction from olive residues have reported the same behaviour [62,63,109], claiming that, at a constant temperature, the solubility of a substance in an SCF increases with pressure.

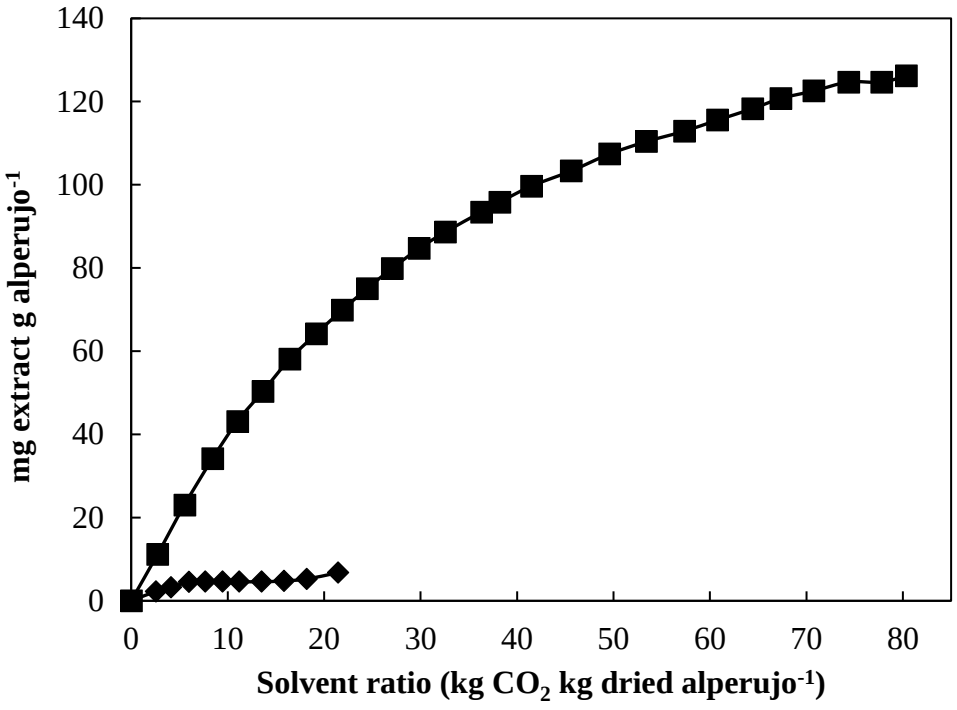

Figure 4.5. Effect of pressure on oil yield: 20 MPa (♦) and 30 MPa (■). Conditions: T = 373.2 K; Q = 0.18 kg h^{-1}; MD = < 0.80 mm and alperujo water mass fraction, 1 %.

Another set of experiments were conducted in order to study the effect of temperature on the supercritical extraction from alperujo. All other parameters were fixed; meanwhile, the temperature was increased from 323.2 K to 373.2 K. These temperatures were selected taking into account preliminary tests, which showed conditions for comparison of hydroxytyrosol extraction yield. The influence of temperature on the cumulative content of oil extracted is shown in Figure 4.6.

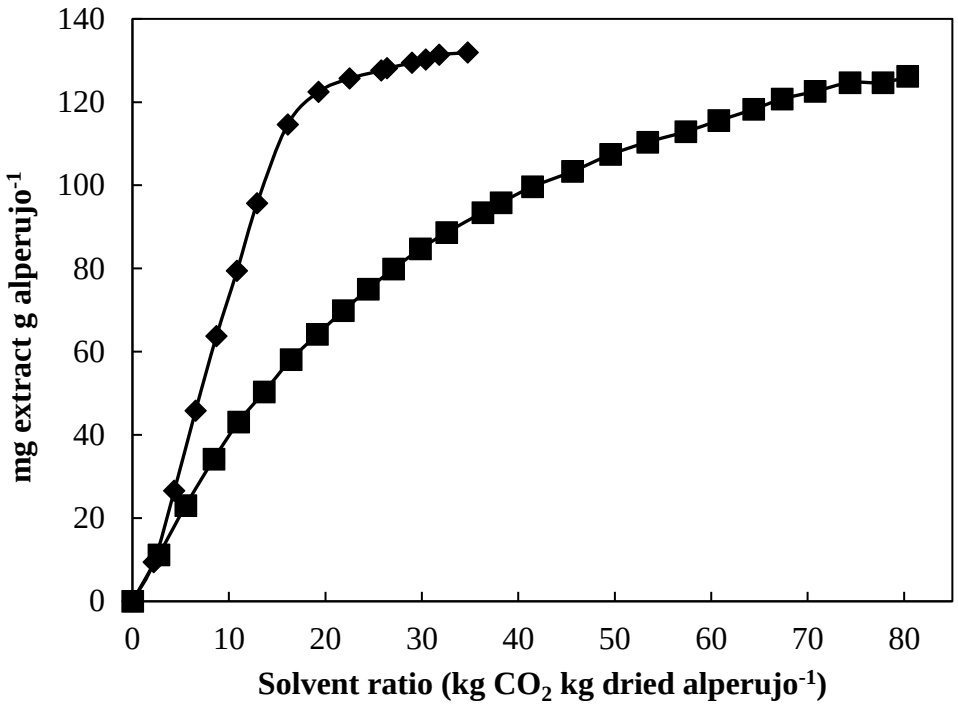

Figure 4.6. Effect of temperature on oil yield: 323.2 K (♦) and 373.2 K (■). Conditions: P = 30 MPa; Q = 0.18 kg h^{-1}; MD = < 0.80 mm and alperujo water mass fraction, 1 %.

As can be seen in Figure 4.6, the highest extraction yield was found at the lowest temperature due to the fact that under these conditions, sc-CO_2 had the highest solvent power, as a consequence of its higher density [49]. During sc-CO_2 extraction, at constant pressure, the change in temperature affects the density of the CO_2, the vapour pressure of

the solutes, and their desorption from the solid matrices. At higher temperatures, the solute becomes more volatile, however, the sc-CO_2 density decreases. For vegetable oils the crossover pressure is about 30 MPa [110]. At relatively low pressures and below the crossover pressure, like those used in this work (≤ 30 MPa), an decrease of density and solvent power with increasing temperature prevails, while an increase in vapour pressure prevails at relatively high pressures [49].

Although the highest extract yield extraction was obtained by using the lowest temperature, further experiments showed that the highest temperatures resulted in the highest total phenol content as will be shown later, so the highest temperature (373.2 K) was selected to study the other process parameters and solid conditions described below.

As claimed before, once values of pressure and temperature are selected, the solvent ratio becomes the most important parameter for the supercritical fluid extraction, since this parameter is able to enhance the extraction rate more than by changing process parameters in a relatively narrow limit. Figure 4.7 shows the extraction curves that resulted from the use of three different CO_2 mass flow rates that ranged from 0.06 kg h^{-1} to 0.30 kg h^{-1}, operating at 30 MPa and 373.2 K with a length-to-diameter ratio of approximately 4:1 of the alperujo fixed bed.

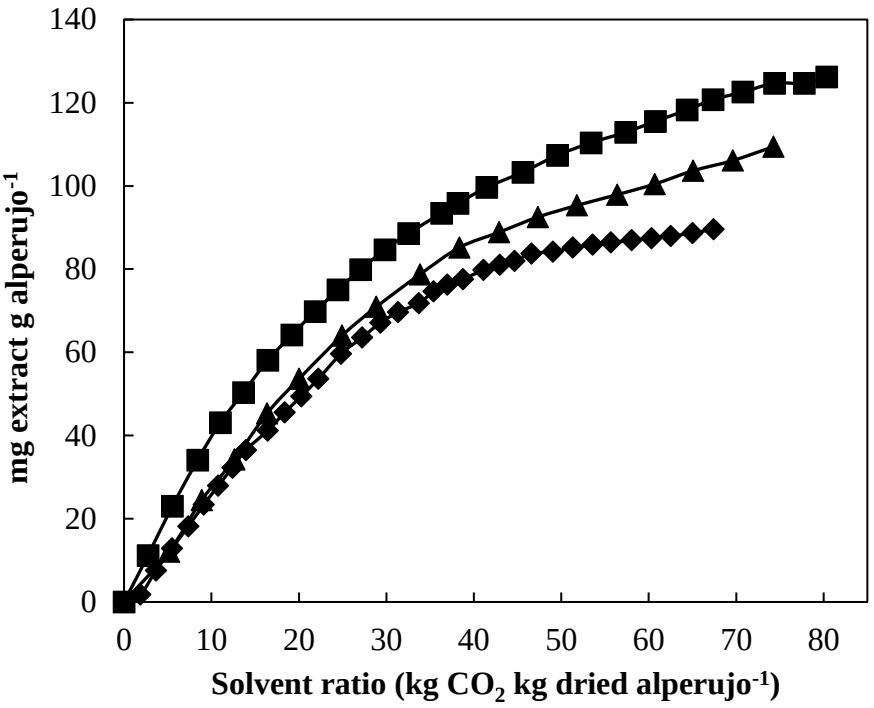

Figure 4.7. Effect of solvent mass flow on oil yield: 0.06 kg h^{-1} (♦), 0.18 kg h^{-1} (■) and 0.30 kg h^{-1} (▲). Conditions: P = 30 MPa; T = 373.2 K; MD = < 0.80 mm and alperujo water mass fraction, 1 %.

As can be seen in Figure 4.7, an increase in flow rate led to a higher extraction yield and to shorter extraction times. However, the highest yield and rate were maxima when working at 0.18 kg h^{-1}. These results could be confirmed in Figure 4.8, which shows that at a solvent hourly ratio of 7.5 kg CO_2 h^{-1} kg dried alperujo^{-1} (0.18 kg h^{-1}) the extraction rate was the highest at every moment. These results could be explained by the fact that the flow rate from 0.06 kg h^{-1} to 0.18 kg h^{-1} enhanced superficial solvent velocity (see Table 4.2) which benefited turbulence and reduced the film layer of stagnant fluid around the solid, thus increasing the external mass transfer coefficients; however, larger flow rates (0.30 kg h^{-1}) reduced the residence time (see Table 4.2), which reduced the time for oil solubilization [107].

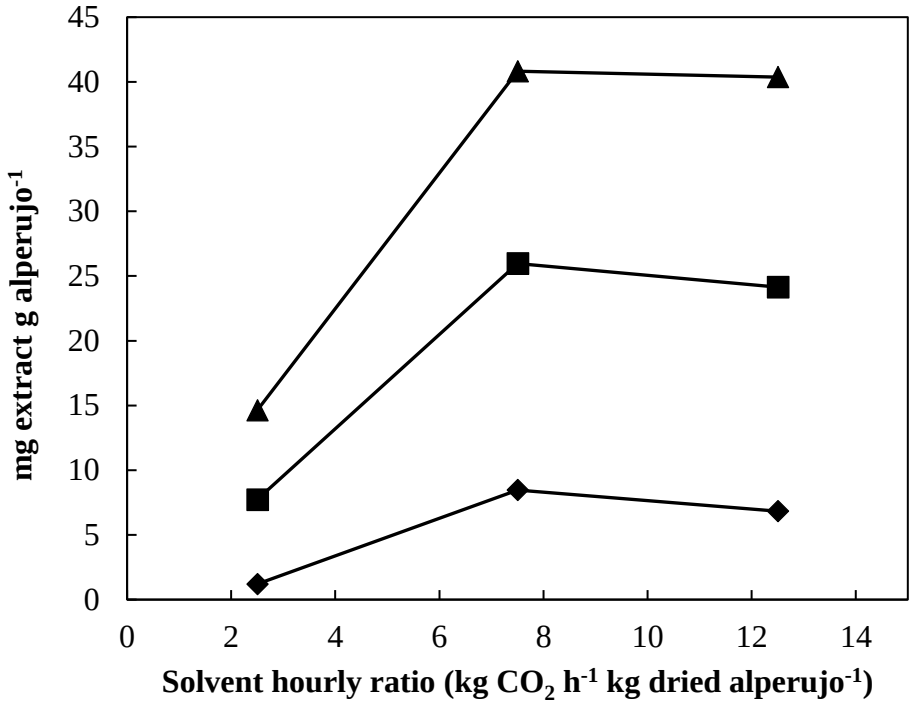

Figure 4.8. Extraction rate for increasing solvent ratios at three moments: 10 min (♦), 30 min (■), 50 min (▲). Conditions: P = 30 MPa; T = 373.2 K; MD = < 0.80 mm and alperujo water mass fraction, 1 %.

Table 4.2. Solvent velocities (*u*) and residence times at different CO_2 flow rates. Conditions: 30 MPa, 373.2 K and 662 kg CO_2 m^{-3}.

CO_2 flow rate (kg h^{-1})	***u* (mm s^{-1})**	**Residence time (min)**
0.06	0.1	55
0.18	0.2	18
0.30	0.3	11

Finally, the influence of the solvent flow rate cannot be discussed without considering economic consequences. This is, for commercial purposes, the solvent flow

rate should be optimized in terms of extraction time and solvent volume used per operation because these influence operational and investment costs. The cost of the SCF installation increases as the square root of the solvent flow rate does, as it has been demonstrated by Perrut [111]. Therefore, it is necessary to optimize this parameter in order to design and run a profitable facility. Table 4.3 shows a summary of the solvent ratio as a function of the oil extraction yield from alperujo at the most favourable conditions of pressure, temperature and solvent flow rate (30 MPa, 323.2 K and 0.18 kg CO_2 h^{-1}), within a period of 280 min. As can be seen in Table 4.3, up to 94 % oil extraction yield could be achieved by using 35 kg CO_2 kg dried alperujo^{-1}. However, using only 30 kg CO_2 kg dried alperujo^{-1} it was possible to achieve an extraction yield of 93 %; i.e. by reducing CO_2 consumption by 15 %, an almost similar efficiency was achieved (only 1 % lower). Similarly, by using 23 kg CO_2 kg dried alperujo^{-1}, an extraction yield of about 90 % oil extract was achieved. In order to extract a further 4 %, approximately 12 kg CO_2 kg dried alperujo^{-1} was required.

4.1.3 Characterisation of the hydroxytyrosol-rich oil extracts

In order to confirm the selective extraction of hydroxytyrosol-rich oil extracts by using sc-CO_2, oil extracts obtained by supercritical fluid extraction were compared with those obtained by conventional Soxhlet extraction with n-hexane. For this, analysis of hydroxytyrosol content, total phenol content and antioxidant capacity of the oil extracts from alperujo were carried out. The results are summarized in Table 4.4.

Table 4.3. CO_2 consumption as a function of temperature and extraction rate of hydroxytyrosol-rich oil from alperujo. Conditions: 30 MPa, 323.2 K and 0.18 kg h^{-1}.

Solvent ratio (kg CO_2 kg dried alperujo^{-1})	**Oil extraction yield (%)**
9	46
11	57
13	68
16	82
19	87
23	90
26	91
26	92
30	93
32	94
35	94

During the supercritical fluid extractions, the highest values of hydroxytyrosol, total phenol content and therefore, antioxidant capacity, were found in the oily extracts obtained at the uppermost pressure (30 MPa) and temperature (373.2 K). In the case of the total phenol content (expressed as mg gallic acid equivalent g extract^{-1}), working at 30 MPa and 373.2 K, this content was 2.7 times higher than in the extracts obtained at 30 MPa and 323.2 K. Likewise, in samples obtained at 30 MPa and 373.2 K the hydroxytyrosol content was 1.6 times greater than in samples obtained at the uppermost pressure and 323.2 K. Consequently, the antioxidant capacity of the supercritical extracts was also higher at 30 MPa and 373.2 K. This could be related to the fact that the temperature improved the mass transfer of this type of compounds from the cell [63,109]. These results contrasted with the total extraction yield, which was greater at low temperatures.

Table 4.4. Hydroxytyrosol content, total phenol content and antioxidant capacity of the extracts from alperujo.

Conditions	**mg hydroxytyrosol g extract^{-1}**	**mg gallic acid equivalent g extract^{-1}**	**µM Trolox equivalent g extract^{-1}**
Supercritical fluid extraction			
20 MPa and 323.2 K	Not detected	1.3 ± 0.0	720 ± 18
20 MPa and 373.2 K	0.7 ± 0.0	2.7 ± 0.0	1,454 ± 209
30 MPa and 323.2 K	1.2 ± 0.1	3.5 ± 0.0	1,944 ± 85
30 MPa and 373.2 K	1.9 ± 0.1	9.6 ± 0.1	6,726 ± 156
Conventional Soxhlet extraction with n-hexane			
	Not detected	1.9 ± 0.6	222 ± 37

It could be also considered difficult to extract hydroxytyrosol by using pure sc-CO_2; however, the extraction of an hydroxytyrosol-rich oil extract by sc-CO_2 extraction can be explained by three main facts. First of all, during the olive oil mechanical process, the major proportion of hydroxytyrosol is contained in the aqueous phase, while only a minor percentage (< 2 % in mass fraction) is in the olive oil. After removing most of the water contained in the alperujo, the hydroxytyrosol is concentrated in the dried sample, making it more readily available for subsequent supercritical extraction.

The second explanation is due to the amphiphilic nature of hydroxytyrosol and the lipophilic nature of its conjugated derivatives, which is reported in several works [39,42,43,112]. In fact, the high antioxidant character of hydroxytyrosol and derivatives is partly due to this lipophilic characteristic [112]. As some of these hydroxytyrosol derivatives are highly lipophilic [113], e.g. some flavonoids and the aglycon derivatives of oleuropein and dimethyl oleuropein, they are also more extractable by sc-CO_2.

The third fact is that the olive oil itself contained in the alperujo (about 14 % d.b.) could have acted as a matrix cosolvent during the extraction of this polar compound. This is already known and reported in the literature. Krichnavaruk et al., (2008), for example, reported the sc-CO_2 extraction of astaxanthin (another polar compound) from *Haematococcus pluvialis* by using vegetable oils (soybean oil and olive oil) as co-solvent. Vasapollo et al., (2004), on the other hand, claimed the extraction of lycopene from tomato using sc-CO_2 in the presence of hazelnut oil as co-solvent. Finally, Sun and Temelli (2006) used canola oil as cosolvent during the sc-CO_2 extraction of carotenoids from carrot.

On the other hand, it can be also seen in Table 4.4 that hydroxytyrosol could not be detected in the samples extracted with n-hexane. In general, n-hexane is not a good solvent for phenolic compounds [42,43]. Another possible reason to not find hydroxytyrosol in the extract from this solvent was the harsh conditions and the prolonged duration of the Soxhlet method. The temperature in the distillation flask in contact with the heating element was probably too high; the degradation temperature of hydroxytyrosol starts at approximately 536 K [117]. Moreover, the assays were conducted in the natural light of the laboratory as the Soxhlet apparatus was made of glass. Hydroxytyrosol is also sensitive to light and oxidation [42,43]. This did not happen with the sc-CO_2 extraction, as a high purity CO_2 was used to avoid large amounts of oxygen in the process [94]. The operating temperature was moderate ($\leq$ 373.2 K) and the extract was protected from light in all parts of the installation.

Finally, the hydroxytyrosol content found in the supercritical extracts of this work was higher compared to other values reported in the literature. The maximum hydroxytyrosol concentration of those analysed in this work (1900 ppm), was greater than the value reported by De Marco et al., (2007) in olive mill wastewater (1224 ppm) and significantly superior than that reported by Owen et al., (2000) in extra virgin oil (232 ppm). The difference in hydroxytyrosol content would be mainly related to the different raw material, harvesting conditions or other environmental factors; although it could be connected to the way the extraction was carried out.

4.2 Use of the Hansen approach to predict the best cosolvents for sc-CO_2 to selectively extract bioactive compounds

The suitability of sc-CO_2 to extract neutral lipids from plant matrices is well known. However, this solvent does not have the ability *per se* to extract active compounds of a polar nature; consequently, a cosolvent must sometimes be added to the supercritical gas in order to increase the extraction yield and selectivity of the supercritical extraction. Another objective of this thesis was to extract oils rich in carotenoids and long chain fatty acids; and since these compounds do not solubilise easily in sc-CO_2, it was necessary to consider the addition of cosolvents to the supercritical gas in order to increase the solubility of the target compound, increase the separation factor and thus reduce the operating pressure and CO_2 consumption. However, at supercritical conditions, choosing a proper cosolvent is a quite difficult task because long and expensive experimental tests are needed; therefore, theoretical estimations should be implemented.

The Hansen approach provides a useful estimation for the selection of solvents in the prediction of the miscibility of natural bioactive compounds [96]. Therefore, the aim of this section was to predict the best cosolvents for sc-CO_2 by using the HST to achieve the selective extraction of compounds with nutritional interest from microalgae.

The calculations were made by using a 5 % volume fraction of several organic cosolvents to ensure a supercritical homogeneous mixture. β-carotene and oleic, linoleic and α-linolenic acids as examples of valuable carotenoids and fatty acids, respectively, were used as target compounds for the extraction. The order of the cosolvent ability was

deduced based on minima R_a values in a wide range of operating conditions suitable for the supercritical extraction.

Considering that the mixtures sc-CO_2 + cosolvent should be a single supercritical phase (completely miscible) at the operating conditions to reach the desired entrainer effect [120], the existence of a single homogeneous phase for all the mixtures at the explored interval of conditions in this thesis was corroborated by visual inspection in the high-pressure variable volume view cell described in Section 3.3.4.

4.2.1 Hansen solubility parameters of target compounds

There was not enough data in the literature regarding the physical properties and solubility parameters of the solute-solvent pairs of this thesis. Therefore, the HSP values of the bioactive compounds involved, from the dispersion (δ_d), polar (δ_p) and hydrogen bonding (δ_h) forces were calculated according to the GCM proposed by Hansen [73]. Likewise, the influence of temperature on the HSP values of the target compounds was calculated by using Equation (3.1) described in Section 3.3.1, based on the Jayasri and Yaseen method [95]. As mentioned before, below the critical points of the target compounds, pressure does not exert a considerable influence on their HSP [96]; therefore, this influence was not considered. Finally, critical temperatures required in Equation (3.1) were obtained by using the GCM proposed by Joback [97]. The structures used to carry out the mentioned GGM could be found in Figure 1.1, Figure 1.2, Figure 1.3a, Figure 1.3b and Figure 1.3c.

Table 4.5 shows the HSP for β-carotene, oleic, linoleic and α-linolenic acid at NTP (298.2 K and 0.1 MPa). In order to visualize the effect of temperature on the HSP of the compounds involved in this thesis, Table 4.5 also contains the HSPs of the target compound at 313.2 K, which was a common condition in **Publications II** and **IV**. However, data related to the HSP of each compound at the studied conditions could be retrieved in **Publications II**, **III** and **IV**.

Table 4.5. Hansen solubility parameters of bioactive compound studied in this thesis.

Target compound	**298.2 K and 0.1 MPa**				**313.2 K and 20 MPa**			
	δ_d	**δ_p**	**δ_h**	**δ_T**	**δ_d**	**δ_p**	**δ_h**	**δ_T**
	$MPa^{1/2}$	**$MPa^{1/2}$**	**$MPa^{1/2}$**	**$MPa^{1/}$**	**$MPa^{1/2}$**	**$MPa^{1/2}$**	**$MPa^{1/2}$**	**$MPa^{1/}$**
β-carotene	16.74	2.32	5.39	17.74	16.63	2.30	5.35	17.62
Oleic acid	17.40	2.67	6.43	18.74	17.26	2.65	6.38	18.59
Linoleic acid	18.29	2.94	7.24	19.89	18.14	2.92	7.18	19.73
α-Linolenic acid	18.03	3.03	7.61	19.80	17.89	3.01	7.55	19.65

As can be seen in Table 4.5, for all the target compound involved in this research thesis, δ_d had the highest contribution due to the presence of a long straight-chain hydrocarbon in their structures. It is worth pointing out the high value of the hydrogen contributions (δ_h) in the fatty acids studied, which is mainly caused by the carboxylic group in their structure, which gives polar and hydrogen bonding contributions, respectively. However, the carboxylic group has a bigger impact than the olefin group, and for that reason, the hydrogen bonding forces are higher.

Finally, as can be seen in Table 4.5, the HSP of the studied compounds varied only slightly within the explored temperature interval. However, these minor changes should be considered during predictions, as they could cause practical differences during validations [68,69,96].

4.2.2 Hansen solubility parameters of solvents

Table 4.6 shows the HSP for sc-CO_2 and its SCM with various cosolvents. To visualize the effect of pressure and temperature, HSP values were reported as an example at two different temperatures (313.2 K and 323.2 K) and pressures (10 MPa and 20 MPa). The addition of cosolvents to sc-CO_2 mainly increased δ_d, and therefore δ_T, which reduced the energy difference (R_a) between the target compounds and all the SCM. On the other hand, both temperature and pressure strongly influenced the HSP of the solvents. An increase in temperature decreased the HSP of all the supercritical solvents; δ_d decreased the most, followed by δ_h and δ_p. Contrarily, a rise in pressure at a constant temperature notably increased the solubility parameters by increasing the solvent density.

Table 4.6. Hansen solubility parameters of CO_2 and its supercritical mixtures at a volume fraction of 5 % cosolvent in CO_2.

Solvent	**T**	**P**	**δ_d**	**δ_p**	**δ_h**	**δ_T**
	K	**MPa**	**$MPa^{1/2}$**	**$MPa^{1/2}$**	**$MPa^{1/2}$**	**$MPa^{1/2}$**
sc-CO_2	313.2	10	7.31	4.64	4.12	9.59
		20	10.51	5.36	4.76	12.72
	323.2	10	3.95	3.63	3.18	6.24
		20	9.64	5.18	4.54	11.85
sc-CO_2 + benzene	313.2	10	7.86	4.41	4.01	9.86
		20	10.90	5.10	4.62	12.89
	323.2	10	4.65	3.45	3.11	6.58
		20	10.07	4.93	4.41	12.05
sc-CO_2 + toluene	313.2	10	7.84	4.48	4.01	9.88
		20	10.88	5.17	4.62	12.90
	323.2	10	4.64	3.52	3.11	6.60
		20	10.05	4.99	4.41	12.06
sc-CO_2 + cyclohexane	313.2	10	7.78	4.41	3.92	9.77
		20	10.82	5.10	4.53	12.79
	323.2	10	4.58	3.45	3.03	6.48
		20	9.99	4.93	4.32	11.95
sc-CO_2 + ethanol	313.2	10	7.73	4.85	4.86	10.34
		20	10.77	5.54	5.47	13.29
	323.2	10	4.53	3.88	3.95	7.15

		20	9.95	5.36	5.25	12.46
sc-CO_2 + methanol	313.2	10	7.70	5.02	5.00	10.46
		20	10.74	5.71	5.62	13.40
	323.2	10	4.49	4.06	4.09	7.31
		20	9.91	5.54	5.39	12.57
sc-CO_2 + acetone	313.2	10	7.72	4.93	4.25	10.09
		20	10.76	5.62	4.86	13.08
	323.2	10	4.51	3.96	3.35	6.88
		20	9.93	5.44	4.65	12.24
sc-CO_2 + n-hexane	313.2	10	7.69	4.41	3.91	9.69
		20	10.74	5.10	4.52	12.72
	323.2	10	4.49	3.45	3.02	6.41
		20	9.91	4.93	4.31	11.87
sc-CO_2 + diethyl ether	313.2	10	7.67	4.55	4.16	9.84
		20	10.72	5.24	4.77	12.85
	323.2	10	4.46	3.59	3.26	6.59
		20	9.89	5.07	4.56	12.01

4.2.3 Miscibility predictions for the selection of the best cosolvent

The miscibility of oleic, linoleic and α-linolenic acid (as model fatty acids from microalgae) and β-carotene (as model carotenoid also contained in microalgae) in sc-CO_2 and its mixtures with several organic solvents was estimated by using the R_a parameter. The smaller the R_a value of the SCM, the more the miscibility of the bioactive compound

in the SCF. Consequently, and according to the theory, the SCM with the lowest R_a would represent the most suitable supercritical solvent.

First of all, **Publication II** aimed to predict the best cosolvents to improve the solubilization of oleic and linoleic acid in sc-CO_2 by using the HST and involving eight organic cosolvents to achieve this goal. Some of them were allowed in the manufacture of foodstuff: acetone, cyclohexane, diethyl ether, ethanol, n-hexane and methanol [100]. The remainder solvents were acceptable in pharmaceutical production: benzene and toluene [101]. Since after **Publication II** it was established that HST does not predict a correct interaction between ring-structure cosolvents and the target compounds, these organic cosolvents (cyclohexane, benzene and toluene) did not participate in the predictions of **Publications III** nor **IV**, so only solvents permitted in food production were considered.

Water was not considered as a cosolvent for either case since it was corroborated that a mixture of sc-CO_2 with a volume fraction of 5 % water was not a homogeneous supercritical phase within the explored interval of operating conditions studied in this thesis. On the other hand, in this research, we wanted to obtain oil extracts rich in active compounds, and it was our experience that water forms emulsions with oily extracts, hampering the extraction.

Table 4.7 shows the R_a values between oleic, linoleic and α-linolenic acids and supercritical solvents at a cosolvent volume fraction of 5 % in CO_2. As can be seen, in the case of oleic and linoleic acids, at the conditions tested in **Publication II**, the best

cosolvents, by decreasing order, were benzene, toluene, cyclohexane, ethanol, methanol, acetone, n-hexane and diethyl ether. Likewise, at the conditions tested in **Publication III**, the same cosolvent order was found for α-linolenic acid, but without take into account the ring-structure cosolvents. Moreover, according to Table 4.7, the highest pressure always resulted in the lower R_a values and therefore better miscibility condition, due to the subsequent increase in the solvent density and the corresponding increase in the solvation power.

Table 4.7. R_a values between oleic, linoleic and α-linolenic acids and supercritical solvents at a cosolvent volume fraction of 5 % in CO_2.

Solvent	**Oleic acid**		**Linoleic acid**		**α-Linolenic acid**
	313.2 K				**305.2 K**
	10 MPa	**20 MPa**	**10 MPa**	**20 MPa**	**20 MPa**
sc-CO_2 + benzene	16.18	10.25	20.77	14.78	-
sc-CO_2 + toluene	16.22	10.30	20.81	14.83	-
sc-CO_2 + cyclohexane	16.34	10.41	20.94	14.94	-
sc-CO_2 + ethanol	16.39	10.51	20.95	14.98	13.76
sc-CO_2 + methanol	16.47	10.62	21.02	15.06	13.84
sc-CO_2 + acetone	16.49	10.62	21.06	15.10	13.89
sc-CO_2 + n-hexane	16.52	10.58	21.12	15.12	13.89
sc-CO_2 + diethyl ether	16.54	10.62	21.13	15.13	13.90
sc-CO_2	17.26	11.05	21.85	15.57	14.29

Finally, for β-carotene, the most adequate cosolvents at the operating conditions explored in **Publication IV**, were ethanol, hexane, acetone and methanol, as can be seen in Table 4.8. As an interesting result, this ranking did not correspond to the solubility of

β-carotene in the cosolvents studied at NTP, which were published elsewhere [121] and was by decreasing order: n-hexane, acetone, ethanol and methanol.

Table 4.8. R_a values between β-carotene and supercritical fluids (sc-CO_2 and its mixtures) at 20 MPa, 313.2 K and a cosolvent volume fraction of 5%.

Solvent	**R_a**
sc-CO_2 + ethanol	12.14
sc-CO_2 + hexane	12.14
sc-CO_2 + acetone	12.21
sc-CO_2 + methanol	12.26
sc-CO_2	12.63

The entrainer effect is obtained when there are specific interactions between the cosolvent and the target compound, such as dipole-dipole, dipole-induced dipole, induced dipole-induced interactions (dispersion) and other specific interaction such as hydrogen bonding [120]. The long chain target compounds studied in this thesis mainly interacted through dispersion forces, due to the non-polar nature of all of them. Regarding this, in all cases studied in this thesis, the addition of an organic cosolvent to the sc-CO_2 improved the miscibility of the bioactive compound due to the fact that the addition of cosolvents increased mainly the dispersion (δ_d) contributions in sc-CO_2 (see Table 4.6), thus decreasing the energy difference (R_a) between the target compound and the SCM.

4.2.4 Prediction of the impact of the amount of cosolvent on the miscibility enhancement

In addition to predicting the best cosolvent to improve the selectivity of sc-CO_2 extraction, the impact of the amount of cosolvent on the miscibility enhancement was investigated. As model compounds, oleic and α-linolenic acids were chosen. Figure 4.9 shows the miscibility enhancement of oleic (see Figure 4.9a) and α-linolenic acid (see Figure 4.9b) with increasing ethanol concentrations at raising pressures predicted by the Hansen approach. To do so, the percentage reduction of the R_a values of the mixture sc-CO_2 + ethanol in relation to pure sc-CO_2 was plotted as a function of increasing volume fraction of ethanol, as described Equation (3.6). For both cases, a non-linear relationship between miscibility enhancement and the cosolvent concentration was observed, mainly at the highest pressures. Moreover, the miscibility enhancement was higher at low cosolvent concentrations and low pressures, being almost linear at 10 MPa for both oleic and α-linolenic acid. At higher pressures, the miscibility in the solvent mixture decreased at ethanol concentrations above a volume fraction of 15 % for oleic acid and 25 % with α-linolenic acids. This behaviour has been also experimentally detected for different systems [66,120,122] and could be explained due to the reduction of the molar volume of the solvent mixture with the increase of pressure and the cosolvent fraction and to the self-association of the cosolvent. Although these cannot be the only explanations, given that for the same cosolvent, the reduction in the miscibility enhancement does not always occur at the same pressure and concentration, as can be seen by comparing Figure 4.9a and Figure 4.9b. Therefore, it must also be related to the target compound. To sum up and based on the predictions made by the HST, the lower the miscibility of the compound of

interest in sc-CO_2 alone, the higher the concentration of cosolvent and the pressure needed to observe the bending phenomenon of the miscibility enhancement curves.

4.2.5 Validation of predictions: Selective extraction of fatty acids

As has been mentioned previously, predictions were first validated with equilibrium data and afterwards with extraction yields of oleic, linoleic and α-linolenic acids from *T. suecica* and β-carotene from *D. salina*. First of all, predictions done in **Publication II** and **Publication III** and reported in Table 4.7 were validated with bubble pressures of oleic, linoleic and α-linolenic acids in sc-CO_2 and its SCM with cosolvents used in food and pharmaceutical applications. The experimental data were obtained in a high-pressure variable volume view cell, following the static synthetic method described in Section 3.3.4 and with a 5 % mass fraction of cosolvent in the SCM. Considering the conditions specified in **Publications II** and **III**, the bubble pressures of oleic and linoleic acid in the supercritical solvents were obtained at 313.2 K and a molar fraction of 0.003 fatty acid. In the case of α-linolenic acid, the bubble pressures were obtained at 305.2 K and a molar fraction of 0.0015. Table 4.9 compiles this information, where the standard deviations in bubble pressures were on average 0.1 MPa. Due to equipment limitations, it was not possible to measure neither the bubble pressures of oleic acid in the SCM with methanol nor those bubble pressures of α-linolenic acid in the SCM made up of sc-CO_2 with methanol, acetone and diethyl ether.

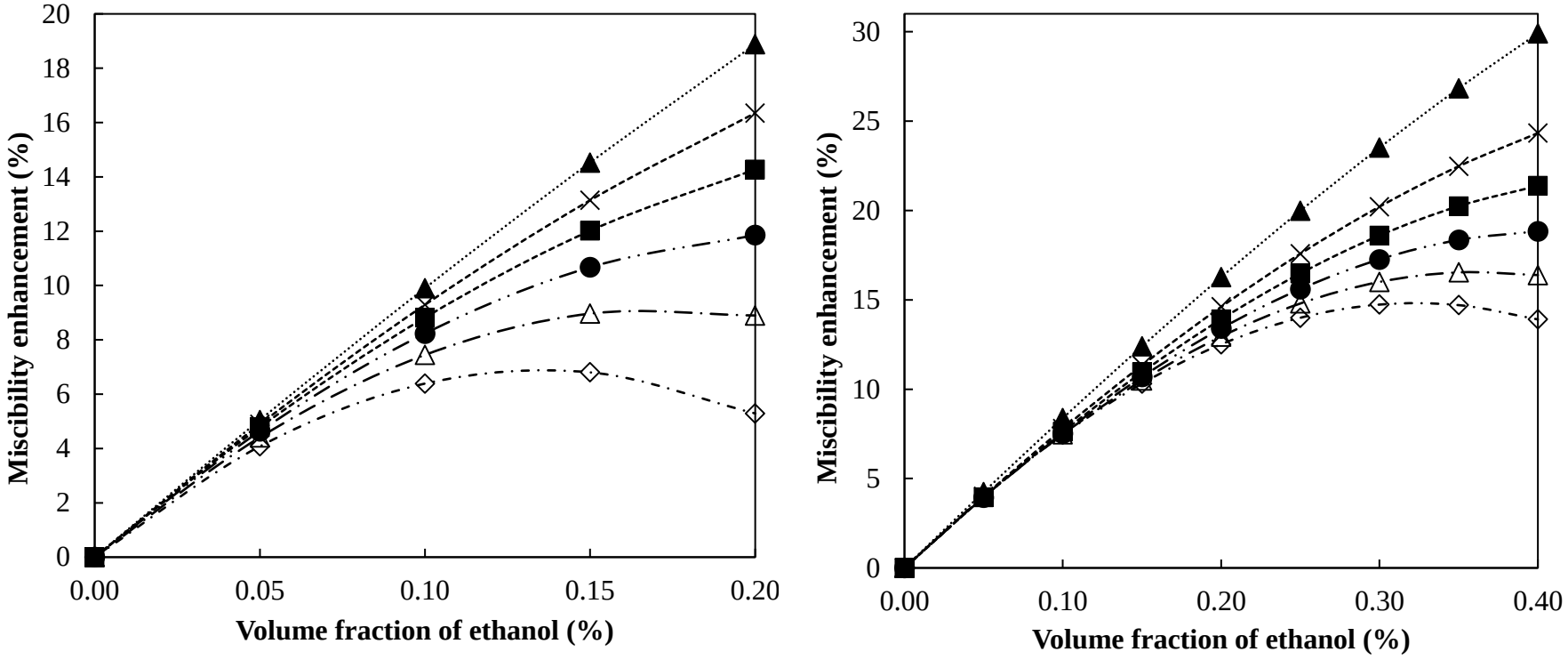

a) b)

Figure 4.9. Predicted miscibility enhancement of a) oleic and b) α-linolenic acid in CO_2 + ethanol at 313.2 K and 10 MPa (▲), 20 MPa (x), 30 MPa (■), 40 MPa (●), 50 MPa (Δ) and 60 MPa (◊) by the Hansen approach.

Table 4.9. Bubble pressures (MPa) for oleic, linoleic and α-linolenic acids with a cosolvent mass fraction of 5 % in sc-CO_2.

Solvent	**Oleic acid**	**Linoleic acid**	**α-Linolenic acid**
	313.2 K and *x* = 0.003*		**305.2 K and *x* = 0.0015***
sc-CO_2 + benzene	16.2	16.3	-
sc-CO_2 + toluene	15.8	18.0	-
sc-CO_2 + cyclohexane	17.2	17.4	-
sc-CO_2 + ethanol	10.4	9.6	12.1
sc-CO_2 + methanol	Not measured	10.6	-
sc-CO_2 + acetone	12.8	12.4	-
sc-CO_2 + n-hexane	16.9	15.5	12.8
sc-CO_2 + diethyl ether	17.1	17.4	-
sc-CO_2	22.3	22.2	13.0

*x: fatty acid molar fraction

In Table 4.9, the lower the bubble pressure the higher the miscibility. Therefore, by comparison of the cosolvent order predicted and shown in Table 4.7 with the equilibrium pressures reported in Table 4.9, it could be seen that the experimental results agreed with predictions made through the HST, except for the cosolvents with a ring structure. This result was not expected, but apparently, at supercritical conditions the ring structure in the cosolvents tested (cyclohexane, benzene and toluene) provided to the molecule with stability that was not predicted by the GCM used in the Hansen approach, avoiding the required entrainer – solute interactions to promote the cosolvent effect. As a

result, the best cosolvents for the solubilisation of oleic, linoleic and α-linolenic acids, at the conditions specified, were the short-chain alcohols, being ethanol the best.

Then, the utility of the HST to reach the selective extraction of oleic, linoleic and α-linolenic acid from *T. suecica* was tested (**Publication III**). Pure sc-CO_2 and two mixtures of sc-CO_2 with 5 % of ethanol (best predicted) or n-hexane (worse predicted) were used as solvents at 20 MPa and 305.2 K to validate the predictions reported in Table 4.7. To do so, the fatty acids concentration was analysed in the extract. The initial oil content in *T. suecica* was quite low (0.03 kg oil extract kg dried *T. suecica*$^{-1}$), as shown in Table 3.1. However, 50 % of the total oil contained in the microalgae was extracted at 20 MPa and 305.2 K by using 18 kg CO_2 kg dried *T. suecica*$^{-1}$ over a 180 min period.

Table 4.10 shows that the amount of the three fatty acids was much higher in the oil obtained with sc-CO_2 and ethanol. i.e., the obtained extract with pure sc-CO_2 contained approximately 14.9 %, 3.7 % and 15.7 % of oleic, linoleic and α-linolenic acid, respectively; while the obtained extract with the sc-CO_2-ethanol mixture contained 52 %, 54 % and 61 % more. The mean standard deviation for the fatty acid concentration in Table 4.10 was 0.5 % mass fraction. The use of both cosolvents improved the selective extraction of fatty acids from the microalgae, with the largest increase occurring in the mixture made up of CO_2 + ethanol, which agreed with the predictions based on the R_a values contained in Table 4.7.

Table 4.10. Fatty acids content in the oil extracts obtained from *Tetraselmis suecica* at 305.2 K, 20 MPa and a cosolvent mass fraction of 5 % in sc-CO_2.

Solvent	Mass fraction of the fatty acid in the extract (%)		
	Oleic acid	**Linoleic acid**	**α-Linolenic acid**
sc-CO_2	14.9	3.7	15.7
sc-CO_2 + n-hexane	15.7	3.9	16.1
sc-CO_2 + ethanol	22.7	5.7	25.3

4.2.6 Validation of predictions: Selective extraction of β-carotene

Firstly, equilibrium pressures of β-carotene in sc-CO_2 and its mixtures with a 5 % mass fraction of acetone, ethanol, n-hexane and methanol as cosolvents were measured. Results are reported in Table 4.11 and as can be seen, the best cosolvent for the solubilization of β-carotene in sc-CO_2 was ethanol followed by n-hexane, acetone and methanol. Accordingly, the addition of a mass fractions of 5 % ethanol to the sc-CO_2 significantly reduced the equilibrium pressure from 26.0 MPa to 14.6 MPa, which was consistent with the predictions made through the HST and reported in Table 4.8.

Extraction data from our laboratory was also used to validate the predictions from Table 4.8. The total extraction time during the supercritical fluid extractions for these validations was set at the beginning of the plateau of the time versus extraction yield curve, at the highest CO_2 density (30 MPa and 308.2 K). Figure 4.10 shows that, at these conditions, the beginning of the plateau was observed around 180 min. Moreover, these assays were carried out using a solvent flow rate of 0.18 kg CO_2 h^{-1}, which provided a

CO_2 consumption of 54 kg CO_2 kg dried *D. salina*$^{-1}$. By using this solvent ratio of pure sc-CO_2 a yield of 64 g oil extract kg dried *D. salina*$^{-1}$ (6.4 %) was obtained, which was equivalent to roughly 30.5 % of the total extractable oil in the microalgae based on the Soxhlet extraction (see Table 3.1 and Table 4.12). The higher total yield with n-hexane was probably due to the less selective extraction for neutral lipids of this organic solvent.

Table 4.11. Bubble pressures (MPa) for β-carotene at 333.2 K and a molar fraction of 4 10^{-7} in sc-CO_2 and supercritical mixtures with a cosolvent mass fraction of 5 % in sc-CO_2. Mean standard deviation: 0.2 MPa.

Solvent	**Equilibrium pressure (MPa)**
sc-CO_2 + ethanol	14.6
sc-CO_2 + n-hexane	16.1
sc-CO_2 + acetone	17.7
sc-CO_2 + methanol	18.2
sc-CO_2	26.0

However, it was decided to proceed with the comparisons in the extraction yield and selectivity to carotenoids, using 20 MPa instead of 30 MPa, as one of the purposes of using cosolvent during supercritical extractions is to reduce operating conditions, which are directly related to operation and capital expenditure.

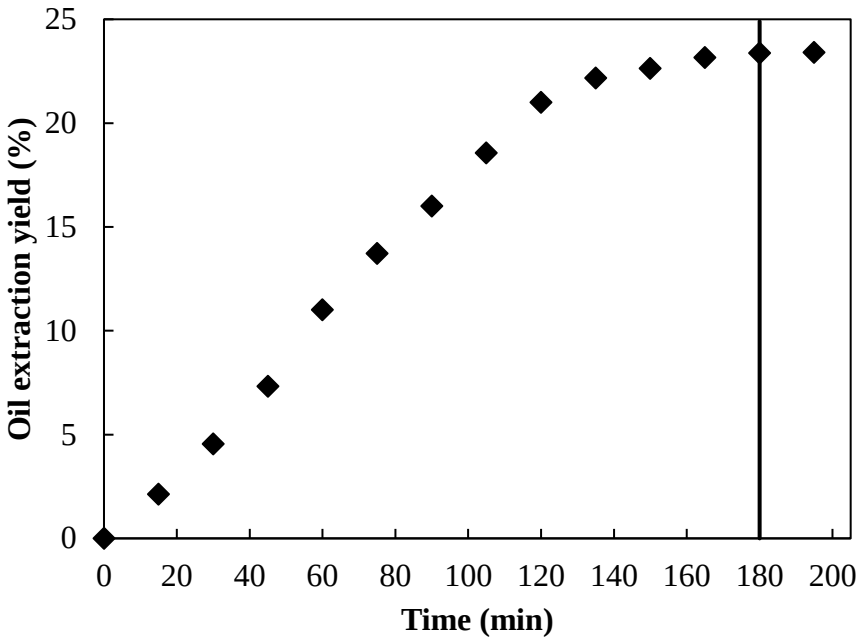

Figure 4.10. Oil extraction yield as a function of time of carotenoid-rich oil from *Dunaliella salina* at 30 MPa, 308.2 K and 0.18 kg CO_2 h^{-1}. A time of 180 min was selected to perform the following supercritical extractions.

Table 4.12 shows the total oil and carotenoids extraction yield from *D. salina* at 180 min, 54 kg solvent (pure CO_2 or solvent mixture) kg dried microalgae^{-1} and different operating conditions when using sc-CO_2 and its mixtures with methanol and ethanol at a mass fraction of 5 %. Again, the cosolvent remaining could not be tested due to safety considerations. Moreover, based on the analysis of the microalgae provider, the β-carotene represented a mass fraction of 86 % of the total carotenoids content. Therefore, the β-carotene was assumed as the most abundant compound present in the enriched-carotenoid extract reported in Table 4.12. In Table 4.12, the maximum standard deviation was 4 % in mass fraction and 10 % in mass fraction for oil and carotenoids yield, respectively.

Table 4.12. Total oil and carotenoids extraction yield from *Dunaliella salina* at 180 min and 54 kg solvent (pure CO_2 or solvent mixture) kg dried microalgae^{-1}.

Pressure (MPa)	**Temperature (K)**	**Oil extraction yield (g oil extract kg microalgae^{-1})**	**Carotenoids extraction yield (g carotenoids kg microalgae^{-1})**	**Ratio Carotenoids/Oil**
Pure sc-CO_2				
	308.2	33	4	0.12
20	318.2	38	6	0.16
	328.2	45	12	0.27
	308.2	56	15	0.27
30	318.2	58	18	0.31
	328.2	64	23	0.36
sc-CO_2 + 0.05 kg methanol kg solvent^{-1}				
20	308.2	40	6	0.15
	318.2	42	9	0.21
sc-CO_2 + 0.05 kg ethanol kg solvent^{-1}				
20	308.2	49	11	0.22
	318.2	54	25	0.46

The addition of a mass fractions of 5 % ethanol to the sc-CO_2 significantly increased the affinity of sc-CO_2 for the β-carotene, which agreed with the prediction made by the Hansen approach. As shown, extraction from *D. salina* at 318.2 K and 20 MPa, resulted in a carotenoid extraction yield of 25 g carotenoids kg microalgae^{-1}, which was more than four times than in pure sc-CO_2 (6 g carotenoids kg microalgae^{-1}). Furthermore, the selectivity of the extraction was enhanced as the carotenoid concentration in the extract was increased from 16 % when using sc-CO_2 alone to 46 % if a mixture sc-CO_2-5 % ethanol was utilized.

The β-carotene extraction yields notably increased with pressure due to the subsequent increase of the solvent density and solvent capacity. However, the impact of temperature was not well foreseen. R_a values were lower at higher temperatures suggesting a higher extraction yield with all the SCF involved. On the contrary, the β-carotene content in the extract was higher at the highest temperature in all cases. As an example, carotenoids content in the extract obtained using sc-CO_2 + 0.05 kg ethanol kg solvent^{-1} at 20 MPa and 318.2 K was 25 g carotenoids kg dry microalgae^{-1}, while at 308.2 K it was 11 g carotenoids kg microalgae^{-1}. This positive impact of temperature on carotenoids extraction yield was initially unexpected since a rise in temperature reduces the density of the supercritical solvent, which reduces its solvent power as reflected in the R_a values. However, temperature positively affects the mass transfer. For instance, temperature increases the solute´s effective diffusivity within the solid and external transportation into the bulk of the supercritical phase and promotes the cell wall to rupture, so the sc-CO_2 could then extract more lipids [107] and so more carotenoids.

Moreover, a rise in temperature increases the solute vapour pressure as expressed in the Antoine equation. At low pressures, the density effect is predominant and therefore the extraction is better at low temperature, whereas if the pressure is high, higher temperatures benefit the extraction due to the increase in the solute vapour pressure. Therefore, the isotherms in the pressure-solubility diagrams intersect at a point called the crossover point, which represents the pressure at which the operating temperature increase, benefits the extraction [49]. Mendes *et al.*, [123] reported the crossover point of β-carotene between 15 MPa and 17 MPa. Then, at higher pressures, the solubility of this compound both in pure and ethanol-modified CO_2 increased when raising temperature from 313.2 K to 333.2 K. The Hansen theory approach takes into account neither the increase of the solute volatility with temperature, nor the enhancement of the kinetic which could turn into an inconvenient for the HSP approach when predicting the best conditions for an extraction.

As another interesting finding, the carotenoids extraction yields reported in this research thesis represent the highest values reported in the literature. As examples, the highest carotenoids content reported by Jaime *et al.* [124] was 4.74 g carotenoids kg dry microalgae^{-1} at 43.7 MPa, 298.85 K, working at the subcritical condition of CO_2, and 120 kg CO_2 kg dry microalgae^{-1}. Macías-Sánchez *et al.* [125], on their part, reported almost 15 g carotenoids kg dry microalgae^{-1} at 30 MPa, 333.2 K using 360 kg CO_2 kg dry microalgae^{-1}. However, in this work, by using only 54 kg CO_2 kg dry microalgae^{-1}, 23 g carotenoids kg dry microalgae^{-1} were extracted at 30 MPa and 328.2 K. Even better extraction yield (25 g of carotenoids kg of dry microalgae^{-1}) was obtained with the same

CO_2 consumption, using ethanol as a cosolvent under milder conditions of both pressure (20 MPa) and temperature (318.2 K).

4.3 Encapsulation of astaxanthin by continuous Supercritical Fluid Extraction of Emulsions

One of the objectives of this thesis was the subsequent encapsulation by advanced supercritical techniques (SFEE in this case) of the bioactive compounds extracted by supercritical fluid extraction. In **Publication IV**, the selective supercritical extraction of β-carotene was performed with the help of the Hansen approach; however, Professor María José Cocero's research group from Valladolid had already studied the encapsulation of this compound by means of the SFEE technique [126]. Moreover, the encapsulation by SFEE of hydroxytyrosol-rich oil extracts and the high-value fatty acid-rich oil extracts were also studied by our own research group in the works published by Calvo *et al*., [127] and Prieto and Calvo [128], respectively; so scientific novelty was compromised. In view of the above, it was decided to encapsulate astaxanthin (another interesting carotenoid from the microalgae *H. pluvialis*) by SFEE. Nevertheless, considering that Cocero's research group, by modifying a SAS equipment encapsulated the extract of shrimp residue rich in astaxanthin using SFEE [129], it was decided to encapsulate this compound in ethyl cellulose, a starch recently proposed as a possible food-grade carrier [78], by means of a high-pressure packed tower in counter-current mode. For this, research stay of almost four months was done in Professor Ernesto Reverchon’s laboratory at the University of Salerno (Italy), from which **Publication V** was derived.

Therefore, as a final section of this thesis, the effectiveness of the SFEE technology in a continuous layout for the encapsulation of astaxanthin in ethyl cellulose was addressed. The micronisation of ethyl cellulose alone and the study of the impact of its concentration in the organic phase was first studied. The surfactant (Tween 80) concentration in the aqueous phase was also examined. Afterwards, the antioxidant capacity of the elaborated particles containing astaxanthin and its release behaviour in SIF were investigated. Into the bargain, looking for a final food-grade product, all the component involved in the production of the particles were approved by the FDA [93].

4.3.1 The influence of the operating conditions

It is relevant to choose the right pressure and temperature to perform the SFEE process, since these operating conditions should enhance the extraction of the organic solvent from the emulsion, avoiding the dissolution of the polymer and the bioactive compound in the sc-CO_2 and circumventing the emulsion loss by washing out in the sc-CO_2 stream. Thus, the high-pressure vapour–liquid equilibria (VLE) of the pseudo-binary system ethyl acetate/CO_2 was used to establish the operating conditions above the critical point of the SCM that should maximise the solvent extraction from the emulsion. The literature reports that at 311.2 K the mixture ethyl acetate/sc-CO_2, with a CO_2 molar fraction of 0.9, is supercritical at 8 MPa [92,130]. It is also well known that water is only slightly soluble in sc-CO_2 at these operating conditions [131]. Besides, a temperature of 311.2 K is also compatible with the glass transition temperature of ethyl cellulose, which is located at about 406.2 K [132].

On the other hand, to reduce energy costs, it was not considered to use a higher pressure since in a previous work carried out by Reverchon's group at the University of Salerno [92], a solvent residue of less than 50 ppm ethyl acetate was achieved when performed the micronisation of poly(lactic-co-glycolic acid) (PLGA) at 311.2 K and 8 MPa and the same length of the column used in this work, which allows the use of the obtained particles in the pharmaceutical [101] and food industry [100] (the limit is 5000 ppm). Furthermore, in the same work [92], microspheres coalescence was observed working at higher pressures. Another of the reasons why it was decided to work at the lowest pressure, was that the density difference between the emulsion and the sc-CO_2 was larger. By fixing the temperature at 311.2 K and operating at 8 MPa, the maximum difference in density between the emulsion and sc-CO_2 is obtained because they are of 1000 kg m^{-3} against 300 kg m^{-3}, respectively [92]. This favoured the existence of two distinct phases along the column and, therefore, its proper functioning avoiding flooding.

Finally, the ratio between the emulsion and the sc-CO_2 (L/G) was fixed at 0.1 according to previous works, which optimised CO_2 and emulsion flow rate [133]. In that work, when an overall amount of 0.40 kg CO_2 was contacted with 0.04 kg emulsion for 40 min, low values of solvent residue (between 40 ppm and 50 ppm) were obtained. Consequently, a CO_2 flow rate of 1.4 kg h^{-1} and an emulsion flow rate of 1.4 10^{-4} m^3 h^{-1} were used to perform the astaxanthin encapsulation in this thesis.

4.3.2 Selection of the starting emulsion

Considering that the dispersed phase of the emulsion acts as a template for future particles, special attention must be paid to the starting formulation of the emulsion to be processed by SFEE. Based on the selection of components and composition, a droplet size can be provided and therefore the future structure and stability of the particles.[90]. In view of the above, different emulsion formulations were prepared and processed by SFEE varying polymer and surfactant concentration. The results obtained in terms of MD are presented in Figure 4.11. Additionally, the ANOVA test developed revealed that surfactant and polymer concentration, and their interactions, had a statistically significant effect on MD at a 95 % confidence level.

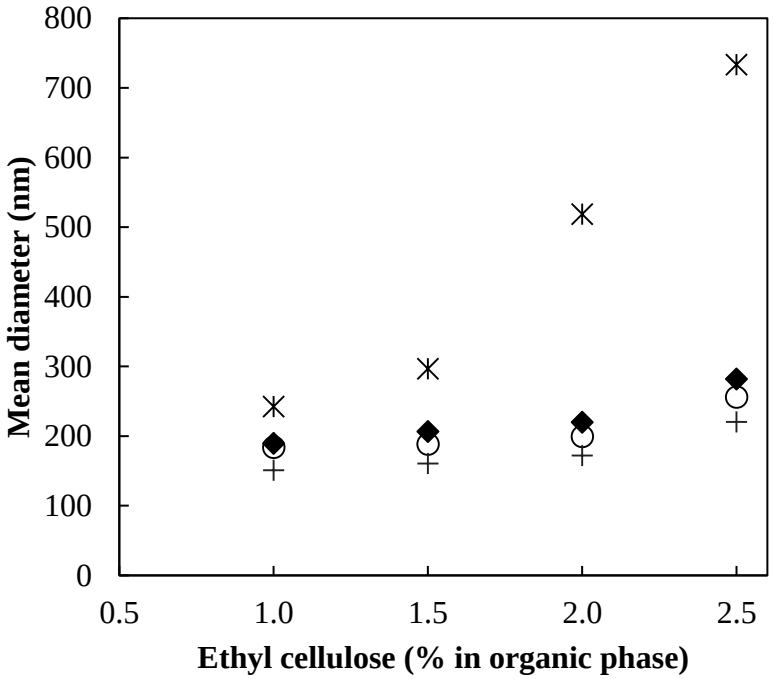

Figure 4.11. Effect of surfactant and polymer concentration on the particle mean diameter. Tween 80 concentration of 0.1 % (✳), 0.2 % (♦), 0.3 % (○) and 0.6 % (Δ).

As can be appreciated in Figure 4.11 the increase in the polymer concentration increased the MD of particles. This behaviour has already been reported in the literature and can be explained by the fact that increasing polymer concentration increases the viscosity of the dispersed phase, and, the droplet size of the dispersed organic phase [134]. In fact, viscosity measurements were carried out on the four different organic phases used in our formulations. As a result, by increasing the polymer concentration, the viscosity of dispersed phase progressively increased, being 3.0 mPa.s, 4.0 mPa.s, 5.0 mPa.s and 6.5 mPa.s for 1.0 %, 1.5 %, 2.0 % and 2.5 % polymer concentrations, respectively, and the final particle size varied accordingly as proposed Calderbank (1958) in the empirical Equation (4.1):

$$d_{32} = A\left(\frac{\mu_d}{\mu_c}\right)^{0.25} \quad (4.1)$$

In Equation (4.1), d_{32} is the average diameter (Sauter's diameter) of the spheres, μ_d is the viscosity of the dispersed phase, μ_c the viscosity of the continuous phase and A is a coefficient which depends on many other factors [134]. As it is described in Equation (4.1) and shown in Figure 4.12, there was a linear relationship between the increase in particle size and the viscosity of the dispersed phase elevated to one quarter. The viscosity of the continuous phase was not modified and considered close to that of water at 298.2 K such as has been claimed in previous works [134].

It can be also seen in Figure 4.11 that, by setting the polymer concentration in the oil phase and increasing the surfactant concentration, a reduction of nanocarriers MD was observed, in the sub micro- range (from 730 nm to 150 nm). The produced particles had

PDI values from 0.15 to 0.35. Besides, there were no statistically significant differences ($p > 0.05$) among all the polymer concentrations in the PDI response. On the contrary, there were statistically significant differences ($p < 0.05$) depending on surfactant content. Moreover, lower PDI values were reached at lower surfactant contents. However, there were no differences ($p > 0.05$) among the PDI at surfactant concentration of 0.2 % and 0.3 %. A PDI value of 0.15 was achieved by using the lowest surfactant concentration, laying almost in the monodisperse range i.e. PDI lower or equal to 0.1. When the system is defined as monodisperse, all the particulate system can be treated as formed by particles of the same dimensions [136].

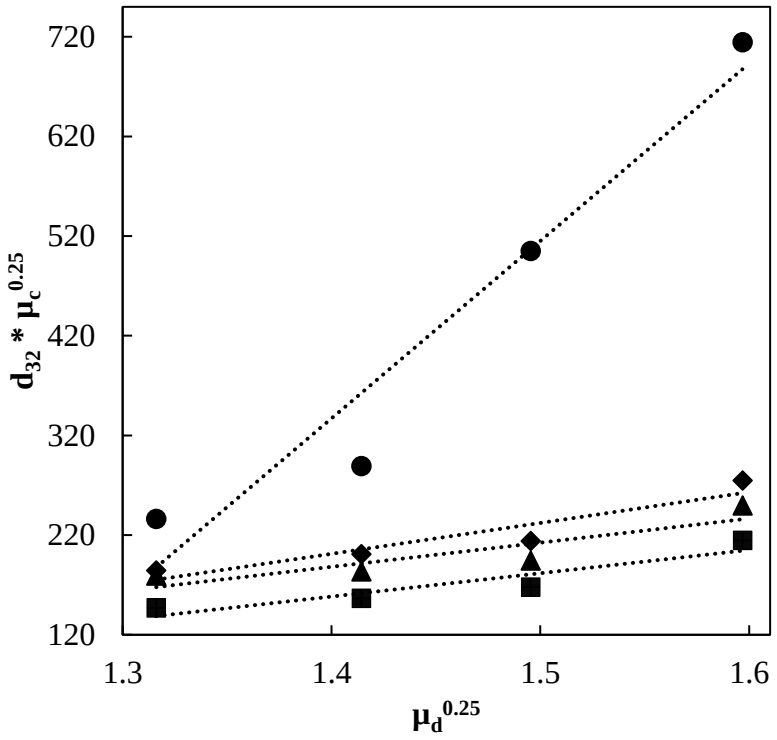

Figure 4.12. The influence of the viscosity of the dispersed phase in the particle size according to Equation (4.1). Tween 80 concentration of 0.1 % (●), 0.2 % (♦), 0.3 % (▲) and 0.6 % (■).

On the other hand, Figure 4.13 shows SEM images of the particles obtained as a function of the surfactant and polymer concentration. As can be seen, the particles obtained were spherical and some of them ellipsoidal. SEM images also show the effect of surfactant and polymer concentration on particles agglomeration and morphology. Beyond 0.3 % Tween 80, agglomeration and formation of unshaped particles was observed at all polymer concentrations. This pact was related to the fact that the higher surfactant concentration leads to a higher number of micelles produced in the emulsion, which leads to the agglomeration of the particles, thus also increasing the PDI [137]. On the other hand, at lower surfactant concentrations (0.1 % and 0.2 %), and exceeding 1.5 % ethyl cellulose, the higher the amount of polymer, the greater the agglomeration and the formation of unshaped particles.

In view of all of the above and taking into account that the surfactant and polymer expenditure could determine the costs of the particles production process [134], a surfactant concentration of 0.1 % in the organic phase was considered as the best. Another factor to choose the percentage of ethyl cellulose to encapsulate astaxanthin was the low solubility of astaxanthin in the organic phase, which conditioned the amount of polymer to use to obtain a higher astaxanthin/polymer ratio. As a result of this circumstance, the proportion of polymer in the organic phase was finally fixed at 1 % to carry out the encapsulation. Finally, an average polymer recovery mass of around 90 % was measured for all the formulations and specifically of 86 % for the formulation selected as optimal (0.1 % Tween 80 and 1.0 % ethyl cellulose), which also reached the lowest PDI value (0.15 ± 0.02).

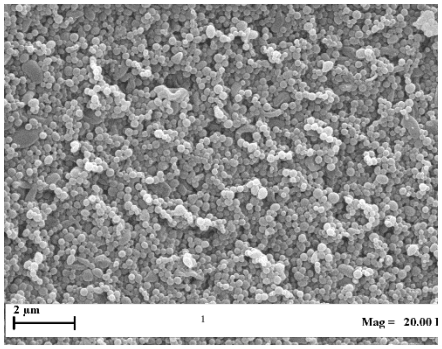

a) 1.0 % ethyl cellulose

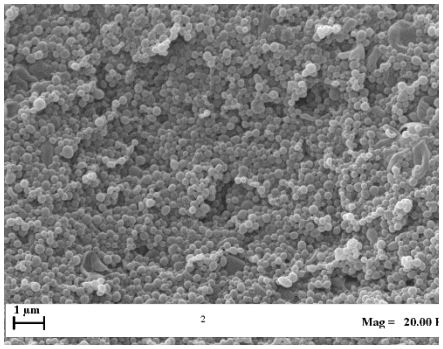

b) 1.5 % ethyl cellulose

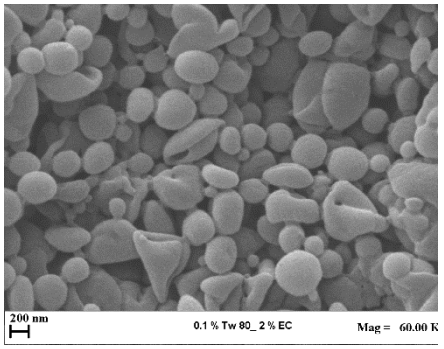

c) 2.0 % ethyl cellulose

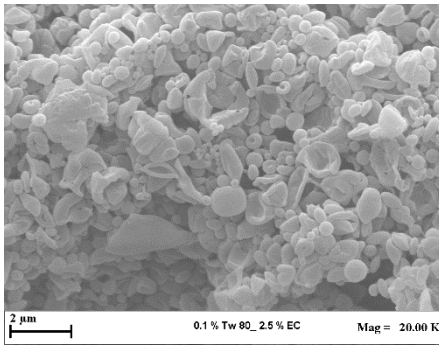

d) 2.5 % ethyl cellulose

0.1 % Tween 80

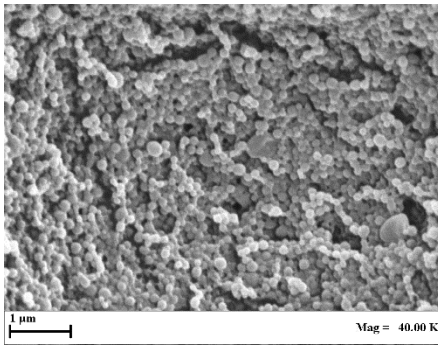

e) 1.0 % ethyl cellulose

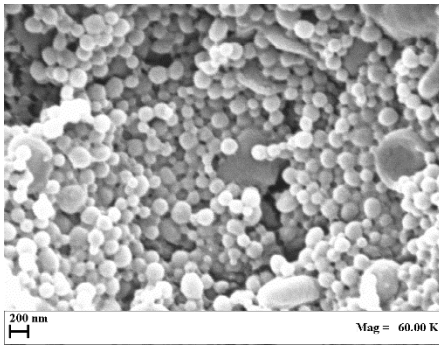

f) 1.5 % ethyl cellulose

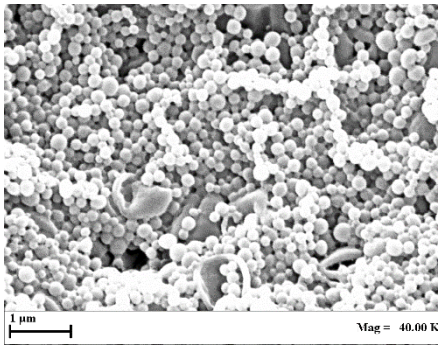

g) 2.0 % ethyl cellulose

0.2 % Tween 80

Large aggregates

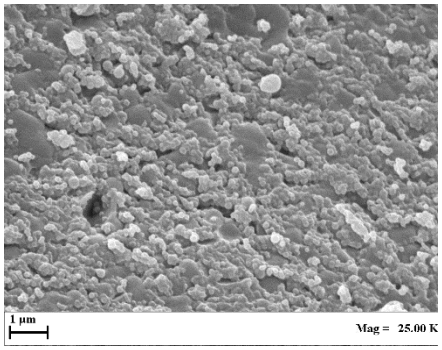

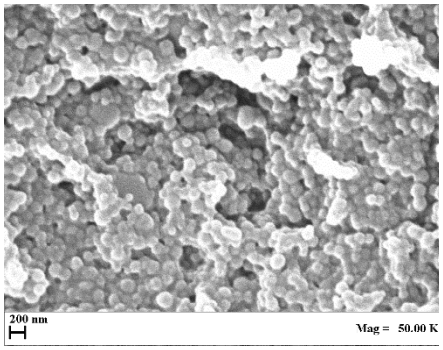

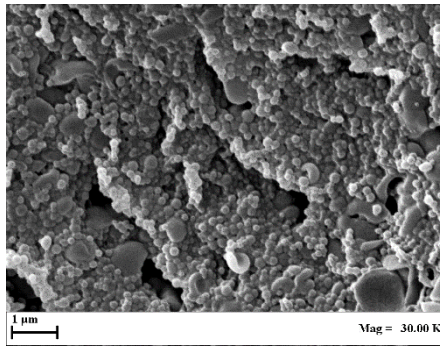

Large aggregates

i) 1.0 % ethyl cellulose j) 1.5 % ethyl cellulose k) 2.0 % ethyl cellulose

0.3 % Tween 80

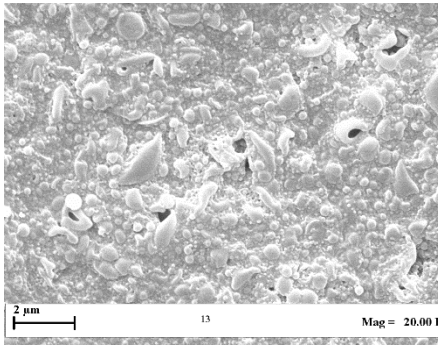

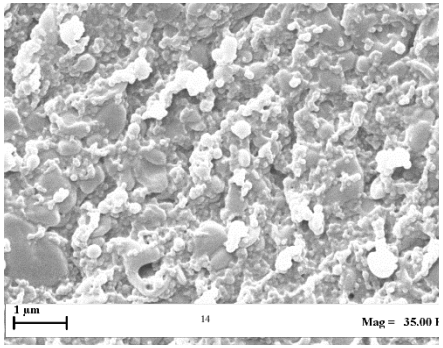

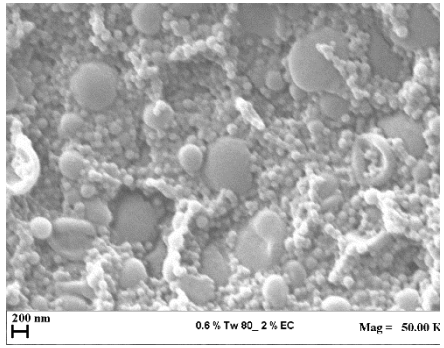

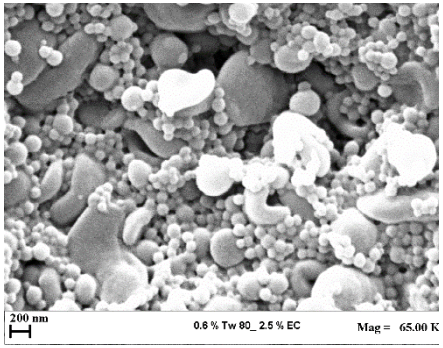

m) 1.0 % ethyl cellulose n) 1.5 % ethyl cellulose o) 2.0 % ethyl cellulose p) 2.5 % ethyl cellulose

0.6 % Tween 80

Figure 4.13. Scanning electron microscopy images of ethyl cellulose microspheres obtained at increasing polymer and surfactant concentrations.

4.3.3 A study on particle size, morphology, encapsulation efficiency, release profile and antioxidant activity of the astaxanthin loaded particles

The selected starting emulsion was further used to encapsulate astaxanthin in ethyl cellulose. As a result, spherical and some ellipsoidal particles with MD of 363 nm ± 7 nm and PDI of 0.21 ± 0.03 were obtained, as can be seen in Figure 4.14. As expected, loaded particles obtained were larger than those obtained when ethyl cellulose was micronized alone, without active compound. Regarding this, the TEM analysis (see Figure 4.15) demonstrate that the astaxanthin was uniformly dispersed within the polymer system. In Figure 4.15, dark and light regions show the stained polymer and astaxanthin, respectively.

On the other hand, an encapsulation efficiency of 84 % ± 2 % was achieved. Accordingly, the loading ratio astaxanthin/polymer was 2.1 10^{-2} kg astaxanthin kg powder^{-1}. Taking into account that there is no Recommended Daily Intake (RDI) for astaxanthin, but most studies reported beneficial results from a daily intake of 4 10^{-6} kg [138]; it would be enough for a person to take 1.9 10^{-4} kg of the powder obtained in this work to promote health benefits. This is a relatively small amount, considering that a person would need to consume from 0.6 kg of salmon to reach the recommended consumption. Alternatively, a person would have to consume roughly 0.26 kg of the shrimp, but only if the shells were also consumed [138,139]. In addition, this dose could improve many blood parameters that may well be beneficial to heart disease [139].

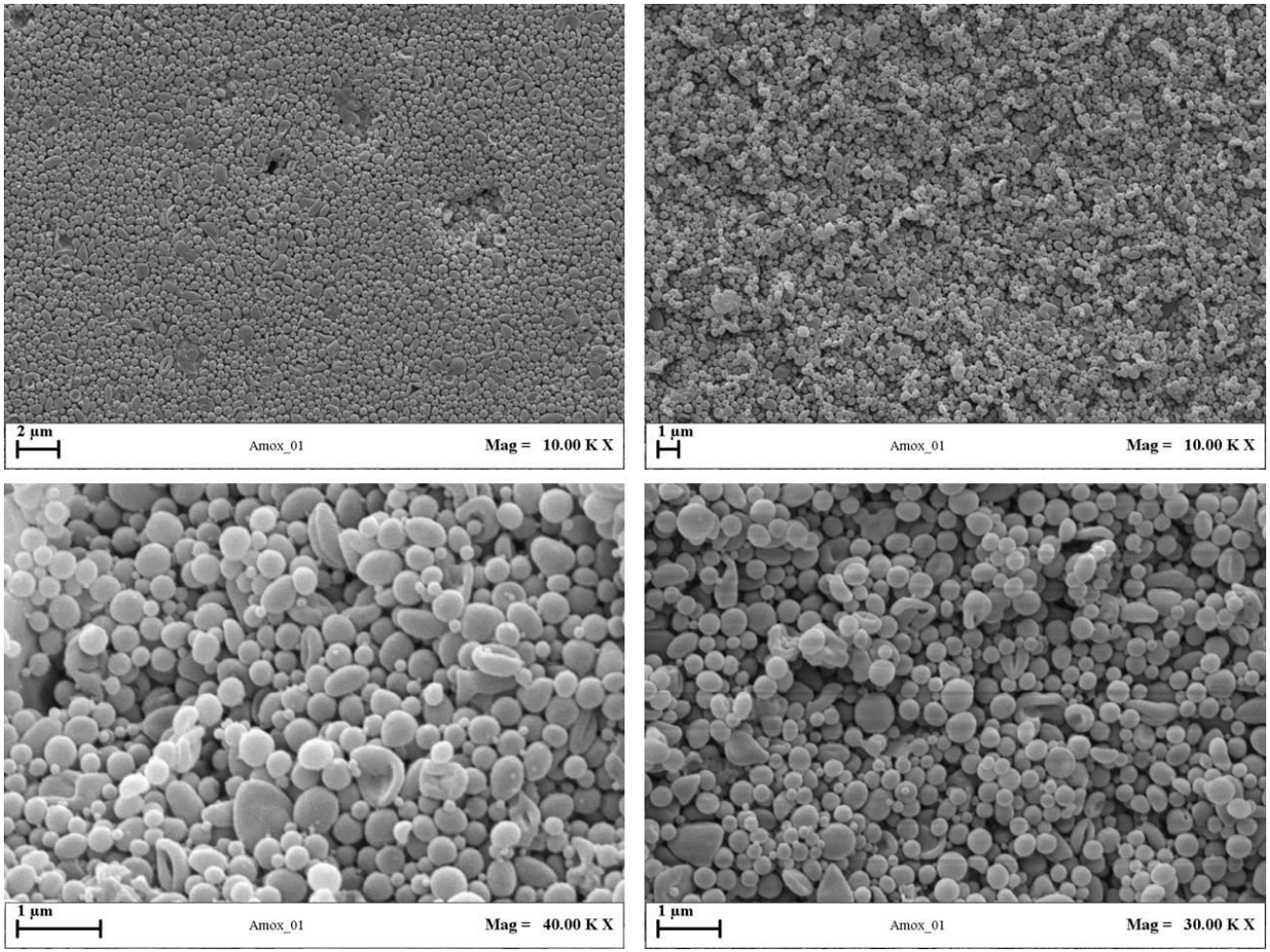

Figure 4.14. Scanning electron microscopy images at different magnifications of astaxanthin encapsulated in ethyl cellulose nanospheres produced with the optimised formulation.

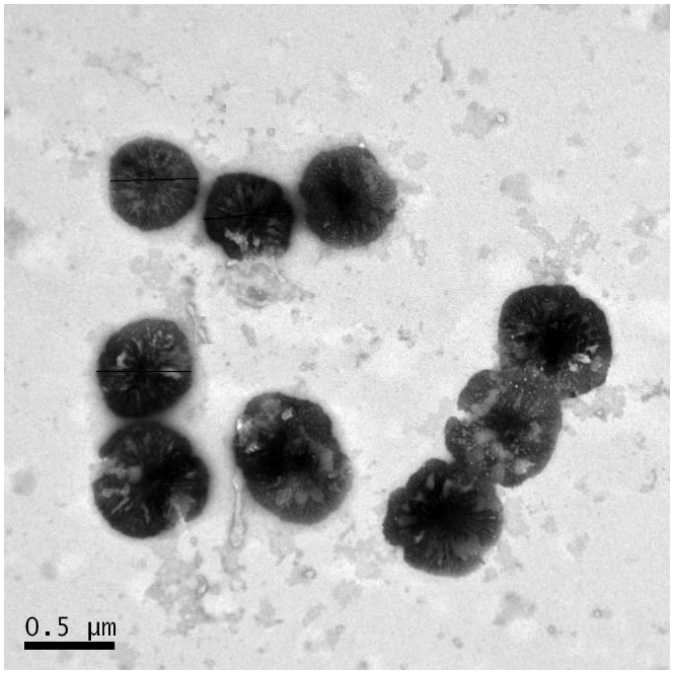

Figure 4.15. Transmission electron microscopy image of astaxanthin-loaded particles obtained by continuous Supercritical Fluid Extraction of Emulsions

Another aspect evaluated was the efficiency of ethyl cellulose as a matrix on sustaining the release of astaxanthin. To do so, experiments were performed in a SIF media with a pH value of 7.2 at 310.2 K to simulate physiological temperature. Figure 4.16 shows the obtained release profile, which was fast for the first 6 h but slowed down after about 7 h. As much as 70 % astaxanthin was released after 10 h, which could be probably caused by the looseness and solubilization of the ethyl cellulose structure in the SIF [106,140].

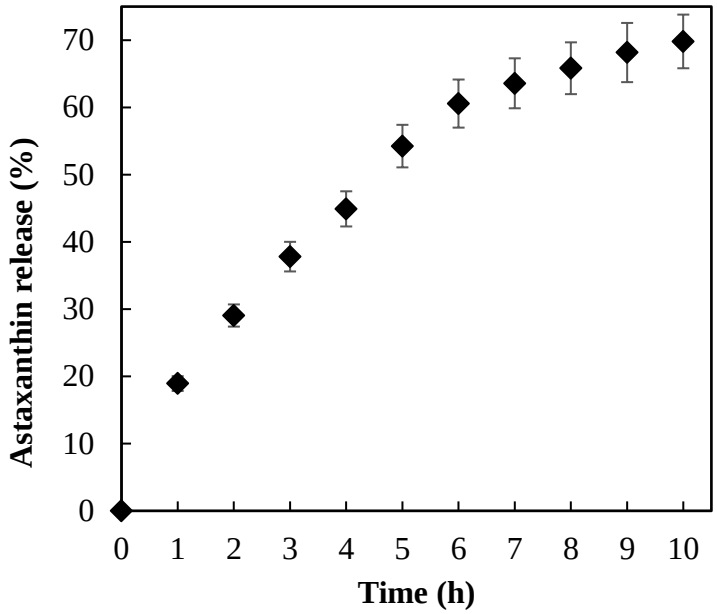

Figure 4.16. Release profiles of astaxanthin from ethyl cellulose nanocapsules in simulated intestinal fluid at pH 7.2.

Finally, the antioxidant capacity of the elaborated particles containing astaxanthin was measured by using radical scavenging assays with DPPH; and as a result, the TEAC of the encapsulated astaxanthin was (77.26 ± 2.60) M Trolox equivalent kg powder^{-1}. By dividing this antioxidant capacity by the encapsulation efficiency (2.1 10^{-2} kg astaxanthin kg powder^{-1}) approximately 3,700 M Trolox equivalent per kg of astaxanthin was found. Thus, this value corresponds to the antioxidant capacity of the astaxanthin contained within the particles. Additionally, the antioxidant capacity of the astaxanthin before being encapsulated was measured to investigate the impact of the SFEE procedure. The TEAC value of the free astaxanthin was (3,900 ± 200) mM Trolox equivalent per kg astaxanthin^{-1}, which means that the astaxanthin did not significantly deteriorate during the processing and encapsulation, probably due to the low temperature and the high speed of the SFEE procedure, as well as the non-oxidizing atmosphere of the CO_2.

5. Conclusions

The initial solid condition before a supercritical fluid extraction has demonstrated to be very important to maximize the extraction yield and to improve the quality of the extract. On the one side, the initial water content must be optimised when the raw material is subjected to supercritical fluid extraction. This is not such a simple task, as there could be several scenarios. Insufficient moisture in vegetable matrices could cause the cell structure to shrink and consequently hinders diffusion, which reduces yield. However, excess water may create an extra barrier for transportation and may generate the co-extraction of polar substances, thereby reducing selectivity. This causes that the optimum moisture content for each raw material can vary greatly. For example, alperujo had to be dried to 1 % moisture as this amount of water was the best to maximize extraction. The extraction of oils rich in carotenoids and nutritive fatty acids from microalgae was best at 6 %. By chance, in both cases, the moisture content in equilibrium with the Madrid environment was the best. However, to achieve these moisture contents, it was necessary to dry the excess water content, demanding a considerable amount of energy that should be considered to run a profitable supercritical extraction process.

On the other hand, mass transfer in sc-CO_2 extraction from solid substrates in most cases depends heavily on the transport rate in the solid phase. The length of the transport path determines mass transport in the solid phase. Particles of dried alperujo with a large diameter (greater than 0.80 mm) hindered the penetration of the supercritical solvent and the solubilisation of the solute. On the contrary, too small particles (usually smaller than 0.40 mm) could represent a risk of formation of preferential channels and blockages during extraction, as discussed by the specialized engineering company Natex [108]. We observed this negative effect above all when microalgae were used, as their mean

diameter was 45 μm; so sea-sand had to be mixed with it to enhance the bed porosity. On an industrial scale, in order to make use of the material exhausted after the supercritical extraction, it would be appropriate to pellet the vegetable material. Moreover, to design the whole supercritical extraction process it must also be taken into account that milling is a very expensive pre-treatment.

Regarding the main operating variables, the increase in pressure improved the extraction rate and yield, as it is directly related to the increase in solvent density and solvent capacity. The maximum operation pressure tested in our installation was 30 MPa. At this pressure, maximum extraction yield was obtained for all the oils obtained. The enrichment of the oils in the bioactive compounds was also the highest. However, caution should be taken, as it was reported for other solids that there is a maximum increase in pressure due to the worsening of the transport properties (increased viscosity and reduced diffusion coefficient), making the internal mass transfer more difficult. A pressure of 40 MPa was established in several raw materials as the limiting value [125,141].

Likewise, the temperature plays a very important role in the extraction processes. Its increase may reduce extraction yields due to a reduction in the sc-CO_2 density. It happened on the total oil yield from microalgae, as for vegetable oils the crossover pressure is about 30 MPa [110]. Contrarily, the increase in temperature could improve the extraction of bioactive compounds, if their vapour pressure is high and because it has a positive impact on diffusion and kinetics; not to mention that temperature could also help to improve the cell opening in vegetable matrices. This indeed happened with the carotenoid concentration in the oil obtained from *Dunaliella salina*. The crossover point

for β-carotene is between 15 MPa and 17 MPa [123], much less than the oil itself. This could explain that the carotenoid proportion in the oil was highest at the highest temperature. Obviously, it is also mandatory not to overpass the deterioration temperature. Carotenoids start to decompose at 323.2 K [142]. On the contrary, the hydroxytyrosol was highest at the maximum explored temperature (373.2 K) since this compound was quite thermostable (thermal decomposition starts at 536 K [117]).

The increase in the flow rate, meanwhile, has an important impact on the extraction rate. It has to be generally high in order to improve turbulence, the mass transfer in the fluid phase and increase productivity. However, there is a maximum because an excessive velocity reduces the residence time in the extractor, hindering the sc-CO_2 to be saturated with the solute. In this sense, the bed length and porosity are important design parameters. Furthermore, the influence of the solvent flow rate cannot be discussed without considering economic consequences. The installation cost of the SCF process increases as the square root of the solvent flow rate as it has been demonstrated by Perrut [111] based on an analysis of the price index of multiple installations from pilot to industrial scale. Additionally, it conditions the consumption of the CO_2 and so the operation time for a specific production. In our installation, the optimum CO_2 flowrate was 18 kg CO_2 h^{-1} (3 g CO_2 min^{-1}) for the raw materials used in this work. The CO_2 consumption varied depending on the raw material used. This ranged from 18 kg CO_2 kg dried *D. salina*$^{-1}$ to obtain an oil extraction yield of about 30.5 % carotenoid-rich oil; through 35 kg CO_2 kg dried alperujo^{-1} in order to achieve roughly 94 % of the oil extract contained in the raw material; up to the employment of 54 kg CO_2 kg

dried *T. suecica*$^{-1}$ to get 50 % of oil extraction yield from *T. suecica*. These values of solvent ratio are in the order of magnitude as those used in large scale applications [143].

The oil extracts obtained by sc-CO_2 extraction in this research could be considered of high quality and rich in compounds of high nutritional value. The concentration of hydroxytyrosol or carotenoids that we have found in our extracts was the highest of those reported in the bibliography. Besides, the extracts were quite pure, which was an indication that they needed little or no further refinement. As a consequence, and although a detailed cost analysis would be necessary, the supercritical extraction of oils rich in antioxidants, carotenoids and fatty acids could be economically viable. Specifically, it seems to be feasible in the case of hydroxytyrosol-rich olive oil as the raw material is a waste.

When the yield or the selectivity of the extraction is low, or the operating pressure or CO_2 consumption are to be reduced, a cosolvent may be added to the supercritical solvent. The Hansen solubility theory can be used to predict the best cosolvent for sc-CO_2 in the solubilization of bioactive compounds from natural matrices within a specific interval of operating conditions. The choice of a cosolvent is not obvious because it is not the best solvent under conventional conditions, as demonstrated for β-carotene. Interestingly, another fact demonstrated by this theory is that a similar benefit cannot be attributed a priori to cosolvents of the same functional type. Methanol and ethanol led to very different results on the selective extraction of carotenoids from microalgae. The solubility enhancement effect is obtained when there are specific intermolecular interactions between the cosolvent and the solute. The goodness of the theory relies on

the fact that it considers three contributions to these interactions. Therefore, the Hansen model could justify why ethanol was the best cosolvent for sc-CO_2 in both, the solubilization of fatty acids and carotenoids by the increase of the dispersion and dipole-dipole interactions that happened under supercritical conditions with this specific cosolvent.

Another aspect that Hansen theory can correctly predict is the impact of cosolvent concentration with operating pressure. In the two cases studied in this thesis, the miscibility enhancement was predicted to be higher at low cosolvent concentrations and low pressures. Theoretically, this behaviour was explained due to the reduction of the molar volume of the solvent mixture with the increase of pressure and the cosolvent fraction. Experimentally, this conduct was related to the self-association of the cosolvent. Although these cannot be the only explanations, given that for the same cosolvent, the reduction in the miscibility enhancement did not occur at the same pressure and concentration for the two fatty acids investigated. Thus, it must also be related to the target solute. Based on the predictions we made with Hansen theory, the lower the miscibility of the compound of interest in sc-CO_2 alone, the higher the concentration of cosolvent and the pressure needed to improve its miscibility in the supercritical fluid mixture.

However, some limitations must be taken into account when implementing the Hansen approach. First of all, its use is limited regarding the predictions of the best conditions to perform the substance solubilisation and therefore the supercritical extraction. In Hansen theory, the main parameter of modification with operating

conditions is the molar volume, a purely thermodynamic property. Therefore, the effect of pressure is well predicted due to the direct relationship between pressure and density; however, the influence of temperature in extraction from a solid matrix is complex involving several mechanisms that cannot be predicted with this single approach. First, the model does not consider any kinetic phenomena that can be dominant in extraction involving solids. Regarding the thermodynamic aspects affecting the solubility, the Hansen theory does not consider a competing phenomenon that occurs when increasing temperature, i.e. the increase of solute vapour pressure; however, this effect becomes relevant at high pressures involved in supercritical extraction. A contribution of the impact of temperature on solute vapour pressure should be added to the Hansen model for this specific application for a better prediction, e.g. a term with the Antoine equation.

In the attempt to apply the Hansen solubility theory to multicomponent systems, care should be taken. Considering that the Hansen theory predicts the miscibility of pure compounds, the presence of other compounds in the matrix could interfere with the solubilization of the target compounds, improving its extraction or functioning as an anti-solvent. Clearly in the cases studied, where the oil content of the raw material was high and because its solubility is relatively high in the sc-CO_2, the main component of the extract was the oil, and therefore the extraction of the minority bioactive compounds was conditioned by this major component. Seemingly, the oil itself acted as a matrix cosolvent in the extraction of hydroxytyrosol and carotenoids, as those are quite insoluble in supercritical CO_2. This can be hardly predicted by Hansen theory.

Finally, the SFEE technology was an effective method to protect the bioactive compounds extracted by sc-CO_2 in a covering polymer. In this way, submicron structures can be obtained that would allow the incorporation of these bioactive compounds in the formulation of cosmetic and para-pharma products as well as in hydrophilic foods as all the ingredients are food approved. It was possible by tuning the initial emulsion formulation to obtain particles of varied sizes within a narrow distribution and low polydispersity. From an optimised starting formulation and working conditions, spherical particles could be produced. Besides, a homogeneous dispersion of the astaxanthin in the ethyl cellulose and a high degree of encapsulation was achieved, thus preserving its original antioxidant capacity to ensure a good-enough release.

The main particle size manipulation parameter was the viscosity of the organic phase that grew with the concentration of coating polymer. However, the amount of the polymer was constrained by the aggregation of the particles. To prevent it, it was necessary to increase the concentration of surfactant in the aqueous phase. One of the most important limitations of this technology is the solubility of the bioactive compound in the organic solvent; for astaxanthin was quite low. However, and despite its low concentration in the starting emulsion (5 g astaxanthin kg starting emulsion^{-1}), it was possible the continuous production in a packed column, increasing the production capacity and easing the scale-up. The use of a packed column also offered a greater product homogeneity and recovery.

Other drawbacks of the technology are: a) particles are obtained in aqueous suspensions that should be dried off if solid particles are required; b) the toxicological

hazards related to the addition of nanoparticles in food has yet to be reviewed [144]; c) consumption of CO_2 to exhaust the organic solvent could be quite high. For example, to reach concentrations of less than 50 ppm (which is the amount established for ethyl acetate in food products [101]) it would be necessary to use 50 kg CO_2 kg ethyl acetate^{-1} operating at 8 MPa and 311.2 K based on solubility data [92,130]; d) after CO_2 and organic solvent separation (e.g. by distillation), the CO_2 should be recycled; e) SFEE is strongly protected by patents of FERRO Corp. and by the group of Prof. Reverchon of the University of Salerno, which could jeopardize its commercialization. To evaluate the feasibility of commercial production by using this technology it would be essential to conduct a rigorous economic evaluation.

References

[1] S. Prabu, T.K. Suriyaprakash, C. Kumar, S. Kumar, Nutraceuticals and their medicinal importance, Int. J. Heal. Allied Sci. 1 (2012) 47. doi:10.4103/2278-344X.101661.

[2] P.M. Kris-Etherton, K.D. Hecker, A. Bonanome, S.M. Coval, A.E. Binkoski, K.F. Hilpert, A.E. Griel, T.D. Etherton, Bioactive compounds in foods: their role in the prevention of cardiovascular disease and cancer, Am. J. Med. 113 (2002) 71–88. doi:10.1016/S0002-9343(01)00995-0.

[3] M. Plaza, S. Santoyo, L. Jaime, G. García-Blairsy Reina, M. Herrero, F.J. Señoráns, E. Ibáñez, Screening for bioactive compounds from algae, J. Pharm. Biomed. Anal. 51 (2010) 450–455. doi:10.1016/j.jpba.2009.03.016.

[4] D.P. Zagklis, C.A. Paraskeva, Isolation of organic compounds with high added values from agro-industrial solid wastes, J. Environ. Manage. 216 (2018) 183–191. doi:10.1016/j.jenvman.2017.04.083.

[5] H.-K. Biesalski, L.O. Dragsted, I. Elmadfa, R. Grossklaus, M. Müller, D. Schrenk, P. Walter, P. Weber, Bioactive compounds: Definition and assessment of activity, Nutrition. 25 (2009) 1202–1205. doi:10.1016/j.nut.2009.04.023.

[6] G. Abdelkarim, B. Soumaya, E. Naima, B. Mohammed, H. Abdellah, What is a bioactive compound? A combined definition for a preliminary consensus, Int. J. Nutr. Food Sci. 3 (2014) 174–179. doi:10.11648/j.ijnfs.20140303.16.

[7] A. Valdés, A. Cifuentes, C. León, Foodomics evaluation of bioactive compounds in foods, TrAC Trends Anal. Chem. 96 (2017) 2–13. doi:10.1016/j.trac.2017.06.004.

[8] E. Jacob-Lopes, M.M. Maroneze, M.C. Deprá, R.B. Sartori, R.R. Dias, L.Q. Zepka, Bioactive food compounds from microalgae: an innovative framework on

industrial biorefineries, Curr. Opin. Food Sci. 25 (2019) 1–7. doi:10.1016/j.cofs.2018.12.003.

[9] J.A. Weststrate, G. van Poppel, P.M. Verschuren, Functional foods, trends and future, Br. J. Nutr. 88 (2002) S233. doi:10.1079/BJN2002688.

[10] D. Martirosyan, J. Singh, A new definition of functional food by FFC: What makes a new definition unique?, Funct. Foods Heal. Dis. 5 (2014) 209–223. doi:10.31989/ffhd.v5i6.183.

[11] L. Contor, Functional food science in Europe, Nutr. Metab. Cardiovasc. Dis. 11 (2001) 20–23.

[12] A. Stein, E. Rodríguez-Cerezo, Functional food in the European Union, Luxembourg, 2008.

[13] "Grand View Research Inc.", Bioactive ingredient market size to reach $51.71 billion by 2024, Bioact. Ingred. Mark. Size. (2016). https://www.grandviewresearch.com/press-release/global-bioactive-ingredients-market.

[14] B. da S. Vaz, J.B. Moreira, M.G. de Morais, J.A.V. Costa, Microalgae as a new source of bioactive compounds in food supplements, Curr. Opin. Food Sci. 7 (2016) 73–77. doi:10.1016/j.cofs.2015.12.006.

[15] I. Michalak, A. Dmytryk, P.P. Wieczorek, E. Rój, B. Leska, B. Górka, B. Messyasz, J. Lipok, M. Mikulewicz, R. Wilk, G. Schroeder, K. Chojnacka, Supercritical algal extracts: A source of biologically active compounds from nature, J. Chem. Article ID (2015) 14. doi:10.1155/2015/597140.

[16] M. Plaza, M. Herrero, A. Cifuentes, E. Ibáñez, Innovative natural functional ingredients from microalgae, J. Agric. Food Chem. 57 (2009) 7159–7170.

doi:10.1021/jf901070g.

[17] M. Oroian, I. Escriche, Antioxidants: Characterization, natural sources, extraction and analysis, Food Res. Int. 74 (2015) 10–36. doi:10.1016/j.foodres.2015.04.018.

[18] M. Gong, A. Bassi, Carotenoids from microalgae: A review of recent developments, Biotechnol. Adv. 34 (2016) 1396–1412. doi:10.1016/j.biotechadv.2016.10.005.

[19] A.C. Guedes, H.M. Amaro, I. Sousa-Pinto, F. Xavier Malcata, Bioactive carotenoids from microalgae, in: Bioact. Compd. from Mar. Foods, John Wiley & Sons Ltd, Chichester, UK, 2013: pp. 131–151. doi:10.1002/9781118412893.ch7.

[20] S.A.R. Paiva, R.M. Russell, β-Carotene and other carotenoids as antioxidants, J. Am. Coll. Nutr. 18 (1999) 426–433. doi:10.1080/07315724.1999.10718880.

[21] K.B. Laurvick, β-carotene-rich extract from Dunaliella salina. Chemical and Technical Assessment (CTA), Rome, Italy, 2017. http://www.fao.org/3/BU603en/bu603en.pdf.

[22] Y. Xu, I. Ibrahim, C. Wosu, A. Ben-Amotz, P. Harvey, Potential of new isolates of *Dunaliella salina* for natural β-carotene production, Biology (Basel). 7 (2018) 14. doi:10.3390/biology7010014.

[23] "Global Market Insights Inc.", Global beta carotene market, Glob. Food Color. Mark. (2019). https://www.gminsights.com/industry-analysis/beta-carotene-market.

[24] J. López-Cervantes, D.I. Sánchez-Machado, Astaxanthin, lutein, and zeaxanthin, in: S.M. Nabavi, A.S. Silva (Eds.), Nonvitamin Nonmineral Nutr. Suppl., Elsevier, Amsterdam, Netherlands, 2019: pp. 19–25. doi:10.1016/B978-0-12-812491-8.00003-5.

[25] L. Jaime, I. Rodríguez-Meizoso, A. Cifuentes, S. Santoyo, S. Suarez, E. Ibáñez, F.J. Señorans, Pressurized liquids as an alternative process to antioxidant carotenoids' extraction from *Haematococcus pluvialis* microalgae, LWT - Food Sci. Technol. 43 (2010) 105–112. doi:10.1016/j.lwt.2009.06.023.

[26] "Global Market Insights Inc.," Astaxanthin market size, Glob. Food Color. Mark. (2019). https://www.gminsights.com/industry-analysis/astaxanthin-market.

[27] L. Zhang, H. Wang, Multiple mechanisms of anti-cancer effects exerted by astaxanthin, Mar. Drugs. 13 (2015) 4310–4330. doi:10.3390/md13074310.

[28] S. Piermarocchi, S. Saviano, V. Parisi, M. Tedeschi, G. Panozzo, G. Scarpa, G. Boschi, G. Lo Giudice, S. Piermarocchi, M. Sartore, G. Monterosso, G. Lo Giudice, I. Fregona, F. Cavarzeran, M.B. Parodi, S. Saviano, G. Di Stefano, M. Varano, V. Parisi, M. Tedeschi, N. Capaldo, G. Panozzo, S. Pignatto, E. Gusson, B. Parolini, G. Boschi, G. Scarpa, C. Del Sal, G. Virgili, Carotenoids in age-related maculopathy Italian study (CARMIS): Two-year results of a randomized Study, Eur. J. Ophthalmol. 22 (2012) 216–225. doi:10.5301/ejo.5000069.

[29] H. Kang, H. Kim, Astaxanthin and β-carotene in Helicobacter pylori-induced gastric inflammation: A mini-review on action mechanisms, J. Cancer Prev. 22 (2017) 57–61. doi:10.15430/JCP.2017.22.2.57.

[30] F.J. Pashkow, D.G. Watumull, C.L. Campbell, Astaxanthin: A novel potential treatment for oxidative stress and inflammation in cardiovascular disease, Am. J. Cardiol. 101 (2008) S58–S68. doi:10.1016/j.amjcard.2008.02.010.

[31] J. Park, J. Chyun, Y. Kim, L.L. Line, B.P. Chew, Astaxanthin decreased oxidative stress and inflammation and enhanced immune response in humans, Nutr. Metab. (Lond). 7 (2010) 18. doi:10.1186/1743-7075-7-18.

[32] B. Capelli, D. Bagchi, G.R. Cysewski, Synthetic astaxanthin is significantly inferior to algal-based astaxanthin as an antioxidant and may not be suitable as a human nutraceutical supplement, Nutrafoods. 12 (2013) 145–152. doi:10.1007/s13749-013-0051-5.

[33] A.C. Rustan, C.A. Drevon, Fatty acids: structures and properties, in: Encycl. Life Sci., John Wiley & Sons, Ltd, Chichester, 2005: pp. 1–7. doi:10.1038/npg.els.0003894.

[34] M.I. Gurr, J.L. Harwood, Fatty acid structure and metabolism, in: Lipid Biochem., Springer US, Boston, MA, 1991: pp. 23–118. doi:10.1007/978-1-4615-3862-2_3.

[35] A.P. Simopoulos, Essential fatty acids in health and chronic disease, Am. J. Clin. Nutr. 70 (1999) 560s-569s. doi:10.1093/ajcn/70.3.560s.

[36] J. Martínez, A. Aguiar, Extraction of triacylglycerols and fatty acids using supercritical fluids - Review, Curr. Anal. Chem. 10 (2013) 67–77. doi:10.2174/1573411011410010006.

[37] S. Takac, A. Karakaya, Recovery of phenolic antioxidants from olive mill wastewater, Recent Patents Chem. Eng. 2 (2010) 230–237. doi:10.2174/1874478810902030230.

[38] "International Olive Council", World statistics on olive oil production, imports, exports and consumption, World Olive Oil Fig. (2019). http://www.internationaloliveoil.org/estaticos/view/131-world-olive-oil-figures.

[39] J. Fernández-Bolaños, G. Rodríguez, R. Rodríguez, A. Heredia, R. Guillén, A. Jiménez, Production in large quantities of highly purified hydroxytyrosol from liquid−solid waste of two-phase olive oil processing or “alperujo,” J. Agric. Food Chem. 50 (2002) 6804–6811. doi:10.1021/jf011712r.

[40] J. Alburquerque, Agrochemical characterisation of "alperujo", a solid by-product of the two-phase centrifugation method for olive oil extraction, Bioresour. Technol. 91 (2004) 195–200. doi:10.1016/S0960-8524(03)00177-9.

[41] C. Bordons, A. Núñez-Reyes, Model based predictive control of an olive oil mill, J. Food Eng. 84 (2008) 1–11. doi:10.1016/j.jfoodeng.2007.04.011.

[42] J. Fernández-Bolaños, O. López, J. Fernández-Bolaños, G. Rodríguez-Gutierrez, Hydroxytyrosol and derivatives: Isolation, synthesis, and biological properties, Curr. Org. Chem. 12 (2008) 442–463. doi:10.2174/138527208784083888.

[43] M. Robles-Almazán, M. Pulido-Morán, J. Moreno-Fernández, C. Ramírez-Tortosa, C. Rodríguez-García, J.L. Quiles, Mc. Ramírez-Tortosa, Hydroxytyrosol: Bioavailability, toxicity, and clinical applications, Food Res. Int. 105 (2018) 654–667. doi:10.1016/j.foodres.2017.11.053.

[44] J. Fernández-Bolaños, Ó. López, M.Á. López-García, A. Marset, Biological properties of hydroxytyrosol and its derivatives, in: Olive Oil - Const. Qual. Heal. Prop. Bioconversions, InTech, 2012: pp. 375–396. doi:10.5772/30743.

[45] N. Allouche, I. Fki, S. Sayadi, Toward a high yield recovery of antioxidants and purified hydroxytyrosol from olive mill wastewaters, J. Agric. Food Chem. 52 (2004) 267–273. doi:10.1021/jf034944u.

[46] M. Brenes, Castro. A., Procedure is for obtaining phenolics extract with high concentration of anti-oxidants and involves ultra-filtration of solutions derived from preparation process of preserved table olive, ES2186467A1, 2004.

[47] L. Villanova, L. Villanova, G. Fasiello, A. Merendino, Process for the recovery of tyrosol and hydroxytyrosol from oil mill wastewaters and catalytic oxidation method in order to convert tyrosol in hydroxytyrosol, US 2006/0070953 A1, 2006.

[48] K. Grodowska, A. Parczewski, Organic solvents in the pharmaceutical industry, Acta Pol. Pharm. 67 (2010) 3–12. doi:10.1021/cg034055z.

[49] G. Brunner, Gas extraction, Steinkopff, Heidelberg, Germany, 1994. doi:10.1007/978-3-662-07380-3.

[50] T. Adschiri, A. Yoko, Supercritical fluids for nanotechnology, J. Supercrit. Fluids. 134 (2018) 167–175. doi:10.1016/j.supflu.2017.12.033.

[51] R.L. Mendes, J.P. Coelho, H.L. Fernandes, I.J. Marrucho, J.M.S. Cabral, J.M. Novais, A.F. Palavra, Applications of supercritical CO_2 extraction to microalgae and plants, J. Chem. Technol. Biotechnol. 62 (1995) 53–59. doi:10.1002/jctb.280620108.

[52] M.M.R. de Melo, A.J.D. Silvestre, C.M. Silva, Supercritical fluid extraction of vegetable matrices: Applications, trends and future perspectives of a convincing green technology, J. Supercrit. Fluids. 92 (2014) 115–176. doi:10.1016/j.supflu.2014.04.007.

[53] F. Sahena, I.S.M. Zaidul, S. Jinap, A.A. Karim, K.A. Abbas, N.A.N. Norulaini, A.K.M. Omar, Application of supercritical CO_2 in lipid extraction – A review, J. Food Eng. 95 (2009) 240–253. doi:10.1016/j.jfoodeng.2009.06.026.

[54] E. Reverchon, I. De Marco, Supercritical fluid extraction and fractionation of natural matter, J. Supercrit. Fluids. 38 (2006) 146–166. doi:10.1016/j.supflu.2006.03.020.

[55] R.P.F.F. da Silva, T.A.P. Rocha-Santos, A.C. Duarte, Supercritical fluid extraction of bioactive compounds, TrAC Trends Anal. Chem. 76 (2016) 40–51. doi:10.1016/j.trac.2015.11.013.

[56] C.G. Pereira, M.A.A. Meireles, Supercritical fluid extraction of bioactive

compounds: Fundamentals, applications and economic perspectives, Food Bioprocess Technol. 3 (2010) 340–372. doi:10.1007/s11947-009-0263-2.

[57] C. Crampon, O. Boutin, E. Badens, Supercritical carbon dioxide extraction of molecules of interest from microalgae and seaweeds, Ind. Eng. Chem. Res. 50 (2011) 8941–8953. doi:10.1021/ie102297d.

[58] H.W. Yen, S.C. Yang, C.H. Chen, Jesisca, J.S. Chang, Supercritical fluid extraction of valuable compounds from microalgal biomass, Bioresour. Technol. 184 (2015) 291–296. doi:10.1016/j.biortech.2014.10.030.

[59] M. Herrero, A. del P. Sánchez-Camargo, A. Cifuentes, E. Ibáñez, Plants, seaweeds, microalgae and food by-products as natural sources of functional ingredients obtained using pressurized liquid extraction and supercritical fluid extraction, TrAC Trends Anal. Chem. 71 (2015) 26–38. doi:10.1016/j.trac.2015.01.018.

[60] D. Chatterjee, P. Bhattacharjee, Supercritical carbon dioxide extraction of antioxidant rich fraction from *Phormidium valderianum*: Optimization of experimental process parameters, Algal Res. 3 (2014) 49–54. doi:10.1016/j.algal.2013.11.014.

[61] C.H. Cheng, T.B. Du, H.C. Pi, S.M. Jang, Y.H. Lin, H.T. Lee, Comparative study of lipid extraction from microalgae by organic solvent and supercritical CO_2, Bioresour. Technol. 102 (2011) 10151–10153. doi:http://dx.doi.org/10.1016/j.biortech.2011.08.064.

[62] A. de Lucas, E. Martinez de la Ossa, J. Rincón, M.. Blanco, I. Gracia, Supercritical fluid extraction of tocopherol concentrates from olive tree leaves, J. Supercrit. Fluids. 22 (2002) 221–228. doi:10.1016/S0896-8446(01)00132-2.

[63] F. Le Floch, M.T. Tena, A. Ríos, M. Valcárcel, Supercritical fluid extraction of

phenol compounds from olive leaves, Talanta. 46 (1998) 1123–1130. doi:10.1016/S0039-9140(97)00375-5.

[64] T.-I. Lafka, A.E. Lazou, V.J. Sinanoglou, E.S. Lazos, Phenolic and antioxidant potential of olive oil mill wastes, Food Chem. 125 (2011) 92–98. doi:10.1016/j.foodchem.2010.08.041.

[65] A. Mouahid, C. Crampon, S.-A.A. Toudji, E. Badens, Supercritical CO_2 extraction of neutral lipids from microalgae: Experiments and modelling, J. Supercrit. Fluids. 77 (2013) 7–16. doi:10.1016/j.supflu.2013.01.024.

[66] G. Brunner, The effect of a modifier or entrainer on solvent power, selectivity, and their pressure and temperature dependence, in: Gas Extr. An Introd. to Fundam. Supercrit. Fluids Appl. to Sep. Process., Springer, Berlin, 1994: pp. 97–105.

[67] J.M. Walsh, G.D. Ikonomou, M.D. Donohue, Supercritical phase behavior: The entrainer effect, Fluid Phase Equilib. 33 (1987) 295–314. doi:10.1016/0378-3812(87)85042-2.

[68] A. del Pilar Sánchez-Camargo, N. Pleite, M. Herrero, A. Cifuentes, E. Ibáñez, B. Gilbert-López, New approaches for the selective extraction of bioactive compounds employing bio-based solvents and pressurized green processes, J. Supercrit. Fluids. 128 (2017) 112–120. doi:10.1016/j.supflu.2017.05.016.

[69] A.P. Sánchez-Camargo, L. Montero, A. Cifuentes, M. Herrero, E. Ibáñez, Application of Hansen solubility approach for the subcritical and supercritical selective extraction of phlorotannins from *Cystoseira abies-marina*, RSC Adv. 6 (2016) 94884–94895. doi:10.1039/C6RA16862K.

[70] J.H. Hildebrand, R.L. Scott, The solubility of nonelectrolytes, Third, Reinhold Pub. Corp., New York, United States, 1950.

[71] C.M. Hansen, 50 Years with solubility parameters - Past and future, Prog. Org. Coatings. 51 (2004) 77–84. doi:10.1016/j.porgcoat.2004.05.004.

[72] C.M. Hansen, The three dimensional solubility parameter and solvent diffusion coefficient, Technical University of Denmark, 1967.

[73] C.M. Hansen, Hansen Solubility Parameters: A User's Handbook, Second, CRC Press, Boca Raton FL, United States, 2007. https://books.google.es/books?id=gprF31cvT2oC.

[74] D. McClements, Nanoparticle- and microparticle-based delivery systems, 1st Editio, CRC Press, Boca Raton, 2014. doi:10.1201/b17280.

[75] V. Đorđević, B. Balanč, A. Belščak-Cvitanović, S. Lević, K. Trifković, A. Kalušević, I. Kostić, D. Komes, B. Bugarski, V. Nedović, Trends in encapsulation technologies for delivery of food bioactive compounds, Food Eng. Rev. 7 (2015) 452–490. doi:10.1007/s12393-014-9106-7.

[76] C.P. Champagne, P. Fustier, Microencapsulation for the improved delivery of bioactive compounds into foods, Curr. Opin. Biotechnol. 18 (2007) 184–190. doi:10.1016/j.copbio.2007.03.001.

[77] B. Hu, Q. Huang, Biopolymer based nano-delivery systems for enhancing bioavailability of nutraceuticals, Chinese J. Polym. Sci. 31 (2013) 1190–1203. doi:10.1007/s10118-013-1331-7.

[78] X. Wu, L. Zhang, X. Zhang, Y. Zhu, Y. Wu, Y. Li, B. Li, S. Liu, J. Zhao, Z. Ma, Ethyl cellulose nanodispersions as stabilizers for oil in water Pickering emulsions, Sci. Rep. 7 (2017) 10. doi:10.1038/s41598-017-12386-4.

[79] M. Younes, P. Aggett, F. Aguilar, R. Crebelli, A. Di Domenico, B. Dusemund, M. Filipič, M. Jose Frutos, P. Galtier, D. Gott, U. Gundert-Remy, G. Georg Kuhnle,

C. Lambré, J. Leblanc, I.T. Lillegaard, P. Moldeus, A. Mortensen, A. Oskarsson, I. Stankovic, P. Tobback, I. Waalkens-Berendsen, M. Wright, A. Tard, S. Tasiopoulou, R.A. Woutersen, Re-evaluation of celluloses E 460(i), E 460(ii), E 461, E 462, E 463, E 464, E 465, E 466, E 468 and E 469 as food additives, EFSA J. 16 (2018). doi:10.2903/j.efsa.2018.5047.

[80] N. Esfandiari, Production of micro and nano particles of pharmaceutical by supercritical carbon dioxide, J. Supercrit. Fluids. 100 (2015) 129–141. doi:10.1016/j.supflu.2014.12.028.

[81] A.Z. Hezave, F. Esmaeilzadeh, Micronization of drug particles via RESS process, J. Supercrit. Fluids. 52 (2010) 84–98. doi:10.1016/j.supflu.2009.09.006.

[82] A. Sane, J. Limtrakul, Formation of retinyl palmitate-loaded poly(l-lactide) nanoparticles using rapid expansion of supercritical solutions into liquid solvents (RESOLV), J. Supercrit. Fluids. 51 (2009) 230–237. doi:10.1016/j.supflu.2009.09.003.

[83] R. Campardelli, E. Reverchon, I. De Marco, PVP microparticles precipitation from acetone-ethanol mixtures using SAS process: Effect of phase behavior, J. Supercrit. Fluids. 143 (2019) 321–329. doi:10.1016/j.supflu.2018.09.010.

[84] R. Adami, S. Liparoti, A. Di Capua, M. Scognamiglio, E. Reverchon, Production of PEA composite microparticles with polyvinylpyrrolidone and luteolin using Supercritical Assisted Atomization, J. Supercrit. Fluids. 143 (2019) 82–89. doi:10.1016/j.supflu.2018.07.020.

[85] J. Jia, J. Wang, K. Zhang, D. Zhou, F. Ge, Y. Zhao, Aescin nanoparticles prepared using SEDS: Composition stability and dissolution enhancement, J. Supercrit. Fluids. 130 (2017) 267–272. doi:10.1016/j.supflu.2017.06.016.

[86] C. Cejudo Bastante, L. Casas Cardoso, M.T. Fernández Ponce, C. Mantell Serrano, E.J. Martínez de la Ossa-Fernández, Characterization of olive leaf extract polyphenols loaded by supercritical solvent impregnation into PET/PP food packaging films, J. Supercrit. Fluids. 140 (2018) 196–206. doi:10.1016/j.supflu.2018.06.008.

[87] B.Y. Shekunov, P. Chattopadhyay, J. Seitzinger, Engineering of composite particles for drug delivery using supercritical fluid technology, in: S. Svenson (Ed.), Polym. Drug Deliv. II, Volume 924, American Chemical Society, Washington DC., 2006: pp. 234–249. doi:10.1021/bk-2006-0924.ch015.

[88] P. Chattopadhyay, R. Huff, B.Y. Shekunov, Drug encapsulation using supercritical fluid extraction of emulsions, J. Pharm. Sci. 95 (2006) 667–679. doi:10.1002/jps.20555.

[89] G. Della Porta, E. Reverchon, Nanostructured microspheres produced by supercritical fluid extraction of emulsions, Biotechnol. Bioeng. 100 (2008) 1020–1033. doi:10.1002/bit.21845.

[90] C. Prieto, Supercritical fluid extraction of emulsions to nanoencapsulate liquid lipophilic bioactive compounds. Process development and scale-up., PhD Dissertation. Complutense University of Madrid, 2017.

[91] C. Prieto, L. Calvo, Supercritical fluid extraction of emulsions to nanoencapsulate vitamin E in polycaprolactone, J. Supercrit. Fluids. 119 (2017) 274–282. doi:10.1016/j.supflu.2016.10.004.

[92] G. Della Porta, N. Falco, E. Reverchon, Continuous supercritical emulsions extraction: A new technology for biopolymer microparticles production, Biotechnol. Bioeng. 108 (2011) 676–686. doi:10.1002/bit.22972.

[93] Food and Drug Administration (FDA), Food additives permitted for direct addition to food for human consumption, Code of Federal Regulations, Title 21, Volume 3, Cite 21CFR172.840, Title 21 - food and drugs, Chapter I - food and drug administration, Department of Health and Human Services, S, Maryland, United States, 2018.

[94] M.J. Cocero, S. González, S. Pérez, E. Alonso, Supercritical extraction of unsaturated products. Degradation of β-carotene in supercritical extraction processes, J. Supercrit. Fluids. 19 (2000) 39–44. doi:10.1016/S0896-8446(00)00077-2.

[95] A. Jayasri, M. Yaseen, Nomograms for solubility parameter, J. Coatings Technol. 52 (1980) 41–45.

[96] K. Srinivas, J.W. King, J.K. Monrad, L.R. Howard, C.M. Hansen, Optimization of subcritical fluid extraction of bioactive compounds using Hansen solubility parameters, J. Food Sci. 74 (2009) E342–E354. doi:10.1111/j.1750-3841.2009.01251.x.

[97] K.G. Joback, R.C. Reid, Estimation of pure-component properties from group-contributions, Chem. Eng. Commun. 57 (1987) 233–243. doi:10.1080/00986448708960487.

[98] A.L. Lydersen, Estimation of critical properties of organic compounds, University of Wisconsin, 1955.

[99] Aspen-Technology, Aspen Plus V 10.0, (2017).

[100] European Parliament and Council of the European Union, Directive 2009/32/EC of the European Parliament and of the Council of 23 April 2009 on the approximation of the laws of the Member States on extraction solvents used in the

production of foodstuffs and food ingredients (Recast), France, 2009. http://eur-lex.europa.eu/legal-content/ES/ALL/?uri=CELEX:32009L0032.

[101] ICH Harmonised Tripartite Guideline, Impurities: guideline for residual solvents Q3C(R6)., 2016.

[102] E. Pérez, A. Cabañas, Y. Sánchez-Vicente, J.A.R. Renuncio, C. Pando, High-pressure phase equilibria for the binary system carbon dioxide+dibenzofuran, J. Supercrit. Fluids. 46 (2008) 238–244. doi:10.1016/j.supflu.2008.01.009.

[103] O. Folin, V. Ciocalteu, On tyrosine and tryptophan determination in protein, J. Biol. Chem. 73 (1927) 627–650.

[104] AOAC, Fatty acid in oils and fats preparation of methyl ester boron trifluoride method, in: Off. Methods Anal. AOAC Int., 16 th, AOAC International Press, Virginia, 1995: pp. 17–22.

[105] A.R. Wellburn, The spectral determination of chlorophylls a and b, as well as total carotenoids, using various solvents with spectrophotometers of different resolution, J. Plant Physiol. 144 (1994) 307–313. doi:10.1016/S0176-1617(11)81192-2.

[106] E. Verhoeven, C. Vervaet, J.P. Remon, Xanthan gum to tailor drug release of sustained-release ethylcellulose mini-matrices prepared via hot-melt extrusion: in vitro and in vivo evaluation, Eur. J. Pharm. Biopharm. 63 (2006) 320–330. doi:10.1016/j.ejpb.2005.12.004.

[107] M. Viguera, A. Marti, F. Masca, C. Prieto, L. Calvo, The process parameters and solid conditions that affect the supercritical CO_2 extraction of the lipids produced by microalgae, J. Supercrit. Fluids. 113 (2016) 16–22. doi:10.1016/j.supflu.2016.03.001.

[108] E. Lack, T. Gamse, R. Marr, Extraction from solids, in: A. Bertucco, G. Vetter (Eds.), High Press. Process Technol. Fundam. Appl., 1st Editio, Elsevier Ltd., Amsterdam, Netherlands, 2001: pp. 378–395.

[109] S. Şahin, M. Bilgin, M.U. Dramur, Investigation of oleuropein content in olive leaf extract obtained by supercritical fluid extraction and soxhlet methods, Sep. Sci. Technol. 46 (2011) 1829–1837. doi:10.1080/01496395.2011.573519.

[110] J.M. Del Valle, J.C. De La Fuente, Supercritical CO_2 extraction of oilseeds: Review of kinetic and equilibrium models, Crit. Rev. Food Sci. Nutr. 46 (2006) 131–160. doi:10.1080/10408390500526514.

[111] M. Perrut, Supercritical fluid applications: Industrial developments and economic issues, Ind. Eng. Chem. Res. 39 (2000) 4531–4535. doi:10.1021/ie000211c.

[112] A. Procopio, C. Celia, M. Nardi, M. Oliverio, D. Paolino, G. Sindona, Lipophilic hydroxytyrosol esters: Fatty acid conjugates for potential topical administration, J. Nat. Prod. 74 (2011) 2377–2381. doi:10.1021/np200405s.

[113] S. Grasso, L. Siracusa, C. Spatafora, M. Renis, C. Tringali, Hydroxytyrosol lipophilic analogues: Enzymatic synthesis, radical scavenging activity and DNA oxidative damage protection, Bioorg. Chem. 35 (2007) 137–152. doi:10.1016/j.bioorg.2006.09.003.

[114] S. Krichnavaruk, A. Shotipruk, M. Goto, P. Pavasant, Supercritical carbon dioxide extraction of astaxanthin from Haematococcus pluvialis with vegetable oils as co-solvent, Bioresour. Technol. 99 (2008) 5556–5560. doi:10.1016/j.biortech.2007.10.049.

[115] G. Vasapollo, L. Longo, L. Rescio, L. Ciurlia, Innovative supercritical CO_2 extraction of lycopene from tomato in the presence of vegetable oil as co-solvent,

J. Supercrit. Fluids. 29 (2004) 87–96. doi:10.1016/S0896-8446(03)00039-1.

[116] M. Sun, F. Temelli, Supercritical carbon dioxide extraction of carotenoids from carrot using canola oil as a continuous co-solvent, J. Supercrit. Fluids. 37 (2006) 397–408. doi:10.1016/j.supflu.2006.01.008.

[117] J.-L. Tu, J.-J. Yuan, Thermal decomposition behavior of hydroxytyrosol (HT) in nitrogen atmosphere based on TG-FTIR methods, Molecules. 23 (2018) 11. doi:10.3390/molecules23020404.

[118] E. De Marco, M. Savarese, A. Paduano, R. Sacchi, Characterization and fractionation of phenolic compounds extracted from olive oil mill wastewaters, Food Chem. 104 (2007) 858–867. doi:10.1016/j.foodchem.2006.10.005.

[119] R.. Owen, A. Giacosa, W.. Hull, R. Haubner, B. Spiegelhalder, H. Bartsch, The antioxidant/anticancer potential of phenolic compounds isolated from olive oil, Eur. J. Cancer. 36 (2000) 1235–1247. doi:10.1016/S0959-8049(00)00103-9.

[120] Ö. Güçlü-Üstündağ, F. Temelli, Solubility behavior of ternary systems of lipids, cosolvents and supercritical carbon dioxide and processing aspects, J. Supercrit. Fluids. 36 (2005) 1–15. doi:10.1016/j.supflu.2005.03.002.

[121] N.E. Craft, J.H. Soares, Relative solubility, stability, and absorptivity of lutein and β-carotene in organic solvents, J. Agric. Food Chem. 40 (1992) 431–434. doi:10.1021/jf00015a013.

[122] M.P. Ekart, K.L. Bennett, S.M. Ekart, G.S. Gurdial, C.L. Liotta, C.A. Eckert, Cosolvent interactions in supercritical fluid solutions, AIChE J. 39 (1993) 235–248. doi:10.1002/aic.690390206.

[123] R.L. Mendes, B.P. Nobre, J.P. Coelho, A.F. Palavra, Solubility of β-carotene in supercritical carbon dioxide and ethane, J. Supercrit. Fluids. 16 (1999) 99–106.

doi:10.1016/S0896-8446(99)00029-7.

[124] L. Jaime, J. a Mendiola, E. Ibáñez, P.J. Martin-Álvarez, A. Cifuentes, G. Reglero, F.J. Señoráns, β-carotene isomer composition of sub- and supercritical carbon dioxide extracts. Antioxidant activity measurement, J. Agric. Food Chem. 55 (2007) 10585–10590. doi:10.1021/jf0711789.

[125] M.D. Macías-Sánchez, C. Mantell, M. Rodríguez, E.J. Martinez de la Ossa, L.M. Lubian, O. Montero, Comparison of supercritical fluid and ultrasound-assisted extraction of carotenoids and chlorophyll a from *Dunaliella salina*, Talanta. 77 (2009) 948–952. doi:10.1016/j.talanta.2008.07.032.

[126] F. Mattea, Á. Martín, A. Matías-Gago, M.J. Cocero, Supercritical antisolvent precipitation from an emulsion: β-Carotene nanoparticle formation, J. Supercrit. Fluids. 51 (2009) 238–247. doi:10.1016/j.supflu.2009.08.013.

[127] L. Calvo, A. Latini, A. Zapata, D.F. Tirado, 17th European Meeting on Supercritical Fluids (EMSF 2019) - 7th European Meeting on High Pressure Technology, in: Form. Coreshell Nanostructures to Entrap Liq. Lipophilic Compd. by SFEE, Ciudad Real, 2019.

[128] C. Prieto, L. Calvo, The encapsulation of low viscosity omega-3 rich fish oil in polycaprolactone by supercritical fluid extraction of emulsions, J. Supercrit. Fluids. 128 (2017) 227–234. doi:10.1016/j.supflu.2017.06.003.

[129] N. Mezzomo, E. De Paz, M. Maraschin, Á. Martín, M.J. Cocero, S.R.S. Ferreira, Supercritical anti-solvent precipitation of carotenoid fraction from pink shrimp residue: Effect of operational conditions on encapsulation efficiency, J. Supercrit. Fluids. 66 (2012) 342–349. doi:10.1016/j.supflu.2011.08.006.

[130] R.L. Smith, T. Yamaguchi, T. Sato, H. Suzuki, K. Arai, Volumetric behavior of

ethyl acetate, ethyl octanoate, ethyl laurate, ethyl linoleate, and fish oil ethyl esters in the presence of supercritical CO_2, J. Supercrit. Fluids. 13 (1998) 29–36. doi:10.1016/S0896-8446(98)00031-X.

[131] M.B. King, A. Mubarak, J.D. Kim, T.R. Bott, The mutual solubilities of water with supercritical and liquid carbon dioxides, J. Supercrit. Fluids. 5 (1992) 296–302. doi:10.1016/0896-8446(92)90021-B.

[132] P. Sakellariou, R.C. Rowe, E.F.T. White, The thermomechanical properties and glass transition temperatures of some cellulose derivatives used in film coating, Int. J. Pharm. 27 (1985) 267–277. doi:10.1016/0378-5173(85)90075-4.

[133] N. Falco, E. Reverchon, G. Della Porta, Continuous Supercritical Emulsions Extraction: Packed tower characterization and application to poly(lactic- co -glycolic acid) + insulin microspheres production, Ind. Eng. Chem. Res. 51 (2012) 8616–8623. doi:10.1021/ie300482n.

[134] M. Li, O. Rouaud, D. Poncelet, Microencapsulation by solvent evaporation: State of the art for process engineering approaches, Int. J. Pharm. 363 (2008) 26–39. doi:10.1016/j.ijpharm.2008.07.018.

[135] P.H. Calderbank, Physical rate processes in industrial fermentation : part 1 : the interfacial area in gas-liquid contacting with mechanical agitation, Trans. Inst. Chem. Eng. 36 (1958) 443–463.

[136] T. Sugimoto, Monodispersed particles, 1st Editio, Elsevier, Amsterdam, Netherlands, 2001.

[137] D.J. McClements, Food emulsions: Principles, practices, and techniques, 3rd Editio, CRC Press, Boca Ratón, 2015. doi:10.1016/S0376-7361(09)70018-4.

[138] L.M.J. Seabra, L.F.C. Pedrosa, Astaxanthin: structural and functional aspects, Rev.

Nutr. 23 (2010) 1041–1050. doi:10.1590/S1415-52732010000600010.

[139] N. Khalid, C.J. Barrow, Critical review of encapsulation methods for stabilization and delivery of astaxanthin, J. Food Bioact. 1 (2018) 104–115. doi:10.xxxx/JFB.2018.00012.

[140] O. Chambin, D. Champion, C. Debray, M.H. Rochat-Gonthier, M. Le Meste, Y. Pourcelot, Effects of different cellulose derivatives on drug release mechanism studied at a preformulation stage, J. Control. Release. 95 (2004) 101–108. doi:10.1016/j.jconrel.2003.11.009.

[141] M. Viguera, C. Prieto, J. Casas, E. Casas, A. Cabañas, L. Calvo, The parameters that affect the supercritical extraction OF 2,4,6-trichloroanisol from cork, J. Supercrit. Fluids. 141 (2018) 137–142. doi:10.1016/j.supflu.2018.03.017.

[142] A.P.R.F. Canela, P.T. V Rosa, M.O.M. Marques, M.A.A. Meireles, Supercritical fluid extraction of fatty acids and carotenoids from the microalgae *Spirulina platensis*, Ind. Eng. Chem. Res. 41 (2002) 3012–3018. doi:10.1021/ie010469i.

[143] A. Bertucco, G. Vetter, High pressure process technology: Fundamentals and applications, 1st Editio, Elsevier, Oxford, UK, 2001.

[144] A. Hardy, D. Benford, T. Halldorsson, M.J. Jeger, H.K. Knutsen, S. More, H. Naegeli, H. Noteborn, C. Ockleford, A. Ricci, G. Rychen, J.R. Schlatter, V. Silano, R. Solecki, D. Turck, M. Younes, Q. Chaudhry, F. Cubadda, D. Gott, A. Oomen, S. Weigel, M. Karamitrou, R. Schoonjans, A. Mortensen, Guidance on risk assessment of the application of nanoscience and nanotechnologies in the food and feed chain: Part 1, human and animal health, EFSA J. 16 (2018). doi:10.2903/j.efsa.2018.5327.

Appendices

ELSEVIER

Publication I

A selective extraction of hydroxytyrosol-rich olive oil from alperujo

D.F. Tirado, E. de la Fuente, L. Calvo

Journal of Food Engineering 263 (2019) 409-416. doi: 10.1016/j.jfoodeng.2019.07.030.

Impact factor Journal of Food Engineering (2018): 3.625

Citations: 0

Journal of Food Engineering 263 (2019) 409–416

Contents lists available at ScienceDirect

Journal of Food Engineering

journal homepage: www.elsevier.com/locate/jfoodeng

A selective extraction of hydroxytyrosol rich olive oil from alperujo

Diego F. Tirado[a], Esther de la Fuente[b], Lourdes Calvo[a,*]

[a] Department of Chemical and Materials Engineering, School of Chemical Sciences, Universidad Complutense de Madrid, Av. Complutense s/n, 28040, Madrid, Spain
[b] Natac Biotech S.L., C/ Electrónica 7, Alcorcón, 28923, Madrid, Spain

ARTICLE INFO

Keywords:
Olive oil
Supercritical extraction
Antioxidant capacity
Total phenol content
Food-grade ingredient

ABSTRACT

Alperujo, the solid-liquid waste generated by the current two-phase method of olive oil extraction, was dried, milled and treated with supercritical carbon dioxide (sc-CO_2) to obtain a hydroxytyrosol (HT)-rich oil. At first, extraction rates were analysed as a function of operating variables and the pre-condition of the raw material. Samples with particle size diameter < 0.80 mm and in equilibrium moisture (1%) with the atmosphere, improved oil extraction yield almost 40% compared with samples with the whole range of particle sizes. Extraction yield improved with solvent flow rate, but a minimum residence time was required. The optimum was 0.18 kg h^{-1} (7.5 kg CO_2 h^{-1} kg biomass^{-1}). Higher pressures and lower temperatures resulted in higher extraction yields; at 30 MPa and 323 K the extraction curve slope was close to the theoretical oil solubility and the yield was 13%, like that obtained with n-hexane by Soxhlet (14%). However, the HPLC-DAD analysis identified higher HT concentration (1900 ppm) in the supercritical extracts at the highest temperature. Consequently, at 373 K, the total phenol content and the antioxidant capacity of the extracts was uppermost. No HT was found in the n-hexane extracts.

1. Introduction

The Mediterranean diet has been widely studied due to its association with improved human health, as it is very effective against cardiovascular diseases, diabetes, inflammation and ageing (Widmer et al., 2015). Many of the benefits associated with the Mediterranean diet are the result of a high intake of antioxidants and anti-inflammatory elements present in several components of this diet, such as olive oil (Robles-Almazán et al., 2018). The olive fruit contains a wide variety of phenolic compounds. They play an important role in the chemical, organoleptic and nutritional properties of virgin olive oil and table olives (Fernández-Bolaños et al., 2008).

The olive oil production process was based on the so-called three-phase system until the nineties, which produced three streams: olive oil, alpechín and olive pomace. To eliminate the alpechín, a two-phase technology emerged, producing only two effluents: olive oil and alperujo (Altieri et al., 2013; Fernández-Bolaños et al., 2002). A schematic representation of the two and three-phase centrifugation procedures for olive oil extraction from olives can be found in the Supplementary file 1. The alperujo contains all the substances that in the three-phase system were contained in the alpechín and in the olive cake and it still has a significant oil content (Arjona et al., 1999). The yearly production of alperujo from the Spanish (largest producer worldwide) (Bordons and Núñez-Reyes, 2008) olive oil industry may approach four million tons.

The high moisture content of alperujo, together with the sugars and fine solids, give to the alperujo sludge a doughy consistency that makes drying difficult, demanding much energy (Arjona et al., 1999). However, generally the alperujo is used to obtain oil by means of a second centrifugation that, being a mechanical method in cold, generates an oil which requires refining with organic solvents for its consumption.

Most phenols (> 98% in mass fraction) remain in the alperujo, with a concentration of 10 to 100-fold higher than that of olive oil (Fernández-Bolaños et al., 2002, 2008). Therefore, alperujo seems to be an affordable and abundant source of natural antioxidants and interesting compounds, hydroxytyrosol (HT) among the most important ones (Fernández-Bolaños et al., 2008).

HT is an amphipathic phenol with a phenyl ethyl-alcohol structure. It is also called 3,4-dihydroxyphenylethanol, 3,4-dihydroxyphenolethanol or 4-(2-Hydroxyethyl)-1,2-benzenediol by the International Union of Pure and Applied Chemistry (IUPAC) system (Robles-Almazán et al., 2018). The origin of HT is the hydrolysis of oleuropein which happens during the ripening of the olives and during the storage and elaboration of table olives (Brenes and de Castro, 1998; Ramírez et al., 2016). Many studies have demonstrated the antioxidant, antimicrobial, anti-inflammatory and antiatherogenic effects of HT

* Corresponding author. Universidad Complutense de Madrid Av. Complutense s/n, 28040, Madrid, Spain.
E-mail address: lcalvo@ucm.es (L. Calvo).

https://doi.org/10.1016/j.jfoodeng.2019.07.030
Received 30 October 2018; Received in revised form 13 July 2019; Accepted 29 July 2019
Available online 30 July 2019
0260-8774/

ELSEVIER

Publication II

Prediction of the best cosolvents to solubilise fatty acids in supercritical CO_2 using the Hansen solubility theory

D.F. Tirado, M.J. Tenorio, A. Cabañas, L. Calvo

Chemical Engineering Science 190 (2018) 14–20. doi:10.1016/j.ces.2018.06.017.

Impact factor Chemical Engineering Science (2018): 3.372

Citations: 8

Chemical Engineering Science 190 (2018) 14–20

Contents lists available at ScienceDirect

Chemical Engineering Science

journal homepage: www.elsevier.com/locate/ces

Prediction of the best cosolvents to solubilise fatty acids in supercritical CO_2 using the Hansen solubility theory

Diego F. Tirado [a], María José Tenorio [b], Albertina Cabañas [b], Lourdes Calvo [a,*]

[a] Department of Chemical and Materials Engineering, Universidad Complutense de Madrid, Av. Complutense s/n, 28040 Madrid, Spain
[b] Department of Physical Chemistry I, School of Chemistry, Universidad Complutense de Madrid, 28040 Madrid, Spain

HIGHLIGHTS

- The Hansen theory was used to choose the best cosolvent for sc-CO_2 extraction.
- The best cosolvents for fatty acids solubilization were short-chain alcohols.
- The predictions were validated with bubble pressures.
- The experimental results agreed with the predictions.

ARTICLE INFO

Article history:
Received 21 December 2017
Received in revised form 18 May 2018
Accepted 4 June 2018
Available online 5 June 2018

Keywords:
Hansen solubility parameters
Miscibility
Cosolvent effect
Carbon dioxide
Supercritical fluid extraction

ABSTRACT

Cosolvents are employed to improve the extraction efficiency and modify the selectivity of the main solvent. However, choosing a proper cosolvent in supercritical extraction is an arduous task. This study aimed to predict the best cosolvents for the supercritical CO_2 extraction of oleic and linoleic acids using the Hansen solubility theory. Calculations were performed for eight organic cosolvents used in food and pharmaceutical production. The best cosolvents for the solubilization of both fatty acids were short-chain alcohols, ethanol and methanol. The predictions were validated with bubble pressures of the mixtures with a 0.003 fatty acid molar fraction at temperatures of 313.2 K and 323.2 K. The experimental results agreed with the predictions. The effect of pressure was well predicted via the direct relationship between pressure and the solvent density. However, the impact of temperature was not properly foreseen because the variation of solute vapour pressure was not considered. The Hansen theory predicted that the miscibility enhancement of the solute in the supercritical mixture is maximum at low pressures and low cosolvent concentrations, as was experimentally confirmed.

1. Introduction

Linoleic acid ($C_{18}H_{32}O_2$) is a polyunsaturated omega-6 fatty acid (C18:2 *cis*-9,12). The human body requires sufficient amounts of linoleic acid in its diet because it cannot produce omega-6 fatty acids. Omega-6 fatty acids, including linoleic acid, support healthy cellular activity and play an essential role in the health and function of cells (Rustan and Drevon, 2005). When linoleic acid replaces saturated fats in the diet, it can cause cholesterol levels to decrease, thereby reducing the risk of heart diseases (Harris et al., 2009) and enhancing brain health (Wainwright, 2002). Alternatively, oleic acid ($C_{18}H_{34}O_2$) is a monounsaturated omega-9 fatty acid (C18:1 *cis*-9). Omega-9 fatty acids, in contrast to omega-6 fatty acids, can be produced by the body. However, it is also beneficial to obtain oleic acid from food because oleic acid, similar to other omega-9 fatty acids, can help to reduce the risk of heart diseases by raising levels of high-density lipoprotein and lowering low-density lipoprotein (Rustan and Drevon, 2005).

Supercritical carbon dioxide (sc-CO_2) has been selected as the solvent for the extraction of some fatty acids and other bioactive compounds because of factors such as its non-flammability, non-toxicity, low cost and availability. A cosolvent, modifier, or entrainer may be added to the supercritical gas to increase solute solubility, increase separation factor, and reduce operating pressure and CO_2 consumption. Both of these last two operating variables directly affect operation and capital expenditure (Perrut, 2000).

The cosolvent effect is obtained when there are specific intermolecular interactions between the pair cosolvent – solute (Walsh et al., 1987). However, the entrainer increases the critical locus of the mixtures and might contaminate the product; therefore, a further separation stage is required. After the extraction,

* Corresponding author.
E-mail address: lcalvo@ucm.es (L. Calvo).

https://doi.org/10.1016/j.ces.2018.06.017
0009-2509/

AIDIC / Associazione Italiana di Ingegneria Chimica

Publication III

The selective supercritical extraction of high-value fatty acids from Tetraselmis suecica using the Hansen solubility theory

D.F. Tirado, A. Rousset, L. Calvo

Chemical Engineering Transactions 75 (2018) 133-138. doi: 10.3303/CET1975023.

Impact factor Chemical Engineering Transactions (2018): -

Citations: 0

CHEMICAL ENGINEERING TRANSACTIONS
VOL. 75, 2019
A publication of AIDIC
The Italian Association of Chemical Engineering
Online at www.cetjournal.it
Guest Editors: Sauro Pierucci, Laura Piazza

ISBN 978-88-95608-72-3; **ISSN** 2283-9216
DOI: 10.3303/CET1975023

The Selective Supercritical Extraction of High-value Fatty Acids from Tetraselmis suecica using the Hansen Solubility Theory

Diego F. Tirado, Amandine Rousset, Lourdes Calvo*

Department of Chemical and Materials Engineering, Complutense University of Madrid, Av. Complutense s/n, 28040 Madrid, Spain.
lcalvo@ucm.es

The aim of this work was to test the utility of the Hansen theory to predict the best cosolvent for supercritical carbon dioxide (sc-CO_2) to reach the selective extraction of fatty acids from *Tetraselmis suecica*. The order in the cosolvent power was established with five organic solvents used in food production: acetone, diethyl ether, ethanol, n-hexane and methanol. Predictions focused on the selective extraction of oleic, linoleic and α-linolenic acid. The cosolvent power depended on the fatty acid, but in general, the best cosolvent for the three target compounds was ethanol. Predictions were validated through equilibrium data and extraction yields from *T. suecica*. Operating at 305.15 K and 20 MPa, the extracted oil with the sc-CO_2-ethanol (5 % mass fraction) mixture significantly improved the content of the target fatty acids compared with pure sc-CO_2; e.g. the α-linolenic acid content was 16 % in the oil obtained with pure sc-CO_2 while it was 25 % in the oil obtained with sc-CO_2 + 5 % ethanol. However, the Hansen theory predicted that the miscibility enhancement of the fatty acids caused by increasing ethanol concentrations in the supercritical solvent mixture was not progressive. In fact, at high pressures and high ethanol concentrations, it was predicted up to less than half the miscibility enhancement.

1. Introduction

Microalgae have received widespread attention in the world population due to the high amounts of bioactive compounds within their structure. Some of these valuable compounds include mono (MUFAs) and polyunsaturated fatty acids (PUFAs) (Viso and Marty, 1993). *Tetraselmis suecica*, for example, is a marine green microalga extensively used in aquaculture, which has already demonstrated its potential as a feedstock for the production of bioactive compounds such as MUFAs and PUFAs (Pérez-López *et al.,* 2014). There is a special interest in the extraction of these fatty acids from natural matrices since functional roles and effects on human health are attributed to them (Calder, 2015). Regarding this, the supercritical carbon dioxide (sc-CO_2) extraction seems to be a suitable technology to achieve the extraction of high-value fatty acids from natural sources (Martínez and Aguiar, 2013). The use of sc-CO_2 has become an alternative solvent for oil extraction from microalgae and plants, because it can achieve good oil yield with respect to the conventional organic solvent extraction, with better product quality and offering the possibility of obtaining a product without the presence of traces of a residual solvent in the final product, which makes the process attractive from the health and environmental point of view. Moreover, CO_2 has easy achievable supercritical conditions (304.13 K and 7.38 MPa are the critical temperature and pressure, respectively) (Mendes *et al.,* 1995).
On the other hand, in order to increase the solubility of specific compounds in sc-CO_2, and therefore improve their extraction, a cosolvent is added in the fluid to increase the separation factor and/or reduce operating pressure and CO_2 consumption. However, the selection of the best cosolvent requires long and expensive experimental effort. For that reason, theoretical estimations should be implemented and the Hansen solubility theory (HST) has already demonstrated to be a useful tool for this sort of evaluations (Tirado *et al*., 2018). In this theory, the total solubility parameter (δ_T) of a substance is divided into three components: dispersion (δ_d), polar (δ_p) and hydrogen-bonding (H-bonding, δ_h) forces, later on, known as Hansen solubility parameters

Paper Received: 29 March 2018; Revised: 20 August 2018; Accepted: 7 November 2018

Please cite this article as: Tirado D.F., Rousset A., Calvo L., 2019, The Selective Supercritical Extraction of High-value Fatty Acids from Tetraselmis Suecica Using the Hansen Solubility Theory, Chemical Engineering Transactions, 75, 133-138 DOI:10.3303/CET1975023

(HSP) (Hansen, 1967). Thus, δ_T is calculated as the square root of a sum of each Hansen component squared. On the other hand, the Hansen theory provides a numerical estimation of the degree of interaction among materials and solvents through the R_a parameter, which can be a good indicator of their miscibility. This last represents the distance between the three-dimensional coordinates of a target compound (δ_{d1}, δ_{p1} and δ_{h1}) and those of the solvent (δ_{d2}, δ_{p2} and δ_{h2}) and can be calculated by Eq. (1). The smaller the value of R_a, the larger the miscibility between the compound and the solvent. Consequently, and according to the Hansen theory, supercritical systems with the lowest R_a value would represent the most suitable one.

$$R_a = \sqrt{4(\delta_{d1} - \delta_{d2})^2 + (\delta_{p1} - \delta_{p2})^2 + (\delta_{h1} - \delta_{h2})^2} \quad (1)$$

In previous work, Tirado *et al.,* (2018) demonstrated the suitability of the HST to predict the best cosolvent for sc-CO_2 in the solubilization of fatty acids within a specific interval of operating conditions. Moreover, the same research group proved that this theoretical approach was also useful to predict the best cosolvent for the extraction of carotenoids from *Dunaliella salina* (Tirado and Calvo, 2019). However, the extension of the Hansen theory to the supercritical extraction of fatty acids from natural matrices has not yet been demonstrated. Therefore, this study aimed to validate the Hansen approach to predict the best supercritical mixture to reach the selective SFE of oleic, linoleic and α-linolenic acid from *T. suecica*. Emphasis was placed on these fatty acids because of their interest in the food industry. In addition, the initial content of these fatty acids in the microalgae was enough to notice the impact of cosolvent power after the SFE.

2. Materials and Methods

2.1 Reagents

Acetone (≥ 99.9 %, Sigma-Aldrich), anhydrous sodium sulphate (≥ 99 %, Sigma-Aldrich), boron trifluoride (1.5 M in methanol, ACROS Organics™), butylated hydroxytoluene (≥ 99 %, Sigma-Aldrich), ethanol (≥ 99.8 %, Fisher Chemical), heptadecanoic acid (≥ 98 %, Sigma-Aldrich), n-hexane (≥ 99 %, Fisher Chemical), methanol (≥ 99.9 %, Fisher Chemical), fatty acid methyl esters (FAME Mix C8 - C22, Sigma-Aldrich), sodium hydroxide (≥ 98 %, Sigma-Aldrich), sodium chloride (≥ 99.5 %, Sigma-Aldrich), α-linolenic acid (99 %, ACROS Organics™), helium (≥ 99.99 %, Air Liquide), nitrogen (≥ 99.99 %, Air Liquide), hydrogen (≥ 99.99 %, Air Liquide) and CO_2 (≥ 99.98 %, Air Products) were used in this work. All substances were acquired in Spain and used without any pre-treatment.

2.2 Computational methods

The modelling of the Hansen theory implemented in this work was carried out such as it was described in previous works (Tirado *et al.*, 2018; Tirado and Calvo, 2019) using Microsoft Excel.

2.2.1 Hansen solubility parameters of fatty acids

The HSP at 298.15 K and 0.1 MPa of the oleic (C18:1 *cis*-9), linoleic (C18:2 *cis*-9,12) and α-linolenic (C18:3 *cis*-9,12,15) acids were calculated by using the group contribution method (GCM) proposed by Hansen (Hansen, 2007). The influence of temperature on the HSP values was calculated by the Jayasri and Yaseen method (Jayasri and Yaseen, 1980). Working below the critical points of the target compounds, pressure does not exert a considerable influence on their HSP (Tirado *et al.,* 2018), therefore, this influence was not considered. The critical temperatures were calculated by the GCM proposed by Joback (Joback and Reid, 1987).

2.2.2 Hansen solubility parameters of solvents

The mixtures sc-CO_2 + cosolvent should be in the supercritical state (completely miscible) at the operating conditions to reach the desired cosolvent effect (Tirado *et al.,* 2018). Therefore, calculations were performed at a constant cosolvent volume fraction of 5 % (0.05 m^3 m^{-3}) to ensure the selection of the best cosolvent at supercritical conditions. The existence of a single homogeneous phase for all the mixtures at the explored conditions was corroborated by visual inspection in a high-pressure variable volume view cell (see Section 2.3). The reference solubility parameters values for CO_2 and the cosolvents at 298.15 K and 0.1 MPa were obtained from the Hansen Handbook (Hansen, 2007); while the molar volume as function of the temperature and pressure studied (20 MPa and 305.15 K) were calculated by using the Reference Fluid Properties (REFPROP) model from the National Institute of Standards and Technology (NIST), with help of the Aspen Plus V 10.0 software. Finally, for the mixtures consisting of sc-CO_2 and a volume fraction of 5 % cosolvent, the solubility parameters were determined with a linear blend rule. The total HSP value of the mixture was equal to the sum of the product of the respective volume fractions of the components present in the mixture, and their corresponding HSP value.

2.2.3 Prediction of miscibility enhancement

The miscibility enhancement was defined by Eq. (2) as the percentage reduction of the R_a values of the mixture sc-CO_2 – cosolvent in relation to pure sc-CO_2 as a function of the cosolvent volume fraction at different pressures (Tirado *et al.,* 2018).

$$\text{Miscibility enhancement (\%)} = \left[1 - \left(\frac{R_{a\ sc-CO_2+cosolvent}}{R_{a\ pure\ sc-CO_2}}\right)\right] x100\ \% \quad (2)$$

2.3 Apparatus and experimental procedure of the assays performed at supercritical conditions

SFE of fatty acid rich-oil from *T. suecica* was carried out at 20 MPa and 305.15 K using sc-CO_2 and its mixtures with a mass fraction of 5 % (0.05 kg kg^{-1}) cosolvent. The procedures to fill up the raw material, start-up and stop the equipment could be consulted in previous work (Tirado and Calvo, 2019). Additionally, the predictions were validated for α-linolenic acid with equilibrium data obtained in a high-pressure variable volume view cell, following the static synthetic method. Bubble pressures at 305.15 K using a molar fraction of 1.5 10^{-3} α-linolenic acid in sc-CO_2 and the supercritical mixture formed by sc-CO_2 + 5 % mass fraction of cosolvent were measured. The bubble pressures of oleic and linoleic acids were already reported (Tirado *et al.,* 2018). For both validation methods, mass fraction and not volume fraction was used due to practical limitations. e.g., during SFE, the flow rate in the experimental set up was measured in mass. However, considering the low amount of cosolvent, the variation with respect to the volume fraction was insignificant (Tirado and Calvo, 2019).

2.4 Fatty acids analysis

First, the supercritical extracts were derivatized following the procedure described by the AOAC Official Method 969.33 (AOAC, 1995). Subsequently, the samples were analysed by gas chromatography (GC) with a Shimadzu 2010 Plus gas chromatograph (Shimadzu Corporation, Japan) equipped with a Flame Ionization Detector (FID) and a Zebron ZB-1HT capillary column (20 m × 0.18 mm i.d. × 0.18 µm film thickness). The separation was carried out with helium (1.8 10^{-6} m^3 min^{-1}) as a carrier gas. The column temperature was programmed starting at a constant value of 393.15 K during 3 min, heated to 458.15 K at 3 K min^{-1}, held at 458.15 K during 3 min, heated again to 523.15 K at 15 K min^{-1} and finally held at 523.15 K for 5 min. The equilibration time was 5 min. A split injector (50:1) at 523.15 K was used. The FID was also heated at 553.15 K. The injection volume was 1 10^{-9} m^3. The fatty acid methyl esters (FAMEs) were identified by comparison of their retention times with those of chromatographic standards. The compounds were quantified related to the area of the internal standard.

2.5 Statistical analysis

The experiments were repeated at least three times. Analyses were performed in duplicate for each replicate (n = 3 × 2). Means and standard deviations were calculated for all data. The experimental error was deduced from selected tests that were repeated six times. The maximum standard deviation for the fatty acid concentration was 0.5 % mass fraction of the fatty acid in the extract and the standard deviations in the bubble pressures were on average 0.1 MPa.

3. Results and Discussion

First, the miscibility of the fatty acids with sc-CO_2 and its mixtures with a volume fraction of 5 % cosolvent was estimated using the HST. Five organic solvents approved for the manufacture of food products (European Parliament and Council of the European Union, 2009) were used for the predictions: acetone, diethyl ether, ethanol, n-hexane and methanol. The miscibility predictions were compared with the concentration of the fatty acids in the oil extracted by SFE from *T. suecica* by using pure sc-CO_2, sc-CO_2 + ethanol and sc-CO_2 + n-hexane. Also, equilibrium data (bubble pressures) of α-linolenic acid in the supercritical mixtures was compared. To match the conditions used in the experimental validation, 20 MPa and 305.15 K were selected for the HST estimations.

3.1. Hansen solubility parameters of fatty acids

Table 1 shows the HSP for oleic, linoleic and α-linolenic acids at 298.15 K and 0.1 MPa, and at the selected conditions for the supercritical extraction. In the three fatty acids, the dispersion force (δ_d) had the highest contribution, due to the presence of a long straight-chain hydrocarbon in their structures. Furthermore, these fatty acids contain unsaturations (olefin groups) and one carboxylic group, which gives polar (δ_p) and H-bonding contributions (δ_h), respectively. However, the carboxylic group has a bigger impact than the olefin

group, and for that reason, the H-bonding forces are higher. On the other hand, the HSP of the three fatty acids varied only slightly within the explored temperature interval, as it was before described (Tirado *et al.,* 2018).

Table 1: Hansen solubility parameters of the fatty acids studied in this work at room and supercritical conditions.

Fatty acid	298.15 K and 0.1 MPa			305.15 K and 20 MPa		
	δ_d $MPa^{1/2}$	δ_p $MPa^{1/2}$	δ_h $MPa^{1/2}$	δ_d $MPa^{1/2}$	δ_p $MPa^{1/2}$	δ_h $MPa^{1/2}$
Oleic acid	17.40	2.67	6.43	17.35	2.66	6.42
Linoleic acid	18.29	2.94	7.24	18.24	2.93	7.22
α-Linolenic acid	18.03	3.03	7.61	17.99	3.02	7.59

3.2 Hansen solubility parameters of the supercritical solvent mixtures

Table 2 shows the HSP of sc-CO_2 and its mixtures with a volume fraction of 5 % cosolvent. The addition of cosolvents to sc-CO_2 mostly increased δ_d. The highest value of δ_d happened in the sc-CO_2-ethanol mixture.

Table 2: Hansen solubility parameters of sc-CO_2 and its supercritical mixtures with several cosolvents (5 % volume fraction) at 305.15 K and 20 MPa.

Supercritical fluid	δ_d $MPa^{1/2}$	δ_p $MPa^{1/2}$	δ_h $MPa^{1/2}$
sc-CO_2	11.30	5.52	4.97
sc-CO_2 +acetone	11.53	5.77	5.07
sc-CO_2 + ethanol	11.54	5.69	5.69
sc-CO_2 +diethyl ether	11.49	5.40	4.97
sc-CO_2 +n-hexane	11.51	5.25	4.72
sc-CO_2 + methanol	11.51	5.87	5.83

3.3 Prediction of the best cosolvent

Table 3 shows the R_a values between all the studied fatty acids and the supercritical mixture at 305.15 K and 20 MPa. The cosolvent order depended on the fatty acid. For oleic acid, the most adequate cosolvents by increasing miscibility (minor R_a), at the tested operating conditions, were ethanol and n-hexane. In the case of linoleic and α-linolenic acids, the best cosolvents were both alcohols. These differences in the cosolvent order could be explained by the different affinities of the fatty acids (due mainly to their structural differences) with the supercritical mixture since the cosolvent effect is obtained when there are specific intermolecular interactions between the pair cosolvent – solute (Walsh *et al.,* 1987). In any case, the best cosolvent power for all the studied fatty acids was given by ethanol, as the supercritical mixture containing this alcohol provoked the highest reduction in R_a in relation to pure sc-CO_2.

Table 3: R_a values between fatty acids and supercritical solvents at 305.15 K, 20 MPa and a cosolvent volume fraction of 5 %.

Supercritical fluid	R_a between the fatty acid		
	Oleic acid	Linoleic acid	α-Linolenic acid
sc-CO_2	12.514	13.845	14.286
sc-CO_2 +acetone	12.127	13.438	13.881
sc-CO_2 + ethanol	12.031	13.297	13.759
sc-CO_2 +diethyl ether	12.126	13.463	13.902
sc-CO_2 +n-hexane	12.093	13.456	13.887
sc-CO_2 + methanol	12.132	13.376	13.843

3.4. Validation of the predictions

Validations were performed using ethanol (as better) and n-hexane (as worse) cosolvent. The R_a values provided by these cosolvents differed sufficiently enough to find experimental variations on the equilibrium pressures and on the fatty acid content in the supercritical extracts. Table 4 shows the fatty acid content of the extracts obtained with pure sc-CO_2 and with its mixture with an ethanol and n-hexane mass fractions of 5 % at 305.15 K and 20 MPa. The use of both cosolvents improved the selective extraction of fatty acids from the microalgae, with the largest increase occurring in the mixture made up of CO_2 + ethanol, which agreed with the predictions based on the R_a values. The obtained extract with pure sc-CO_2 contained 14.9 %, 3.7 % and 15.7 % of oleic, linoleic and α-linolenic acid, respectively; while the obtained extract with the sc-CO_2-ethanol mixture contained roughly 53 %, 54 % and 61 % more.

Table 4: Fatty acids content in the oil extracts obtained from Tetraselmis suecica at 305.15 K, 20 MPa with a cosolvent mass fraction of 5 % in sc-CO_2. Bubble pressures for α-linolenic acid at 305.15 K.

Supercritical fluid	Mass fraction of the fatty acid in the extract (%)			Bubble pressure (MPa) for α-linolenic acid
	Oleic acid	Linoleic acid	α-Linolenic acid	
sc-CO_2	14.9	3.7	15.7	13.0
sc-CO_2 + n-hexane	15.7	3.9	16.1	12.8
sc-CO_2 + ethanol	22.7	5.7	25.3	12.1

Additionally, Table 4 shows the bubble pressures obtained by the static synthetic method at 305.15 K for a molar fraction of 1.5 10^{-3} α-linolenic acid in sc-CO_2 and sc-CO_2 + 5 % mass fraction of ethanol or n-hexane. Lower bubble pressure values indicated higher miscibility. Therefore, the best cosolvent for the solubilization of α-linolenic in sc-CO_2 was ethanol followed by n-hexane, which was consistent with the predictions made using the HST. Similar results were obtained for oleic and linoleic acids. For example, the bubble pressure of a 0.003 molar fraction of linoleic acid at 313.2 K was 9.6 MPa in the mixture CO_2-ethanol, 15.5 MPa in the mixture CO_2-hexane and 22.2 MPa in pure sc-CO_2 (Tirado *et al*., 2018).

3.5. The impact of the amount of cosolvent on the miscibility enhancement

Figure 1 shows the miscibility enhancement predicted by the Hansen theory of α-linolenic with raising ethanol concentrations at increasing pressures. The percentage reduction of the R_a values of the mixture sc-CO_2 + ethanol in relation to pure sc-CO_2 was plotted as a function of increasing volume fraction of ethanol. In Figure 1, a non-linear relationship between the miscibility enhancement and the cosolvent concentration was observed, mainly at the highest pressures. Thus, at ethanol concentrations in the supercritical solvent mixture higher than 25 %, the miscibility enhancement curves were not linear. Above 50 MPa, the lines even curved down. Similar behaviour was previously predicted for oleic acid in the same supercritical solvent mixture; however, it happened at a lower ethanol concentration of 10 % (Tirado *et al.,* 2018). It was also experimentally detected for different systems (Brunner, 1994; Ekart *et al.,* 1993; Güçlü-Üstündağ and Temelli, 2005).

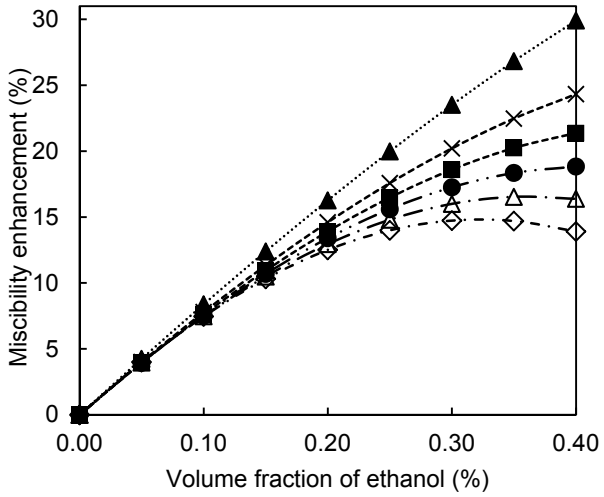

Figure 1: Predicted miscibility enhancement of α-linolenic acid in sc-CO_2 + ethanol at 313.15 K and 10 MPa (▲), 20 MPa (x), 30 MPa (■), 40 MPa (●), 50 MPa (Δ) and 60 MPa (◊) by the Hansen theory.

Theoretically, this behaviour was explained due to the reduction of the molar volume of the solvent mixture with the increase of pressure and the cosolvent fraction. Besides, Güçlü-Üstündağ and Temelli (2005) related this conduct to the self-association of the cosolvent. Although these cannot be the only explanations, given that for the same cosolvent, the reduction in the miscibility enhancement does not always occur at the same pressure and concentration. It must also be related to the target solute. Based on the predictions we have made with Hansen's theory, the lower the miscibility of the compound of interest in sc-CO_2 alone, the higher the concentration of cosolvent and the pressure needed to observe the bending phenomenon of the miscibility enhancement curves.

4. Conclusions

In this study, the Hansen solubility theory was validated to choose the best supercritical solvent mixture to reach the selective extraction of oleic, linoleic and α-linolenic acids. According to this theory, the best cosolvent for supercritical carbon dioxide (sc-CO_2) in the extraction of the three fatty acids from *Tetraselmis suecica* was ethanol, as it was experimentally corroborated. Consequently, the Hansen solubility parameters could be a suitable tool to at least reduce the number of experiments for the selection of the best cosolvent for sc-CO_2 in the extraction of a target compound from a natural complex matrix.

Acknowledgements

Diego F. Tirado thanks the "Bolívar Gana con Ciencia" program from the Department of Bolívar (Colombia) for a PhD grant.

References

AOAC, 1995. Fatty acid in oils and fats preparation of methyl ester boron trifluoride method, in: Official Methods of Analysis of AOAC International. AOAC International Press, Virginia, pp. 17–22.

Brunner, G., 1994. The effect of a modifier or entrainer on solvent power, selectivity, and their pressure and temperature dependence, in: Gas Extraction: An Introduction to Fundamentals of Supercritical Fluids and the Application to Separation Processes. Springer, Berlin, pp. 97–105.

Calder, P.C., 2015. Functional roles of fatty acids and their effects on human health. J. Parenter. Enter. Nutr. 39, 18S–32S.

Ekart, M.P., Bennett, K.L., Ekart, S.M., Gurdial, G.S., Liotta, C.L., Eckert, C.A., 1993. Cosolvent interactions in supercritical fluid solutions. AIChE J. 39, 235–248.

European Parliament and Council of the European Union, 2009. Directive 2009/32/EC of the European Parliament and of the Council of 23 April 2009 on the approximation of the laws of the Member States on extraction solvents used in the production of foodstuffs and food ingredients (Recast). France.

Güçlü-Üstündağ, Ö., Temelli, F., 2005. Solubility behavior of ternary systems of lipids, cosolvents and supercritical carbon dioxide and processing aspects. J. Supercrit. Fluids 36, 1–15.

Hansen, C.M., 2007. Hansen Solubility Parameters: A User's Handbook, Second. ed. CRC Press, Boca Raton FL, United States.

Hansen, C.M., 1967. The three dimensional solubility parameter and solvent diffusion coefficient. Technical University of Denmark.

Jayasri, A., Yaseen, M., 1980. Nomograms for solubility parameter. J. Coatings Technol. 52, 41–45.

Joback, K.G., Reid, R.C., 1987. Estimation of pure-component properties from group-contributions. Chem. Eng. Commun. 57, 233–243.

Martínez, J., Aguiar, A., 2013. Extraction of triacylglycerols and fatty acids using supercritical fluids - Review. Curr. Anal. Chem. 10, 67–77.

Mendes, R.L., Coelho, J.P., Fernandes, H.L., Marrucho, I.J., Cabral, J.M.S., Novais, J.M., Palavra, A.F., 1995. Applications of supercritical CO_2 extraction to microalgae and plants. J. Chem. Technol. Biotechnol. 62, 53–59.

Pérez-López, P., González-García, S., Ulloa, R.G., Sineiro, J., Feijoo, G., Moreira, M.T., 2014. Life cycle assessment of the production of bioactive compounds from *Tetraselmis suecica* at pilot scale. J. Clean. Prod. 64, 323–331.

Tirado, D.F., Calvo, L., 2019. The Hansen theory to choose the best cosolvent for supercritical CO_2 extraction of β-carotene from *Dunaliella salina*. J. Supercrit. Fluids 145, 211–218.

Tirado, D.F., Tenorio, M.J., Cabañas, A., Calvo, L., 2018. Prediction of the best cosolvents to solubilise fatty acids in supercritical CO_2 using the Hansen solubility theory. Chem. Eng. Sci. 190, 14–20.

Viso, A.-C., Marty, J.-C., 1993. Fatty acids from 28 marine microalgae. Phytochemistry 34, 1521–1533.

Walsh, J.M., Ikonomou, G.D., Donohue, M.D., 1987. Supercritical phase behavior: The entrainer effect. Fluid Phase Equilib. 33, 295–314.

ELSEVIER

Publication IV

The Hansen theory to choose the best cosolvent for supercritical CO_2 extraction of β-carotene from Dunaliella salina

D.F. Tirado, L. Calvo

The Journal of Supercritical Fluids 145 (2019) 211–218.
doi:10.1016/j.supflu.2018.12.013.

Impact factor The Journal of Supercritical Fluids (2018): 3.481

Citations: 4

The Journal of Supercritical Fluids 145 (2019) 211–218

Contents lists available at ScienceDirect

The Journal of Supercritical Fluids

journal homepage: www.elsevier.com/locate/supflu

The Hansen theory to choose the best cosolvent for supercritical CO_2 extraction of β-carotene from *Dunaliella salina*

Diego F. Tirado, Lourdes Calvo*

Department of Chemical and Materials Engineering, Universidad Complutense de Madrid, Av. Complutense s/n, 28040, Madrid, Spain

GRAPHICAL ABSTRACT

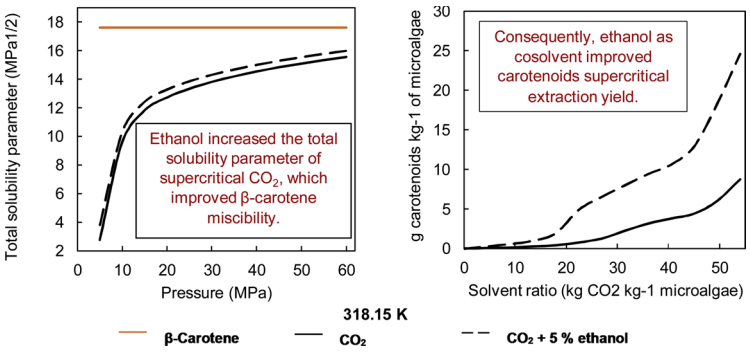

ARTICLE INFO

Keywords:
Hansen solubility parameters
Food-grade ingredients
Supercritical fluid extraction
Cosolvent effect
Carotenoids
Microalgae

ABSTRACT

The Hansen solubility theory was used to predict the best cosolvent for supercritical carbon dioxide (sc-CO_2) to achieve the selective extraction of β-carotene from *Dunaliella salina*. Among four organic cosolvents, ethanol was predicted to be the best based on minima R_a values. The predictions were validated through equilibrium data and extraction curves from the microalgae. The addition of ethanol reduced the bubble pressures, and therefore increased the solubility of the β-carotene. With 5% mass fraction, at 318.15 K and 20 MPa, the extraction yield was 25 g carotenoids kg microalgae^{-1}, much more than in pure sc-CO_2 (6 g).

1. Introduction

The search for natural sources of antioxidants keeps increasing over time. These products are used to reduce the oxidative deterioration of both, food and the human body [1,2]. Microalgae represent one of the sources that are being studied due to the high amounts of bioactive compounds within their structure. Some of these compounds include antioxidants, polyunsaturated fatty acids (PUFAs), sterols and others [1,3].

Carotenoids, for instance, are a class of organic pigments from the group of isoprenoids that have numerous biological functions. They are fat-soluble and therefore, they present high solubility in non-polar solvents. The β-carotene is one of the main types of carotenes, and it is mainly known for being a natural precursor of vitamin A. It is a high-molecular-weight compound that is formed by a hydrocarbon chain without oxygen ($C_{40}H_{56}$) [4]. It is easily degradable by light, heat and air, and its colour can vary from yellow to dark red, depending on its purity, source and location. Some of the main natural sources of β-carotene include plants, algae, microalgae [4] and fungi [5], but most part of its production comes from synthetic methods.

* Corresponding author at: Universidad Complutense de Madrid, Av. Complutense s/n, 28040, Madrid, Spain.
E-mail address: lcalvo@ucm.es (L. Calvo).

https://doi.org/10.1016/j.supflu.2018.12.013
Received 22 October 2018; Received in revised form 18 December 2018; Accepted 18 December 2018
Available online 21 December 2018
0896-8446/

ELSEVIER

Publication V

Astaxanthin encapsulation in ethyl cellulose carriers by continuous supercritical emulsions extraction: A study on particle size, encapsulation efficiency, release profile and antioxidant activity

D.F. Tirado, I. Palazzo, M. Scognamiglio, L. Calvo, G. Della Porta, E. Reverchon

The Journal of Supercritical Fluids 150 (2019) 128-136.
doi:10.1016/j.supflu.2019.04.017.

Impact factor The Journal of Supercritical Fluids (2018): 3.481

Citations: 0

J. of Supercritical Fluids 150 (2019) 128–136

Contents lists available at ScienceDirect

The Journal of Supercritical Fluids

journal homepage: www.elsevier.com/locate/supflu

Astaxanthin encapsulation in ethyl cellulose carriers by continuous supercritical emulsions extraction: A study on particle size, encapsulation efficiency, release profile and antioxidant activity

Diego F. Tirado[a], Ida Palazzo[b], Mariarosa Scognamiglio[b], Lourdes Calvo[a,*], Giovanna Della Porta[b,c,**,1], Ernesto Reverchon[b,1]

[a] Department of Chemical and Materials Engineering, Complutense University of Madrid, Av. Complutense s/n, 28040 Madrid, Spain
[b] Supercritical Fluids Lab., Department of Industrial Engineering, University of Salerno, Via Giovanni Paolo II, 84084 Fisciano, SA, Italy
[c] Translational Medicine Lab., Department of Medicine and Surgery, University of Salerno, Via S. Allende, 84081 Baronissi, SA, Italy

HIGHLIGHTS

- SEE-C was used to encapsulate astaxanthin in ethyl cellulose.
- Carrier size was tuned by modifying the emulsion formulation.
- Encapsulation efficiency of 84% was reached.
- The drug did not lose its biological activity and was released in almost 10 h.

GRAPHICAL ABSTRACT

Nanocarriers of astaxanthin in ethyl cellulose were produced by SEE-C with a high encapsulation efficiency.

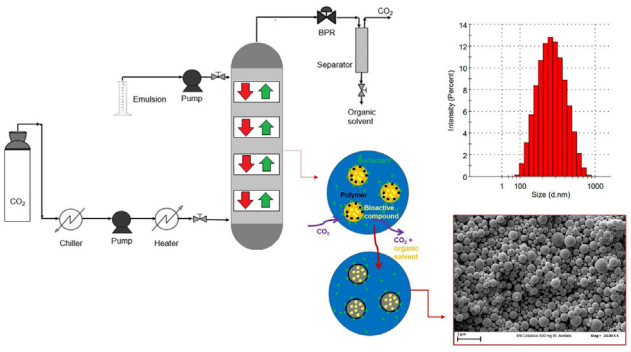

ARTICLE INFO

Article history:
Received 11 March 2019
Received in revised form 24 April 2019
Accepted 29 April 2019
Available online 1 May 2019

Keywords:
Supercritical emulsion extraction
Astaxanthin
Nanocarriers
Controlled release
Antioxidant activity

ABSTRACT

Supercritical emulsions extraction (SEE) technology was used to encapsulate astaxanthin (AXT) in ethyl cellulose (EC). The operating parameters were 8 MPa and 311 K with an L/G ratio of 0.1 (CO_2 flow rate of 1.4 kg/h). Several emulsion formulations were tested, fixing the *oil-water* ratio at 20:80 (ethyl acetate/water) and varying EC concentration in the oily phase from 1.0–2.5% mass and the surfactant amount in the water phase from 0.1 to 0.6% mass. Both parameters influenced carriers morphology, size and distribution; a correlation between the EC amount in oily phase and its dynamic viscosity was proposed to explain the droplets/carriers size variation observed. Carriers aggregation was monitored at surfactant concentration higher than 0.3% mass. The best emulsion formulation was obtained using 1.0% mass of EC in the oily phase and 0.1% mass of surfactant in the water phase; in these conditions spherical nanocarriers with unwrinkled and smooth surface were obtained with a size of 242 nm and Poly Dispersity Index of 0.16. EC mass recovery was of 90%. Higher carrier mean size of 363 nm (Poly Disperity Index of 0.31) was measured when AXT was encapsulated in the same conditions, achieving an encapsulation efficiency of 84%. The carriers were loaded with 21 mg/g of AXT and showed an excellent antioxidant capacity, measured as Trolox equivalent (Trolox equivalent per kg of pure AXT), and

* Corresponding author.
** Corresponding author at: Department of Medicine and Surgery "Scuola Medica Salernitana", University of Salerno, Via S. Allende, Baronissi, SA 84084, Italy.
E-mail addresses: lcalvo@ucm.es (L. Calvo), gdellaporta@unisa.it (G. Della Porta).
[1] The authors shared the co-last authorship.

https://doi.org/10.1016/j.supflu.2019.04.017

Curriculum vitae

Curriculum vitae

Diego Felipe Tirado Armesto

17/12/1990

Colombian

ORCID: 0000-0002-6178-5660
Scopus ID: 56031347300
JCR Publications: 6
Scopus indexed publications: 22
Books: 2
Google scholar citations: 230
***h*-index Google scholar:** 8

Education

Food Engineering
University of Cartagena (Colombia)
December 2012

Master's in environmental engineering
University of Cartagena
May 2016

Work experience

Young Researcher and Innovator
Administrative Department of Science, Technology and Innovation (COLCIENCIAS)
University of Cartagena
Cartagena de Indias (Colombia)
02/2013 – 02/2014

Research Assistant
University of Cartagena
Cartagena de Indias
02/2014 – 10/2015

Participation in research projects during the doctoral period

Preparation of nanomaterials with supercritical CO_2 and their application in catalysis and pharmacology
Ministry of Economy and Competitiveness (CTQ2013-41781-P)
12/2014 – 09/2017
Principal Investigators: Concepción Pando and Albertina Cabañas

Preparation of metal and drug hybrid nanomaterials on biocompatible carriers for controlled release using supercritical CO_2
Santander-Complutense University of Madrid (PR75/18-21583)
01/2019 – Present
Principal Investigator: Albertina Cabañas

Preparation of advanced drug delivery systems incorporating metallic nanoparticles based on supercritical CO_2 technologies
Ministry of Economy and Competitiveness (RTI2018-097230-B-I00)
Principal Investigator: Albertina Cabañas and Lourdes Calvo Garrido
01/2019 – Present

Research stays during the doctoral period

University of Salerno
Department of Industrial Engineering
Supercritical fluid research group

03/09/2018 – 22/12/2019

Topic: *Continuous production by supercritical emulsion extraction (SEE-C) of bioactive compounds contained in biopolymers using a high-pressure packing column in counter-current.*

Supervisor: Ernesto Reverchon

Publications during the doctoral period

D.F. Tirado, M.J. Tenorio, A. Cabañas, L. Calvo. Prediction of the best cosolvents to solubilise fatty acids in supercritical CO_2 using the Hansen solubility theory. Chemical Engineering Science, 190, 14-20 (2018). https://doi.org/10.1016/j.ces.2018.06.017

D.F. Tirado, L. Calvo. The Hansen theory to choose the best cosolvent for supercritical CO_2 extraction of β-carotene from *Dunaliella salina*. Journal of Supercritical Fluids, 145, 211 - 218 (2019). https://doi.org/10.1016/j.supflu.2018.12.013.

D.F. Tirado, I. Palazzo, M. Scognamiglio, L. Calvo, G. Della Porta, E. Reverchon, Astaxanthin encapsulation in ethyl cellulose carriers by continuous supercritical emulsions extraction: A study on particle size, encapsulation efficiency, release profile and antioxidant activity. Journal of Supercritical Fluids, 150, 128-136 (2019). https://doi.org/10.1016/j.supflu.2019.04.017.

D.F. Tirado, A. Rousset, L. Calvo, The selective supercritical extraction of high-value fatty acids from *Tetraselmis suecica* using the Hansen solubility theory. Chemical Engineering Transactions, 75, 133-38 (2019). https://doi.org/10.3303/CET1975023.

D.F. Tirado, E. de la Fuente, L. Calvo, A selective extraction of hydroxytyrosol rich olive oil from alperujo. Journal of Food Engineering, 263, 409-416 (2019). https://doi.org/10.1016/j.jfoodeng.2019.07.030.

Collaboration in teaching activity during the doctoral period

Separation process
BSc in Chemical Engineering
Complutense University of Madrid
Academic years: 2016/2017, 2017/2018, 2018/2019
40 h/year

Advance separation processes
Master's in chemical engineering: Process Engineering
Complutense University of Madrid
Academic years: 2016/2017, 2017/2018, 2018/2019
20 h/year

Participation at congresses during the doctoral period

Oral presentation: Application of the Hansen solubility theory for the selection of co-solvents for supercritical carbon dioxide extraction. 50th Anniversary HSP Conference, 5-7th April 2017, York, United Kingdom.

Poster: The prediction of the best co-solvents for supercritical CO_2 extraction of bioactive compounds with the Hansen solubility theory. 16th European Meeting on Supercritical Fluids (EMSF), 8-11th April 2019, Lisbon, Portugal.

Oral presentation: Extracción con dióxido de carbono supercrítico de compuestos bioactivos a partir de materiales vegetales. IX meeting FLUCOMP, 13-15th June 2018, Madrid, Spain.

Oral presentation: The Encapsulation of Astaxanthin in Ethyl Cellulose By Continuous Supercritical Emulsions Extraction. 17th European Meeting on Supercritical Fluids (EMSF 2019) - 7th European Meeting on High Pressure Technology, 08-11th April 2019, Ciudad Real, Spain.

Oral presentation: A computational approach for the selective supercritical carbon dioxide extraction of high-value nutritional compounds from microalgae. 2nd International Conference on Engineering Future Food, 26-29th May 2019, Bologna, Italy.

Oral presentation: Supercritical extraction of bioactive compounds from vegetable matrices and their encapsulation with supercritical fluid advanced techniques. 3rd ANQUE-ICCE International Congress of Chemical Engineering - 1er Congreso Iberoamericano de Ingeniería Química (CIBIQ), 19-21th June 2019, Santander, Spain.

Courses, seminaries and workshops during the doctoral period

Course on "Bioproducts Engineering and Biorefineries"
University of Valladolid
Valladolid, Spain
2016

Course: Gas safety inside a laboratory
Praxair, Inc.
Madrid, Spain
2016

Chemical Engineering PhD Program Seminar
Complutense University of Madrid
Madrid, Spain
2017

1ª Convocatoria EDUCM PhDay Complutense
Universidad Complutense de Madrid
Madrid, Spain
2017

Aspectos metodológicos para el Doctorado en el ámbito de Ciencias experimentales e Ingenierías
Complutense University of Madrid
Madrid, Spain
2017

Chemical Engineering PhD Program Seminar
Complutense University of Madrid
Madrid, Spain
2018

Chemical Engineering PhD Program Seminar
Complutense University of Madrid
Madrid, Spain
2019

Honours and awards

Honourable mention for ACADEMIC EXCELLENCE to a graduate of the Food Engineering Program
Administrative decision No. 79
University of Cartagena
2012

Grant as a young Researcher and Innovator COLCIENCIAS 2012-2013
Administrative Department of Science, Technology and Innovation (COLCIENCIAS)
2012

First place who finished academically in the second period of 2012, corresponding to the curricular project of the Food Engineering program
University of Cartagena
2012

Master's grant for being a distinguished graduate student with the first position in the Faculty of Engineering
University of Cartagena
2014

International predoctoral grant "Bolívar Gana con Ciencia"
Government of Bolívar (Colombia)
2015

Languages

Spanish	Native proficiency
English	B2, EF Standard English Test (2017)
Italian	Elementary proficiency, University of Salerno